University of Nevada, Reno

Development of a Novel Humidification-Dehumidification Solar Distillation System Prototype

A thesis submitted in partial fulfillment of the
requirements for the degree of Master of Science in
Mechanical Engineering

by

Robert L. Hemenway

Dr. Cahit A. Evrensel/Thesis Advisor

May, 2024

THE GRADUATE SCHOOL

We recommend that the thesis
prepared under our supervision by

Robert L. Hemenway

entitled

Development of a Novel Humidification-Dehumidification Solar Distillation System Prototype

be accepted in partial fulfillment of the
requirements for the degree of

MASTER OF SCIENCE

Cahit A. Evrensel, Ph.D.
Advisor

Robert H. Turner, Ph.D.
Committee Member

S. Kent Hoekman, Ph.D.
Graduate School Representative

Markus Kemmelmeier, Ph.D., Dean
Graduate School

May, 2024

Abstract

This thesis explores a novel solar distillation unit designed to be sufficiently simple and cost-effective that an individual with modest skill and means could reproduce it and use it to distill water. The design centers around solar heated air which heats and evaporates water in a moisturizer filter. Subsequently the nearly saturated air is cooled in an air-to-water heat exchanger, condensing vapor for collection. Two different heat rejection systems were considered and tested, appropriate for different seasons.

A system was built and tested at the Desert Research Institute in Reno Nevada, which features abundant sunshine throughout the year. A mathematical model initially predicted a reasonable estimated distilled water collection. However, the system as built and tested contained a design flaw which was identified only after testing was completed, namely that air velocity through the heat exchanger-condenser blew suspended atomized water droplets past the collection area and returned them to the solar collector, bypassing useful collection and diminishing the apparent system efficiency. A second mathematical model correctly estimated both the expected distilled water collection and also the realized product. The approach can deliver more distilled product than a sloping glass passive solar still, but more research is required for a proper demonstration.

Acknowledgements

This thesis was made possible by the help and support of my wife and children. My parents were also a major support from allowing me to use the workshop at their home to keeping me positive throughout this endeavor. Thank you to my brother-in-law, Donnie Werner, who helped me build the prototype system.

A special thank you to Dr. Bob Turner who took me under his wing and helped me develop this program. His instruction and insights were fundamental to this project.

Thanks, is also due to my Advisor, Dr. Cahit Evrensel, who was willing to work with me and be my advisor. He was willing to take me on when I needed the support.

Thank you to Peter Ross from the Desert Regional Institute for the space and support. This allowed me to better test the practical application of my project and to better understand the complexities of such a design.

I am grateful for all of the support, advice, and assistance I received from everyone. Thank you all!

Table of Contents

List of Tables

List of Figures

Nomenclature:

A	Cross-sectional area of the heat exchanger	44
A_c	Useable area of the solar collector	38
AMTD	Arithmetic Mean Temperature difference	57
C_p	specific heat	38
$C_{p,h}$	Specific heat on the hot side	44
$C_{p,a}$	Specific heat of air	44
$C_{p,c}$	Specific heat on the cold side	44
$C_{p,w}$	Specific heat of water	44
ECHR	Evaporative cooling heat removal using sump water to cool the condenser	81
F	Correction Factor	47
FoM	Figure of Merit	58
$FoM_{Atacama}$	Figure of Merit for the Wilson solar still in the Atacama Desert	83
F_R	Heat removal factor	39
h_1	Enthalpy as read from point SP-1 on the psychrometric chart	54
h_2	Enthalpy as read from point SP-2 on the psychrometric chart	54
h_{fg}	Specific enthalpy change of vaporization	58
h_s	Saturation enthalpy	56

HD	Humidification-Dehumidification system	13
HEHR	Heat exchanger heat removal using ambient air	81
I	Solar intensity on solar collector surface	38
$LMTD$	Log Mean Temperature Difference	44
$\dot{m}_a$	Mass flow rate of the air	45
$\dot{m}_c$	Mass flow rate on the cold side	44
$\dot{m}_h$	Mass flow rate on the hot side	44
$\dot{M}_{sc}$	Potential water evaporation rate of the insolation incident on the solar collector	58
$\dot{m}_v$	Distilled water recovery rate	58
$\dot{m}_{vby}$	Liquid droplet blowby	75
$\dot{m}_{vc}$	Mist that bypassed collection and reentered the solar collector	69
$\dot{m}_w$	Mass flow rate of water	46
MSF	Multi-Stage Flash system	6
NTU	Number of Transfer Units	47
P_{amb}	Ambient Pressure	45
P_{v3}	Partial vapor pressure	53
P_{atm}	Atmospheric pressure	52
Ppm	Parts per million	11
$power_{ECHR}$	Electrical power used by the ECHR heat rejection unit	83
$power_{HEHR}$	Electrical power used by the HEHR heat rejection unit	84

$power_{water}$	Electrical power used if a large body of water is used as the heat rejection unit	84
Q	Total Heat	41
Q_a	Heat lost by the air	46
Q_{Lat}	Latent heat required to evaporate bypassed fog	69
Q_s	The expected heat collected from the solar collector	68
Q_{sen}	Actual sensible heat collected by the solar collector	68
Q_{sl}	Total heat supplied by the solar collector	68
Q_u	Useful collected heat	54
Q_w	Heat gained by the water	46
RH_{amb}	Ambient relative humidity	67
RH_1	Relative humidity in the distillation unit before the evaporative pad	70
RH_2	Relative humidity in the distillation between the evaporative pad and the condenser	70
RH_3	Relative humidity in the distillation after the condenser	70
RO	Reverse Osmosis system	10
SSS	Single Slope Still	2
$T_{a,i}$	Input Temperature of air	46
$T_{a,o}$	Output Temperature of air	46
T_{a1}	Temperature of the air entering the Distillation unit from the solar collector	54

T_{a2}	Temperature of the air between the Evaporative pad, Celdek, and the condenser	57
T_{a3}	Temperature of the air after the condenser	52
T_{amb}	Ambient Temperature	39
$T_{c,i}$	Input Temperature on the cold side	44
$T_{c,o}$	Output Temperature on the cold side	44
T_{ct1}	Water Temperature exiting a cooling tower	49
T_{ct2}	Water Temperature into the cooling tower	49
$T_{h,i}$	Input Temperature on the hot side	44
$T_{h,o}$	Output Temperature on the hot side	44
T_{in}	Arbitrary input Temperature	38
T_{out}	Arbitrary output Temperature	38
$T_{w,i}$	Input Temperature of water	46
$T_{w,o}$	Output Temperature of water	46
T_{w1}	Water Temperature from the bottom of the evaporative cooler	49
T_{w2}	Water Temperature from the returning from the condenser	49
T_{wb}	Ambient wet bulb Temperature	67
T_{2s}	Extrapolated Saturation Temperature of SP-2 on the psychrometric chart	56
T_{wbt}	Arbitrary Ambient wet bulb Temperature	49
UA	Overall heat transfer coefficient	14

U_L	Overall heat loss coefficient	39
V	Volume of ambient air	67
$\dot{V}_a$	Volumetric flow rate of air through the system	45
v_a	Velocity of the air	45

Greek:

α	The absorber absorptivity	39
ΔT	Total Temperature change	39
ΔT^*	Change in Temperature between the air through the condenser and the water in the condenser	44
ΔT_w	Change in water Temperature in the heat rejection loop	50
ε	Heat exchanger effectiveness	47
η_{ct}	Cooling tower efficiency	49
η_c	Efficiency	38
ρ_a	Density of air	45
τ	The normal glazing transmissivity	39
ω	Ambient humidity ratio	53
ω_1	Humidity ratio as read from point SP-1 on the psychrometric chart	53
ω_2	Humidity ratio as read from point SP-2 on the psychrometric chart	57
ω_3	Humidity ratio as read from point SP-3 on the psychrometric chart	53
ω_s	Saturation humidity	56

Introduction

Clean water is a valuable resource. Burgeoning human populations, pollutions in many dimensions, and diminishing resources present humanity with an array of challenges. According to UNESCO:

> "The world's population is growing by about 80 million people a year, implying increased freshwater demand of about 64 billion cubic meters a year. An estimated 90% of the 3 billion people who are expected to be added to the population by 2050 will be in developing countries, many in regions where the current population does not have sustainable access to safe drinking water and adequate sanitation [1]."

While methods exist to create clean water, they are energy intensive, high in cost, create a large amount of waste, require sophisticated technology, and require a large amount of maintenance. These wastes are slowly increasing the cost of clean water while also making it more difficult to access the technologies involved. This thesis will examine a method of creating clean water that is potentially more cost effective, uses solar energy as the primary thermal driver rather than electrical energy, can be operated and maintained by average citizens, and reduces wastewater.

Chapter 1. Literature Review and System Approach Selection

The aim of this thesis is to find or create a “low technology” system that can be built and deployed with a minimum of knowledge and a moderate skill at building. To that end, several common distillation and desalination systems and techniques were explored. Each system was considered based on several criteria. The system should be:

- Sufficiently low-tech that it can be comprehended, built, and operated by people of modest skills
- Fabricated from widely accessible materials and components
- Release minimal pollution to the environment
- Robust and require minimal maintenance
- Capable of being used in a variety of environments
- Capable of being used continuously possibly year-round
- Scalable that a system could be manufactured to meet demands

With these criteria in mind four approaches, single slope still (SSS), Multi-stage flash (MSF), Reverse Osmosis (RO), and humidification-dehumidification (HD) were seriously considered.

1. Single slope solar stills (SSS)

In 1872 Swedish engineer, Carlos Wilson, built a solar still in the Atacama Desert in Chile. “This plant can be considered to be the first industrial installation for exploitation of solar energy. For over thirty years the 4,757-m^2 Carlos Wilson plant provided drinking water for a nearby silver mine and various nitrate (saltpeter) mines. [2]” Wilson’s still used the brackish and non-potable waters of the Las

Salinas silver mine to make fresh clean drinking water. In 1972, Wilson's solar still was recreated in two locations, the first at the original site at Las Salinas and the

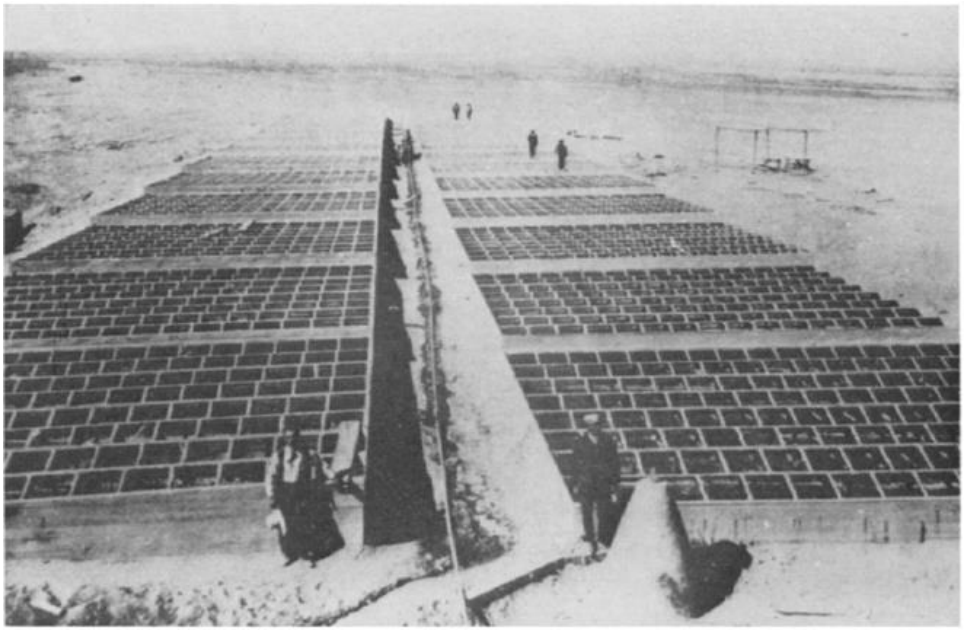

Fig. 1-1: Carlos Wilson's solar still plant in the Atacama Desert in Chile

second at the Solar Energy Laboratory at the Universidad Técnica Federico Santa Maria in Valparaiso, Chile. These recreations allowed engineers to test the output of the still. [2]

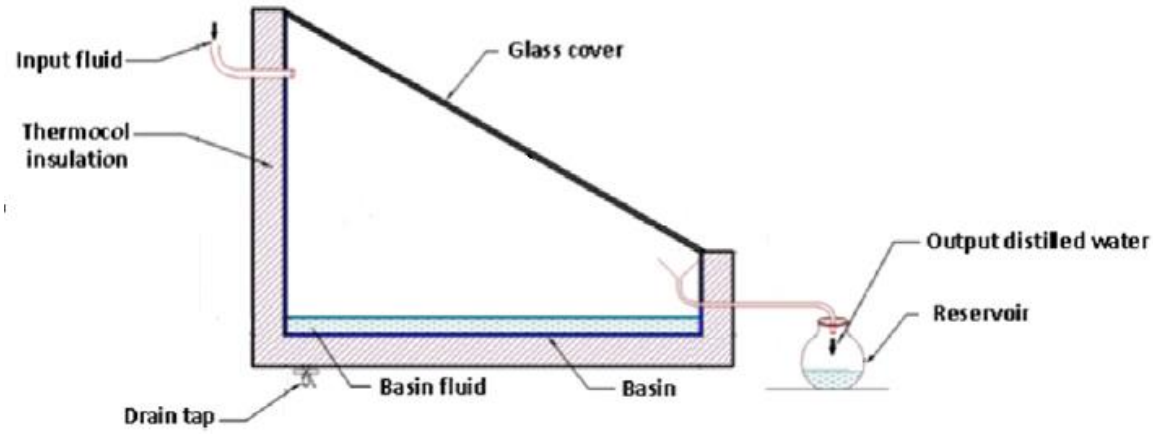

Fig. 1-2: single slope solar still

Wilson's still was not only the first industrial solar still, but it is the basis for one of the most common styles of solar still, the single slope basin still. Single slope basin stills are the most common type of small scale solar still [3].

Single slope solar stills (SSS), while easy and inexpensive to build, are characterized by exceptionally low yields of clean water per area and need to be very large to produce sufficient quantities of water. Wilson's still was ultimately able to produce about 20,000 liters of water per day, but also had a land surface area of 7896 m^2 [4]. This inefficiency in output has relegated solar distillation to be considered infeasible for large scale use in the industrialized world. Several attempts and considerations have been made to increase the efficiency of single slope stills. Many experiments focus on promoting water vaporization through various methods including using a wicking material to increase surface area, an additional internal water heater, using ultrasonic vaporizers, and using fans to create agitation in the water [3, 5, 6, 7]. Other efforts focus on the slope to promote condensation within the basin. Nanomaterials have been used to promote dropwise condensation [8]. The shape of the basin has been redesigned to increase the overall surface area while maintaining a similar or smaller footprint [9]. While most experiments do show improvements in the output, nothing has so drastically changed the amount of water per square area such that single slope solar distillation would be viable on an industrial scale. In comparison to the industry standards such as Reverse Osmosis (RO) and Multi-stage flash (MSF), solar distillation in SSS stills is exceedingly inefficient in space and output.

SSS systems are as simple as can be. There are no moving parts aside from a potential pump to fill the bottom of the tank. They are very easy to build and do not even require complex considerations for incidence to the sun. This makes SSS systems ideal for persons of modest skill to build and maintain.

SSS systems can be made of very accessible materials such as wood or sheet metals. The only potential difficulty comes from the glass pane on the slope. Glass can be difficult to work with and most often it is better to purchase an appropriately sized piece of glass and build the rest of the still around that piece. That being said, glass can be found in a wide range of sizes for very reasonable prices.

SSS systems require draw down to remove brine and contaminates but because of the low yield the brine can be returned to the general water supply without any real upset.

When properly built, the maintenance of a SSS system is very minimal. Cleaning the glass, performing draw down and on occasion removing scale build up within the box. However, if not well maintained, leaks can occur and be difficult to repair.

SSS systems require a good amount of sunlight and Temperatures above freezing but can operate in moderately extreme environments such as the Atacama Desert.

SSS systems can only be used during the day as the driving thermal energy comes from the sun. They can also only be used if the water in the still is not frozen. This limits the use of SSS systems.

SSS systems are easily scaled up as multiple stills can be built and placed in parallel to allow for easy refilling of the stills with simple plumbing. The only limitation on scalability is the amount of open area needed to place the stills. Near the equator the SSS receives approximately equal insolation throughout the year, but in Temperate latitudes the non-adjustable glass slope can have a large seasonally variable input and output. Although SSS stills are simple and amenable to amateur construction and maintenance, the intent here is to identify a better low-tech solar distillation approach. SSS stills take up an unacceptable amount of space to produce a small amount of distillate. This eliminates SSS stills as a viable candidate for consideration.

2. Multi-Stage Flash systems (MSF)

Multi-stage flash is a process which uses multiple stages of varying Temperatures and pressures to precisely control the boiling point of the water or brine passing through. Each stage uses the heat from the previous stage to bring the brine over the boiling point at the pressure in the stage. The brine is quickly

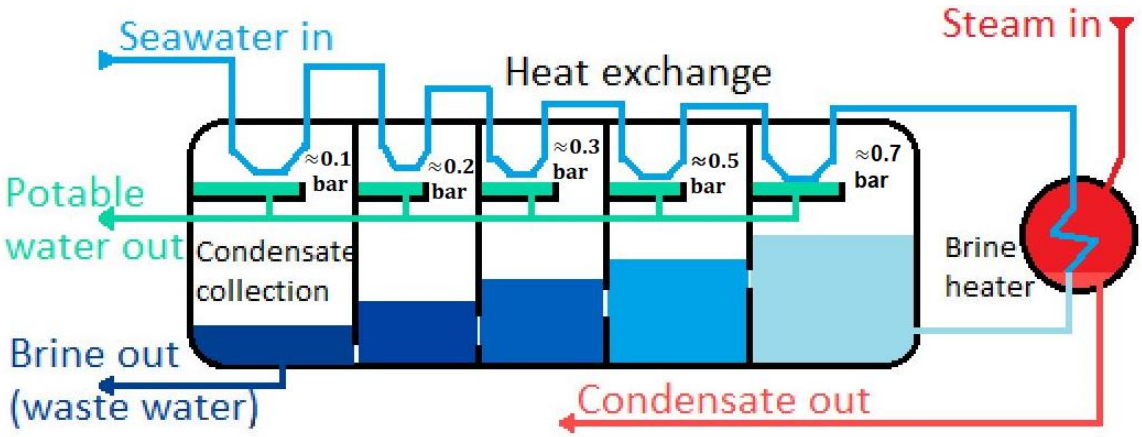

Fig. 1-3: 'Once-through' Multi-stage Flash desalination system

evaporated and condensed, using a heat exchanger, leaving clean distilled water to be siphoned off from each stage while the heat is passed to the next stage. Most MSF systems range from 10 to 30 stages; however, some industrial systems have 40 stages [8]. Typically, the output of an MSF system is between 80-85% of the input water [8,9]. MSF is a well proven and developed technology. It is ideal for desalination on a large industrial scale.

Vacuum distillation units are attractive for several reasons. In a vacuum vapor diffusion from evaporator to condenser surfaces is substantially promoted, because the large relatively heavy nitrogen and oxygen molecules that would otherwise impede diffusion are absent. Also, when air is present it is heated and cooled, to the detriment of the distillation process. In MSF systems precise vacuum is used to adjust the boiling Temperature of the water within each stage and as the water becomes more brackish and fouled in each successive stage the required vacuum is increased. This pressure control allows for substantially more stages with less Temperature drop across each stage. Even though the technology has been well developed MSF systems use a great deal of energy to control the Temperatures and pressures in each stage.

MSF systems are energy intensive systems. Requiring both thermal energy to control the required Temperature ranges, and electrical energy to control the vacuum pressures in each stage. For each cubic meter of freshwater produced MSF plants use 20-25 kWh of electrical energy [10]. To help reduce the energy load required for MSF systems, many MSF plants are integrated with power plants [9]. When MSF systems are integrated into the power plants the MSF system can

utilize the waste heat of the power plant. While MSF systems have fairly high output capacities ranging from 4000 to 30,000 m^3/day, the energy costs have made MSF less attractive in recent years. According to Nevada Energy, the cost per kWh in Northern Nevada, at the time of writing, ranges from $0.002 for large businesses to $0.56 for peak critical times.[11] These rates do not include any other charges or service fees. The standard rate for kWh will be considered to be $0.15. Using $0.15 as the cost of kWh, a cubic meter of fresh water would cost between $3.03 and $3.78 employing the vacuum-based MSF approach. Most large-scale businesses that require distilled water, such as hospitals, have on site distillation units; however, if those systems fail and distilled water needs to be purchased the cost of approximately 1 m^3 of distilled water can be upwards of $1100 [12].

MSF systems are complicated systems requiring a strong understanding of vacuum systems. The system requires a multi-stage pressure vessel or several pressure vessels that can be attached together. Each pressure camber needs to be Temperature controlled and have a heat exchanger of some type and a way to draw down the collected distillate. This makes MSF systems too complicated to be easily constructed by someone with modest general knowledge.

Pressure vessels, heat exchangers, vacuum pumps, and heating elements of the types needed for MSF systems are expensive and have very specific requirements that need to be met to ensure the system is functional and safe.

MSF systems are capable of collecting upwards of 85% of the input water as distillate. However, they also use a great deal more electrical energy as compared to other systems.

MSF systems require a good deal of maintenance to keep the pressure vessels from having any leaks. It is also important to be able to remove any scale build up in any of the chambers. This means MSF systems can require a large amount of maintenance.

MSF systems can be employed in a wide variety of environments. MSF systems are often employed in power plants to utilize the waste heat of the power plant to reduce the energy needed to heat the input water.

With the exception of routine maintenance MSF systems can be used at any time of year and any time of day. MSF systems are completely unaffected by weather conditions.

MSF systems are highly scalable, often having as many as 30 stages in each unit. Each subsequent stage uses the previous stages heat and brine with a lower pressure to distill more water from the brine.

For our considered project searching for a low technology solar distillation unit that could be fabricated and maintained by people of competent skills but not specialists, the disadvantages of vacuum systems are overwhelming. Vacuum technology is expensive to purchase and operate, vacuum containers are inherently heavy (and expensive), sealing technology is difficult for non-experts, and component replacement and maintenance are onerous. Therefore, MSF and other vacuum technology is eliminated as a candidate approach.

3. Reverse Osmosis (RO)

Reverse Osmosis uses approximately half the energy of MSF and can be made more efficient with more advanced RO systems [13]. RO is a type of membrane system which uses high pressures to force a solution through a membrane. The pressure required is called the osmotic pressure and is a thermodynamic property of a solution. For water purification the membrane must be highly permeable to water, but impermeable to any dissolved solutes within the water [14]. RO also has a lower cost for the clean water it produces. This has made RO a very popular solution for water desalination.

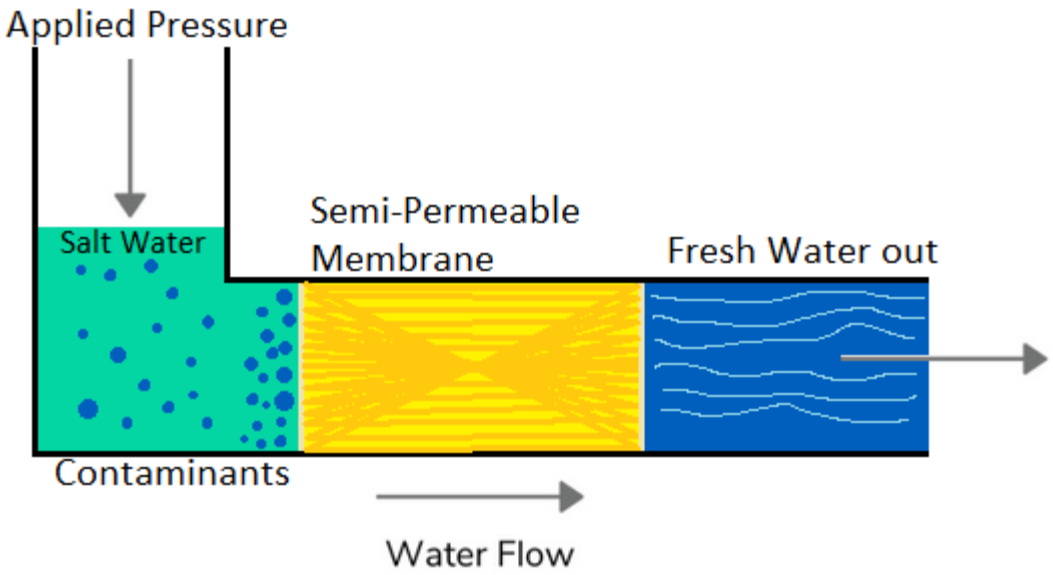

Fig. 1-4: Reverse Osmosis system

However, RO has many drawbacks as well. RO systems cannot get much more than 50% product water to feed water because there is a limit to the amount of pressure that can be used to push water through the membrane before the concentration of dissolved impurities becomes too high and the membrane becomes fouled [14]. This in turn lowers the output of the RO system. Along with

the limited output RO systems produce water with 300-400 parts per million (ppm) [of total solutes] while MSF systems produce water with <50 ppm [13]. RO systems are also not as effective at removing organic contaminates because the water is not boiled or vaporized in any way during the RO process. While organic solutes with higher molecular weights are removed, those with molecular weights less than 200 tend to be poorly rejected by the membrane [14]. There is also a potential issue with biological contamination across the membrane. This requires regular disinfection of the RO system [14].

Upon first consideration RO systems seem to be very simple and comprehendible. There is a pump or a compressor that forces water through a very fine filter. However, the simple concept becomes much more complicated upon implementation. RO systems require a fairly complex plumbing system to not only force the water through the filters in one direction but both directions to keep the filters from becoming fouled. There is also a need for bypass plumbing so that the filters can be changed out for new clean filters.

RO requires specific and costly filters that are not widely available. The pumps or compressors used in the systems are not easily obtained either. The plumbing for the system needs to be done by professionals with knowledge of RO systems to make sure everything is plumbed correctly.

RO systems produce 30-50% freshwater product from the amount of feed water put into the system. The other 50-70% of the feed water slowly accumulates the salts, impurities and contaminates contained within the feed water. This raises the level of contamination or parts per million (ppm) of the water until the pump

can no longer force the water through the filters without fouling them with the contaminates. This requires the system to be flushed periodically to lower the concentration of the feed water. The flushed out contaminates are then disposed of. After some time, the filters become fouled regardless of the system being flushed and must be replaced. While the filters can be cleaned and recycled in many cases it is not always possible and those filters are also disposed of. This means the RO system can potentially have a higher amount of pollution than other methods.

With the need to periodically flush out contaminates, and replace filters, RO systems have a moderately high need for maintenance for a moderately low output of clean water. However, when properly implemented RO systems are very robust.

RO systems only require feed water, and a place to dispose of the fouled water that cannot be filtered. This means RO systems are suitable to be used in nearly any environment or location that has access to feed water.

With the use of bypass plumbing RO systems can have routine maintenance performed on different sections of the system without interrupting the rest of the system. And because RO systems tend to be placed indoors weather has little to no effect on the system allowing it to be used year-round in most locations.

The most attractive aspect of RO systems as compared to other industry standards, such as MSF systems, is how energy efficient RO systems are. Even the largest industrial systems use about half of the energy of comparable systems like MSF. RO systems are moderately easy to scale to meet demands as the

system need only be plumbed and set up properly. Even though RO systems are energy efficient they are complicated and require expensive filters. RO is a sophisticated high-tech approach that requires specialty membranes and hardware that cannot be fabricated by amateurs. Thus, RO is eliminated from our consideration.

4. Non-Vacuum Humidification-Dehumidification (HD) System

Humidification-Dehumidification Systems, as the name suggests, use a humidifier to promote evaporation of brine or contaminated water, leaving behind the contaminates. A dehumidifier or condenser is then used to pull the clean water vapor out of the air. The air is then cycled through the system again repeating the process. HD systems can be fairly simple or moderately complex and can yield a reasonable amount of clean water.

The major advantage of HD systems is their potential simplicity. HD systems only need four main components: (1) a humidification medium, (2) an

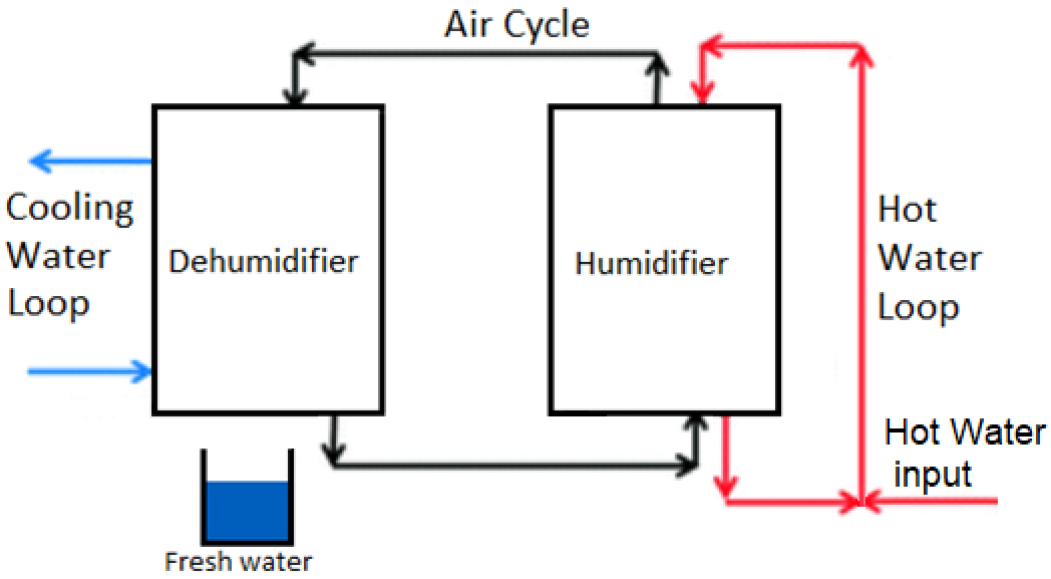

Fig. 1-5: Humidification-Dehumidification system

energy absorber, (3) pumps and blowers for mass transport, and (4) heat exchangers [15]. Humidification via evaporative coolers is a well-known technology and has many common components that are cheaply available. Solar energy can be utilized through a solar air collector, to add thermal energy to the system. The use of pumps and blowers, while vital to the system, can be minimized through thoughtful design, thus minimizing the electrical energy required by the system. A heat exchanger is needed to create a heat differential within the system, with the overall heat transfer coefficient, UA, being the most important system efficiency aspect.

While HD systems are relatively simple, the lack of more sophisticated methods are both potential advantages and disadvantages. The simplicity of the system allows for low-cost systems to be built by persons with moderate skill. With few components the HD system requires less maintenance and is flexible enough to be employed in many varied situations.

A major disadvantage of non-vacuum HD systems is the air in the system (relative to the vacuum method). Air is heated and cooled throughout the process, resulting in parasitic heat penalties in both heating and cooling components. An even bigger penalty is the air itself, which impedes the condensation process, especially in passive systems, as the larger air molecules inhibit vapor molecules from approaching the cool condenser surface. Non-vacuum multi-stage Humidification-Dehumidification distillation systems have been examined extensively including the use of solar heating to promote evaporation [16-21].

While not as simple as SSS systems, HD systems have very few complex parts and can even be built with a bare minimum of four parts, the humidifier, the condenser, the blower, and the circulating pump.

While industrial HD systems may use large and potentially costly materials, HD systems do not require large or costly materials. Since the system is so simple it can be approached in a multitude of ways. That allows for less expensive and less complex components to be used with a reasonable amount of success.

HD systems can use a variety of energy sources, including solar heat, and on the small scale only a few components require electrical power. If designed properly HD systems can utilize up to 75% of the input water and only require draw down on occasion.

HD systems exhibit a notable advantage in requiring relatively minimal maintenance. The inherent simplicity of their design contributes to reduced wear and tear. The primary maintenance tasks constitute inspections to ensure the proper functioning of the components, coupled with occasional cleaning to prevent scaling or fouling. Unlike more complex water distillation technologies, HD systems generally do not involve intricate machinery or extensive plumbing, diminishing the likelihood of frequent breakdowns. When properly maintained, these systems demonstrate robust reliability, making them appealing solutions for sustainable water production in regions facing water scarcity.

HD systems need to be mostly sealed units to prevent the loss of water vapor out of the system. This allows HD systems to be used in a wide variety of

environments without issue. With minimal maintenance requirements HD systems can be used continuously without issue.

HD systems can be scalable in a few different ways. HD systems can use multiple stages in which the cooling provided to the first stage is the heating for the second. HD systems can also be expanded by having several stills in parallel.

After carefully considering each of the four systems it was determined that an HD system would be the most reasonable to design as a low technology solution. HD systems have very few components, require little maintenance, can use solar heating, and do not require complex vacuum chambers or filters while still being capable of producing a reasonable amount of distillate. The literature for such systems did not reveal a system with simple off the shelf components for either the humidification or the dehumidification processes. Both humidification and dehumidification processes have been utilized in industrial and consumer environments. Both processes have common materials and components that are readily available for a low cost. Such an approach appears fabricable by people with average building skills using common components and tools and is therefore worth examination. For the humidification process Evaporative cooler pads and or rigid fiber resin pads can be used. Such evaporative pads are very inexpensive and readily available. Air-to-water heat exchangers are generally expensive. However, an internet search revealed that new after-market automobile radiators are relatively inexpensive. While not necessarily intended for use as a condenser, automobile radiators are intended to be highly effective heat exchangers and can be repurposed by cooling the water

being pumped through the radiator. Each stage will resemble evaporative cooler technology, and all components are readily available. Thus, this approach will be researched in this study.

For the purpose of this study, we shall be focusing on the design and construction of a system that can be easily built with off the shelf parts that are readily available, can be built by persons with modest skill, and which requires little maintenance, energy, and cost. Table 1 shows a direct comparison of each of the four systems considered.

TABLE I

COMPARISONS OF THE FOUR SYSTEMS

	Single Slope	Multi-stage Flash	Reverse Osmosis	Humidification-Dehumidification
Cost	Low	High	High	Low
Maintenance	Low	High	Very High	Medium
Energy usage	Low	High	Low	Low
Yield	Very Low	High	Medium	Low to high Dependent on application

Adapted from [22]

Chapter 2. Concept Development

After carefully considering each of the four systems it was determined that an HD system would be the most reasonable to design as a low technology solution. HD systems have very few components, require little maintenance, can use solar heating, and do not require complex vacuum chambers or filters while still being capable of producing a reasonable amount of distillate.

The HD system will need a solar air heater collector, a humidification device, a condensing device, a blower fan to promote hot air flow through the system, and two circulating pumps, one to circulate water through the humidification device and one to run the cool water loop through the condenser and the heat rejection system. The consideration of each component will be briefly discussed.

Solar Collector Selection

Since distillation depends upon Temperature differences, high Temperature solar collectors have an initial attraction. Point focusing dish collectors (or power towers with hundreds of mirrors) used for thermal power generation can produce Temperatures in excess of 1100^{o}F ~ 600^{o}C [23]. These systems require sophisticated, expensive, and delicate two-axis tracking. Such Temperatures are much too high for distillation purposes, so dish collectors are not considered for this project.

Single-axis linear concentrating trough collectors can produce Temperatures as high as 500^{o}F = 260^{o}C [24]. While such Temperatures might be useful in advanced large scale vacuum distillation systems, the complexity and expense make linear focusing collectors unsuitable for this project.

Flat plate solar collectors are bifurcated into two categories, hydronic (liquid working fluid) collectors and air heaters. Either would be suitable for low Temperature solar distillation. But most hydronic solar collectors are factory fabricated and very expensive (even with some government rebates), which is why there are so few solar heating systems in solar rich states such as Nevada. Liquid-filled solar collector fabrication generally requires expert welding skills. And many factory-fabricated collectors leak after a few years in the field. Furthermore, in many climates there is the risk of losing the collector to freezing.

There are many advantages to solar air heaters. There is no liquid to leak, freeze, overpressure (boil), corrode, or degrade. Factory manufactured air collectors are also expensive by the time they get to the consumer due to shipping, storage, commissions, etc. However, site-built solar air heaters can be built inexpensively from commonly available materials by people of modest skills and are the solar collectors best suited for this project [25, 26, 27]. Construction details are provided in the above references. A study done at the Desert Research Institute found site built solar collectors have a much greater economic efficiency than commercially purchased collectors [28].

Advantages claimed for a site-built air heating solar collector over hydronic (liquid filled) collectors include: (1) Cost; (2) Small leaks are unimportant; (3) Hydronic systems can over-pressure in summer; (4) Freeze problems eliminated; (5) economic efficiency higher; (6) can be built by skilled laymen; (7) maintenance, if necessary, can be provided by the owner; and (8) money for construction stays in the local community, instead of supporting foreign economies.

Humidifier

The humidifier will use the heat generated from the solar collector to evaporate water. Several different humidifiers were considered. Since we are searching for a low tech and accessible component, existing evaporative technology was of particular interest. Evaporative coolers use several different types of evaporative media including rigid cellulose or fiber resin pads (commonly called Celdek), corrugated PVC, organic fibers such as aspen and coconut, and even some porous stones and ceramics. While each type of evaporative media has particular advantages, they all share some key features. “The most studied performance parameters of DEC [Direct Evaporative Cooling] pads are the saturation effectiveness, pressure drop, humidity increase, water evaporation, Temperature drop, cooling capacity, Coefficient of Performance (COP), and the heat and mass transfer coefficients [29].”

After careful consideration, a 4-inch thick Celdek pad was chosen to be the humidification medium. Celdek is inexpensive and readily available in various sizes. The Celdek has a good saturation effectiveness, a low pressure drop, a large amount of water to air surface area, and good heat and mass transfer coefficients [29]. Since the Celdek is a rigid medium there was no need to create a support structure to hold the Celdek in position. After some preliminary tests, sheets of acrylic were used to better direct water flow through the Celdek.

Condensing Heat Exchanger

The condensing heat exchanger was initially considered the most significant component in the system. Typically, condensers are large and

expensive making them not ideal for the application of a low technology distillation system. As a part of the consideration, heat exchanger characteristics and flowrates were developed to verify that a chosen heat exchanger would be adequate for the application.

The solar distillation approach has evolved to a system where saturated air will be blown through a compact heat exchanger which is cooled by water from an outside source. As the air Temperature falls, water vapor within the air will be condensed and the liquid collected.

With certain numerical characteristics developed and considered, the choice of heat exchanger can be matched to those characteristics. We found that after-market car radiators were a cost-effective and easily available solution.

Blower Fan and Circulating Pumps

The blower fan and circulating pumps will need to be sized appropriately for the application. They will also need to be fairly commonplace and accessible to achieve the low tech and accessible requirements.

The circulating pump will need to be able to pump water up to the top of the Celdek which will most likely be about two feet tall. Pumps can be very expensive and complicated. Small fountain pumps or fish tank pumps are very simple submersible pumps that can potentially provide the needed flow rate and head. Fountain pumps are smaller and less expensive than fish tank pumps, but they also tend to have much lower flow rates and head. So then, a submersible fish tank pump will be the best bet.

The blower fan will need to be capable of blowing air through the solar collector, the Celdek (which should be saturated), and the condensing heat exchanger. Since none of these components have a high pressure drop across them the blower fan will not need to have a high static pressure to be able to move the air, thus the focus will be on maximizing air flow through the system.

The considered system featuring all the components is depicted in Figure 2-1; the blower and pumps are not shown, nor is insulation. The solar collector angle of tilt can be seasonally adjusted.

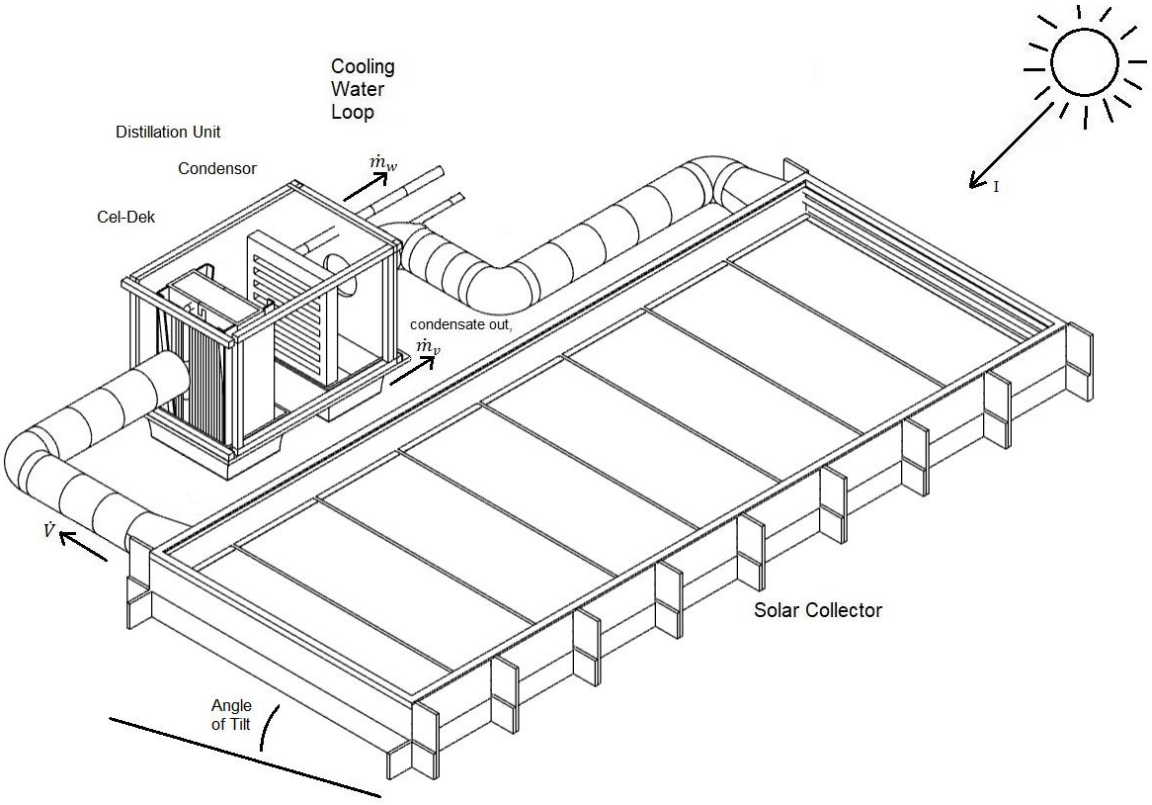

Fig. 2-1: Basic design of the system using the described components

Chapter 3. Building The System

The design of the proposed humidification-dehumidification, HD, system has three main components: 1) the solar heat collector, 2) the distillation unit, and 3) the heat rejection units. Each component was fabricated at a personal workshop and then transported to the Desert Research Institute, DRI, for testing of the system. This chapter will briefly discuss the build process for each component.

Solar air collector

The solar collector was made primarily of metal components. The base of the collector was a four-foot by ten-foot 18-gauge sheet of galvanized steel. The side walls were made of six-inch aluminum c-channel wall studs. Inside the collector there are five layers of aluminum bug screen. Aluminum screen was

Fig. 3-1: The completed solar collector in the workshop.

chosen for its thermal conductivity of $237\frac{W}{m\,K}$ or $137\frac{BTU}{ft\,h\,°F}$ which is orders of magnitude larger than fiberglass's $0.045\frac{W}{m\,K}$ or $0.026\frac{BTU}{ft\,h\,°F}$. The glazing was held on to the collector by one-inch square dowel on the inside of the collector and topped with one-inch by 1.25-inch boards.

To attach the c-channel side walls to the steel sheet self-tapping metal screws were drilled into the bottom of the c-channel and up through the steel sheet in each corner. Then pop rivets were utilized every six-inches to secure the steel sheet to the c-channels. Scrap pieces of c-channel were used to cover any gaps in the corners and then the entire base between the steel sheet and c-channels were sealed with high Temperature sealant. Then the inside of the collector was painted black with high Temperature paint. Two holes were cut into the side of the c-channel on one of the long sides of the collector to accommodate two eight-inch by four-inch register boxes that can be used to connect the collector to the

Fig. 3-2: a) The pop riveted steel sheet and c-channel (b) The inside of the collector painted with high Temperature black paint

distillation unit via six-inch ducting. Two 1-inch by 1.25-inch cross beams were also screwed in just under the top lip of the c-channel to help with rigidity. The cross beams were covered in reflective tape to avoid absorbing heat.

Fig. 3-3: a) Aluminum angle cut into "fingers." (b) "Fingers" three and five holding conduit (c) "Fingers" two, four, and five holding conduit

A 1/16-inch thick by 1-inch high by 3-foot Long Mill Finished Aluminum Solid Angle was cut to five-inch lengths. Notches were cut out on one side of the angle to create five “fingers” approximately half an inch in width. These “fingers were placed in each of the four corners and were used to hold ¾ inch aluminum conduit. On one side “fingers” three and five (starting from the bottom) held conduit and on the other side “fingers” two, four, and five held conduit. Then the “fingers” were

held into place with two self-tapping metal screws, this allowed the conduit to roll in place. Aluminum bug screen was placed in the bottom of the collector. The screen was attached to the base of the collector using a three-foot length of aluminum angle. The screen was then wrapped over the top of the aluminum angle and across to the conduit. The screen was wrapped around the conduit and layered back and forth five times. Until being affixed to the side wall using a one-inch square dowel. When the screen was pulled tight it separated each layer of screen by ¾ of an inch, which is the outer diameter of the conduit, allowing air to flow through each layer unimpeded. 1-inch square dowels were then screwed into the sidewall of the c-channel just underneath the top lip of the c-channel. Foam insulation tape was then placed on top of the top lip of the c-channel. The glazing was then laid on top of the collector and affixed by one-inch by 1.25-inch boards to the panel using screws.

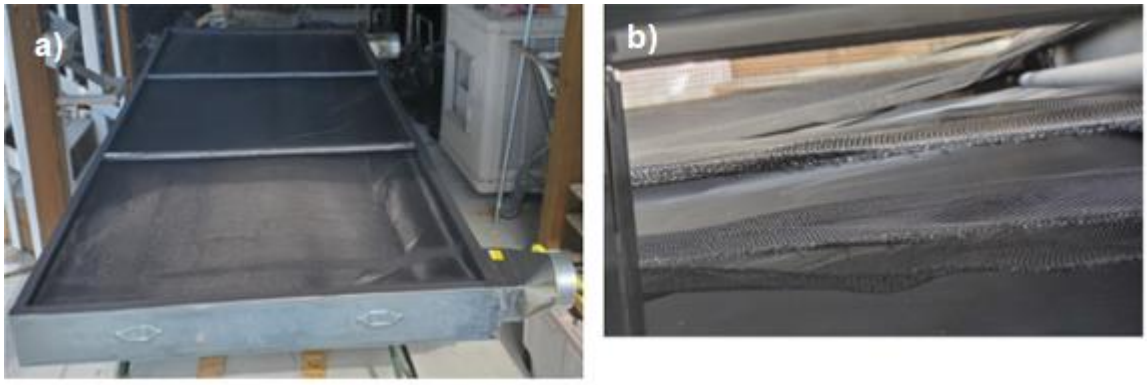

Fig. 3-4: a) The aluminum screen layered in the collector (b) the five layers of the screen before being pulled tight.

A frame was constructed using half-inch thick, four-inch wide OSB, oriented strand board, siding boards. The frame was used to attach fiber-glass insulation to the collector as well as helping to hold the collector at a reasonable angle. Chicken

wire fencing was attached to the bottom of the frame to assist in holding fiber glass insulation. Two automobile jack stands were used to hold up one side of the frame such that the collector was at an optimal angle to the sun.

Fig. 3-5: a) The frame (b) The completed collector on the frame and insulated.

This frame was built with materials that were already on hand to keep costs low. It was not intended to be a permanent fixture and was only used during testing of the system. A more robust frame should be built for a more permanent installation.

Distillation unit

The distillation unit was made from 5/8-inch thick OSB board. The inside was coated with waterproof Flex Seal paint. Two Sterlite plastic bins served as water receptacles. Resin infused Fiber, Celdek, was used as the humidification material. A Honda Civic 3-row 60mm Radiator was used as the condenser for dehumidification.

The box walls were cut to size and 1-inch square dowels were screwed to the outside of each wall to provide better locations for screws. The bottom and top were cut to a larger size to accommodate the walls having the 1-inch dowels. The bottom then had two holes cut into it in which to place the Sterlite bins. Since the bins were hanging out the bottom a stand was built to hold the distillation unit off the ground. Three holes were cut into one side and acrylic was fixed over each hole to act as windows into the box.

Acrylic sheets were used to support the Celdek and direct water flow. In lieu of a distribution pad a 3-d printed casing was placed on top of the Celdek to contain and distribute the water evenly across the Celdek. This 3d print better directed the water and did not allow splashing. A piece of acrylic with evenly spaced holes drilled in it was placed on top of the Celdek to evenly distribute the water throughout. A water pump was placed in the Sterlite bin that contained the Celdek to recirculate the water through the top of the Celdek. A splash guard was placed

Fig. 3-6: Inside of the completed distillation unit

at the edge of the Sterlite bin to keep fouled or dirty water from splashing across to the clean water bin. The Celdek and acrylic were held in place by two pieces of cut Styrofoam lightly compressed between the acrylic and the wall on each side.

A piece of angle aluminum was cut to the width of the box and placed on top of the condensing Sterlite bin. The condenser was placed on top of the piece of angle aluminum. The condenser was angled forward approximately 5 degrees, over the bin, to promote flow of condensation into the Sterlite bin. The condenser was then plumbed up with a rubber hose for the input and output each rubber hose

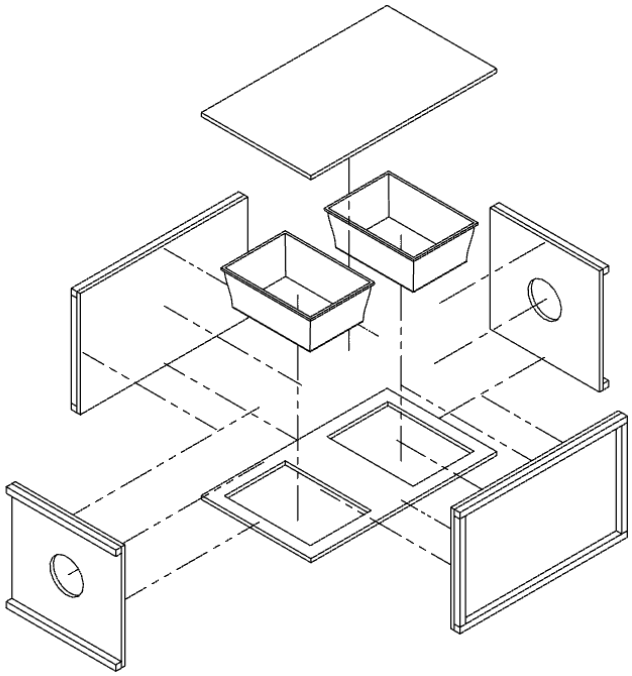

Fig. 3-7: schematic of the distillation box

was attached to a reducing coupler to a ¾ inch plastic tubing. Holes were drilled in the top and bottom of the short side of the box to accommodate the tubing. A piece of acrylic was attached to the bottom of the condenser with construction adhesive to stop any splashing from the Celdek from entering the clean water bin. During testing a plastic sheet was placed vertically between the Celdek and the condenser

to stop any blow through water from hitting the condenser and contaminating the clean water bin. The box was built to be as small as possible to minimize the air gap between the Celdek and the condenser and thus minimize the number of obstructions to the vapor.

The blower fan was bolted to the side of the unit such that it would draw air out of the box and blow it into the solar collector via ducting. The opposite side had a six-inch starting collar attached and ducting from the outlet of the solar collector was then connected making it a closed loop. A piece of plastic was attached to the starting collar to act as a diffuser for the inlet airflow.

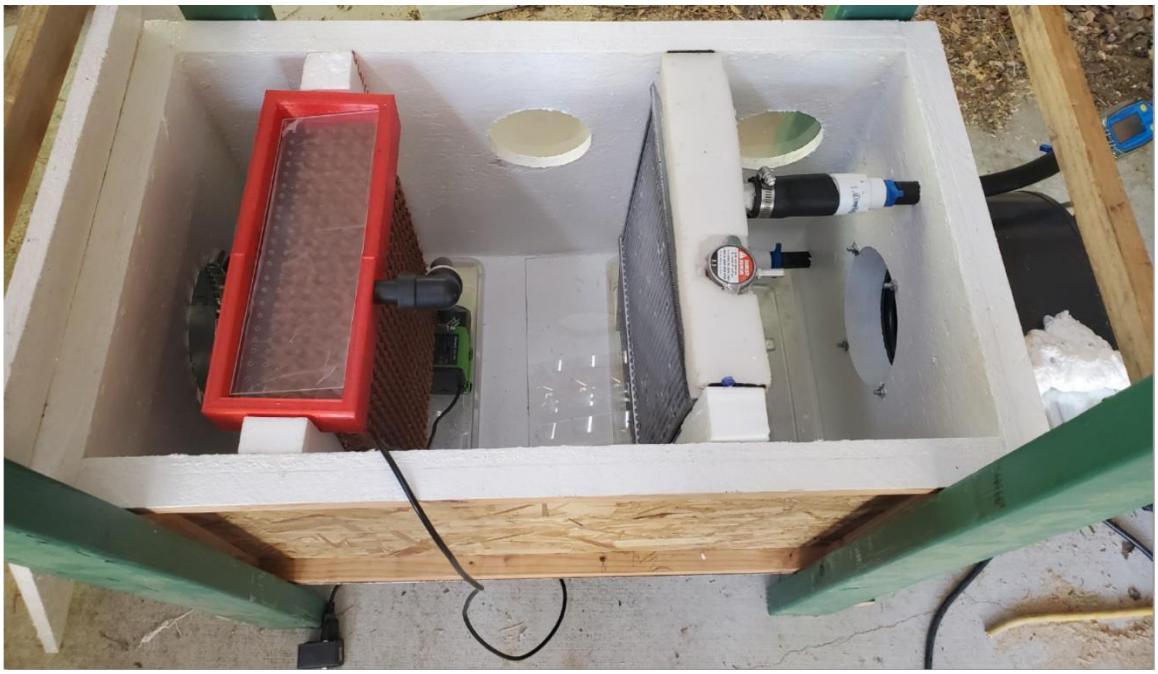

Fig. 3-8: Test fitting the components in the box.

Four small holes were drilled into the side opposite the windows and two small holes were drilled into the inlet side to allow wiring to connect six DHT-22 humidity sensors in the box to an Arduino controller board. Each set of two sensors were placed into each section of the distillation unit, the inlet before the Celdek,

the middle between the Celdek and the condenser, and at the outlet after the condenser. The sensers were calibrated using the saltwater method, which is using the saturation condition of Sodium Chloride to create a humidity of 75% in a sealed container. Thermocouples were also placed in each section to verify and support the humidity sensors.

The top rim of the box was covered with insulation tape and the top was attached to the box by using two spring clamps on each side. A hole was drilled into the bottom of the side of the box to allow for the Celdek water bin to be refilled while the system was running, and a hose was attached to the bottom of the distillate bin allowing for water to be drained out and tested for purity. Rigid insulation was placed on each side of the box to better contain the heat.

Fig. 3-9: Outside of the distillation unit during testing

Heat rejection units

The first of the two heat rejection units was an evaporative cooler and only required plumbing the pump into the system (see Figure 4-1). The second unit, which replaced the evaporative cooler for a second set of testing, was a heat exchanger and blower fan, with cooling derived from the ambient air (see Figure 5-2).

Fig. 3-10: The heat exchanger being placed into the box with closed cell foam.

A second car radiator and blower fan were used to build the heat exchanger side of the cooling unit. A box was built to tightly hold the heat exchanger in the middle and the blower fan was attached to the back side of the box to blow air through the heat exchanger. The heat exchanger was held in place and sealed against the sides of the box using closed cell foam. A pump was placed in a bucket below the box and plumbed up into the heat exchanger inlet. The outlet of the heat

exchanger was plumbed to the inlet of the condenser in the distillation unit. The outlet of the condenser was placed into the bucket containing the pump closing the loop.

Fig. 3-11: blower fan attached to the outside of the heat exchanger box.

System monitoring and data collection

Several data sets were collected during testing: ambient Temperature, outside relative humidity, insolation incident on the collector, flow rate in heat rejection loop, the water Temperature in the bottom of the evaporative cooler, water Temperature exiting the condenser, the Temperature in each section of the distillation unit, the relative humidity in each section, the velocity of the air through the outlet duct, and total water produced. All data were collected every half hour throughout each day of testing. Where possible multiple sensors or devices were used to check data validity.

The ambient Temperature and outside relative humidity were taken from a small hygrometer and verified with local weather data. The insolation, I, was taken using a Fluke IRR1 Solar Irradiance Meter that was fixed to the top frame of the solar collector. The flow rate into the condenser was measured using a one-inch inline digital flow meter. All Temperatures were measured using k-type thermocouples connected to two Danoplus 4 channel thermometers. The water Temperature was measured in the basin of the evaporative cooler, and in the outlet tubing from the condenser. The DHT-22 humidity sensors also measured the Temperature in each section of the distillation unit. The Temperatures from the DHT-22 sensors were verified using a thermocouple in each section of the unit. The humidity sensors were connected to an Arduino Mega control board which was programmed to pole each sensor every two seconds. Readings of the sensor data were taken for one minute every half hour. Each section of the distillation unit had two humidity sensors to verify readings. The air velocity in the duct was measured using a handheld anemometer. The air velocity was measured at several different points across the cross-sectional area and the readings were averaged. The total water collected was measured in the distillation bin. The water was drained and tested for purity using a Total Dissolved Solids (TDS) Digital Meter.

The completed system

The system was made up of three loops, the wetting loop, the air heating loop, and the heat rejection loop. For the heat rejection loop, the system was initially set up with the evaporative cooler as the heat rejection unit. The pump for

the evaporative cooler was plumbed into the condenser inside the distillation unit and the outlet of the condenser was plumbed to the top of the three evaporative pads in the cooler.

For the air heating loop, the blower motor was attached to the distillation unit such that it would draw air out of the distillation unit and the outlet of the blower was connected to the solar collector via insulated ducting. The outlet of the solar collector was connected via insulated ducting back into the inlet of the distillation unit. The solar collector was angled up to approximately $33°$ to be incident to the sun at noon.

The wetting loop was entirely Inside the distillation unit. The Celdek sat in the “dirty” water bin with a circulating pump used to keep the Celdek wet. Hot air from the solar collector was drawn across the Celdek promoting evaporation of the water flowing through the Celdek. The water vapor was then drawn across the condenser and the clean water ran down into the distillate bin.

During the second set of testing, on October 6, 7, and 8, the evaporative cooler was replaced with the heat exchanger and blower fan. The rest of the system was unchanged. The pump from the evaporative cooler was removed and placed in a 5-gallon bucket and plumbed up to the condenser inlet. The condenser was plumbed to the heat exchanger and the heat exchanger outlet went back into the bucket.

The entire system was placed on a concrete slab at DRI with the solar collector facing due south. The distillation unit was placed directly behind the solar collector to easily connect the ducting between the two units. The heat rejection

unit was then placed next to the distillation unit to easily connect the pump to the condenser. See Figure 3-12, which was taken after data collection was complete and a storm had savaged the insulation.

Fig. 3-12: a) The completed system using the evaporative cooler.
b) the completed system using the heat exchanger

Chapter 4. System Modelling

In Chapter 2, the considered system was developed. Figure 4-1 depicts the three-component system consisting of a: (1) solar air heater; (2) distillation unit; and (3) heat rejection system. Here a mathematical model is developed to estimate how the system will perform. This model will be used to systematically reduce collected data in Chapter 5. Using collected data from system testing, some of the variables are assigned numerical values for the observed conditions.

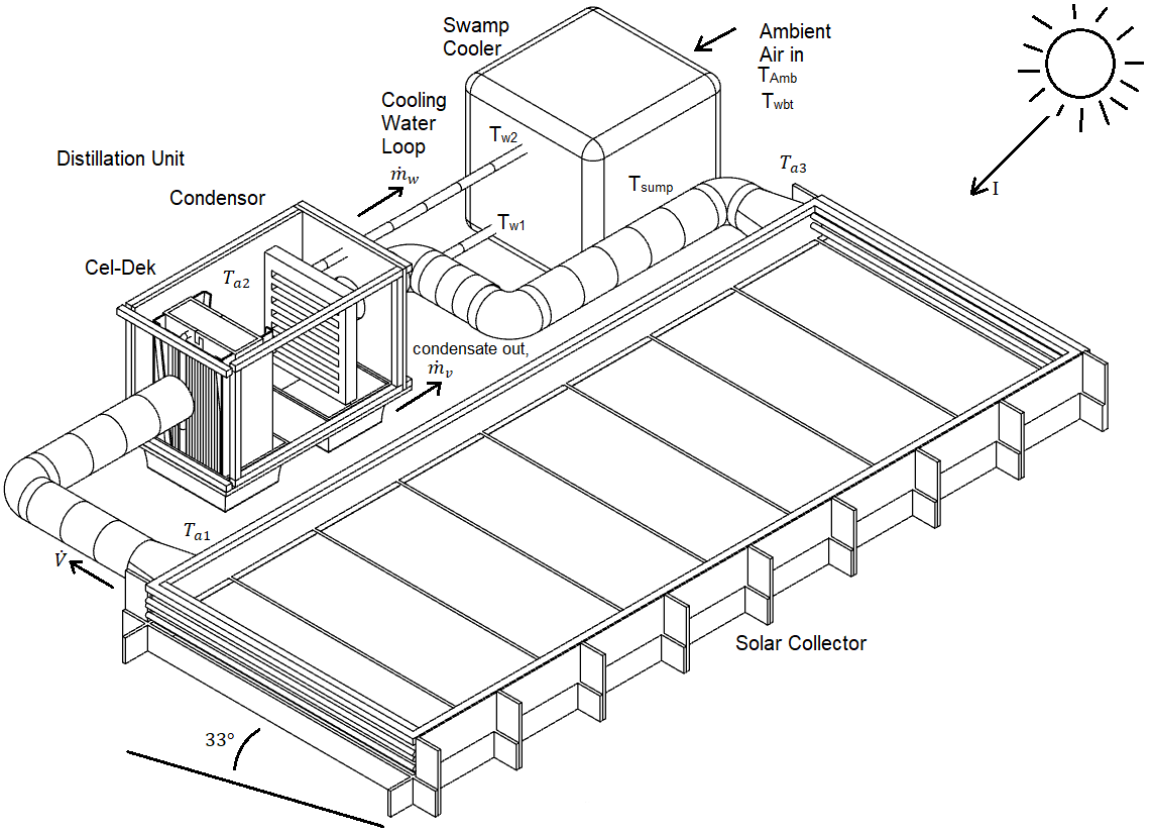

Fig. 4-1: Schematic of the three-component system

For system testing, a solar collector was oriented due south and inclined at 33° from horizontal. The collector was set on September 7th at solar noon (when

the sun was 33° from zenith) to maximize solar gain during the coming system testing period.

1. Solar Collector Efficiency

A series of tests with the collector stand-alone were conducted on July 20, 2023, to determine the solar collector efficiency, η_c, defined as:

$$\eta_c = \frac{Heat\ Obtained}{Insolation\ incident\ on\ collector} = \frac{\dot{m}_a C_p (T_{out} - T_{in})}{IA_c}$$

Where:

$\dot{m}_a$ = mass flow rate of the air

C_p = specific heat

I = Solar intensity on solar collector surface

A_c = useable area of the solar collector

Although the collector nominal size is 4' by 10', the actual useful glazed area (due to battens on the edges) is $A_c = 37.1\ ft^2$. The specific heat of the dry air within the system can be calculated by:

$$C_p = (0.24 + 0.4347H)\frac{BTU}{lb_m\ °F}$$

Where H, is the absolute humidity.

Absolute humidity is the ratio of the mass of water in the air per mass of dry air. Thus, when the air is at atmospheric pressure and the humidity is low the specific heat can be considered a constant of $C_p = 0.24\frac{BTU}{lb_m\ °F}$. Air at different Temperatures was introduced to the collector intake, measured at $\dot{V}_a = 400\ cfm$.

The useful collected heat Q_u and η_c are:

$$Q_u = A_c F_R[\tau\alpha I - U_L(T_{in} - T_{amb})] \quad \frac{BTU}{hr} or\ Watts \tag{1}$$

and

$$\eta_c = \frac{Q_u}{IA_c} = F_R\left[\tau\alpha - U_L\frac{(T_{in} - T_{amb})}{I}\right] \tag{2}$$

Where:

τ = The normal glazing transmissivity

α = The absorber absorptivity

F_R = heat removal factor

U_L = overall heat loss coefficient

The standard way to analyze flat plate solar collector data is to plot η_c versus $\frac{\Delta T}{I}$, which generally gives a downward sloping straight line, Equation 2 [30].

Figure 4-2 shows the data points collected on July 20, 2023, and a best fit linear curve as calculated by Excel is imposed over the data. The ordinate is $\eta_c = 0.80$ and the abscissa is $c = 0.41$, so the slope is the heat removal factor times the overall heat loss coefficient $F_R U_L = -1.95\frac{hr\ ft^2\ °F}{BTU}$. This information allows determination of important operating characteristics of the collector. The ordinate value $\eta_c = \tau\alpha F_R = 0.8$. The normal glazing transmissivity, τ, is estimated by measuring the insolation with a Fluke brand solar meter, then placing the glazing between the sun and solar meter, and again measuring the (diminished) insolation and taking the ratio of the two measurements. A group of 8 closely bunched transmissivity readings averaged at τ = 0.856, which validates the manufacturer's

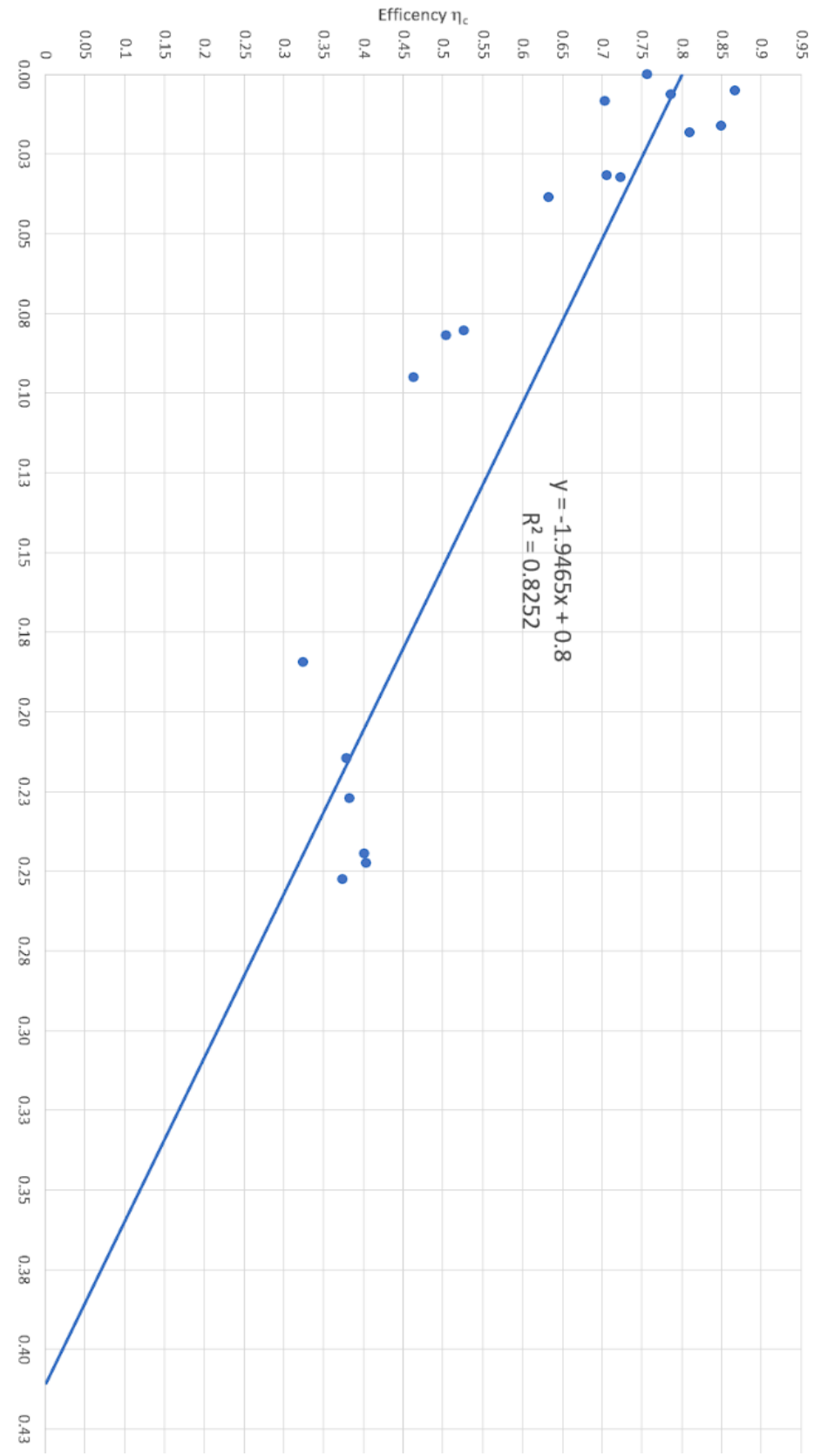

Fig. 4-2: Solar Air Heater Test Data Points with Best Fit Curve

published value of τ = 0.86, which value shall be used henceforth. The absorber absorptivity, α, is expected to be quite high because the 5-screen absorber arrangement traps insolation, and higher placed screen levels intercept radiation from lower screen levels. The heat removal factor F_R is also high, because the screens with their numerous holes provide a large surface area for the absorbed sunlight to be released to the turbulent air flowing over the screens. The product of $\alpha F_R = \frac{0.8}{0.86} = 0.93$, so both α and F_R (whose values are each less than 1.0) are quite high ($\cong \sqrt{0.93} = 0.965$). A good estimate of each, within a few percent is then $\underline{F_R = 0.965}$ and $\underline{\alpha = 0.965}$.

A high value of the heat removal factor, F_R, is important for efficient solar collector operation, because it indicates most of the insolation captured by the absorber is usefully released heat, Q, to the air working fluid, rather than being radiated or reflected to or through the glazing. The necessity for high F_R is seen from the equation for useful heat gain, given by Equation (1).

The negative slope of the curve in Figure 4-2 is the product $F_R U_L = 1.95 \frac{BTU}{hr\ ft^2\ °F} = 11.1 \frac{Watt}{m^2\ °C}$. Then $U_L = \frac{F_R U_L}{F_R} = \frac{1.95}{0.965} = U_L = 2.02 \frac{BTU}{hr\ ft^2\ °F}$. A low value of overall heat loss, U_L, is desirable, because it indicates less heat will be lost from the collector sides, bottom, and top glazing, which motivates good side and bottom insulation. Thus η_c is established to be:

$$\eta_c = 0.80 - 1.95 \frac{(T_{in} - T_{amb})}{I} \qquad (3)$$

2. Distillation Unit

The still consists of two components mounted in a box, so solar heated air must flow first through the humidifier, and then through the condenser heat exchanger, as shown in Figure 4-1. The construction details are presented in Chapter 3. At State Point 1, SP-1, the hot air from the collector passes through the Celdek (aka Munters-fill) moistening pad, it evaporates water flowing down through the Celdek, cooling the air, and increasing the humidity ratio SP-2. Since this is an adiabatic process, on a psychrometric chart the process line follows the upward-left line of constant enthalpy toward the saturation line. The “approach” is defined as the distance between SP-1 and SP-2 divided by the distance between SP-1 and the intersection of the enthalpy line and saturation curve, as can be seen in Figure 4-3. The Munters-fill wetting pad, used in newer home evaporative coolers, was selected because of its high wetting efficiency, or high approach. The system test data from the September runs generally manifested a 95% approach, which is consistent with information from the literature [29]. The moistened air then flows through an air-to-water heat exchanger where it is cooled, causing water to condense on the heat exchanger surface, after which the condensate drops down to a collection bucket. The condenser-heat exchanger is water-cooled by water from the heat rejection system; see Figure 4-1.

While we believed the UA of a car radiator would be suitable for our application, we found that in general UA is not a listed or commonly available specification for car radiators. So, a testing protocol was developed to validate the UA of such a radiator. The specific heat exchanger is a crossflow car radiator. This

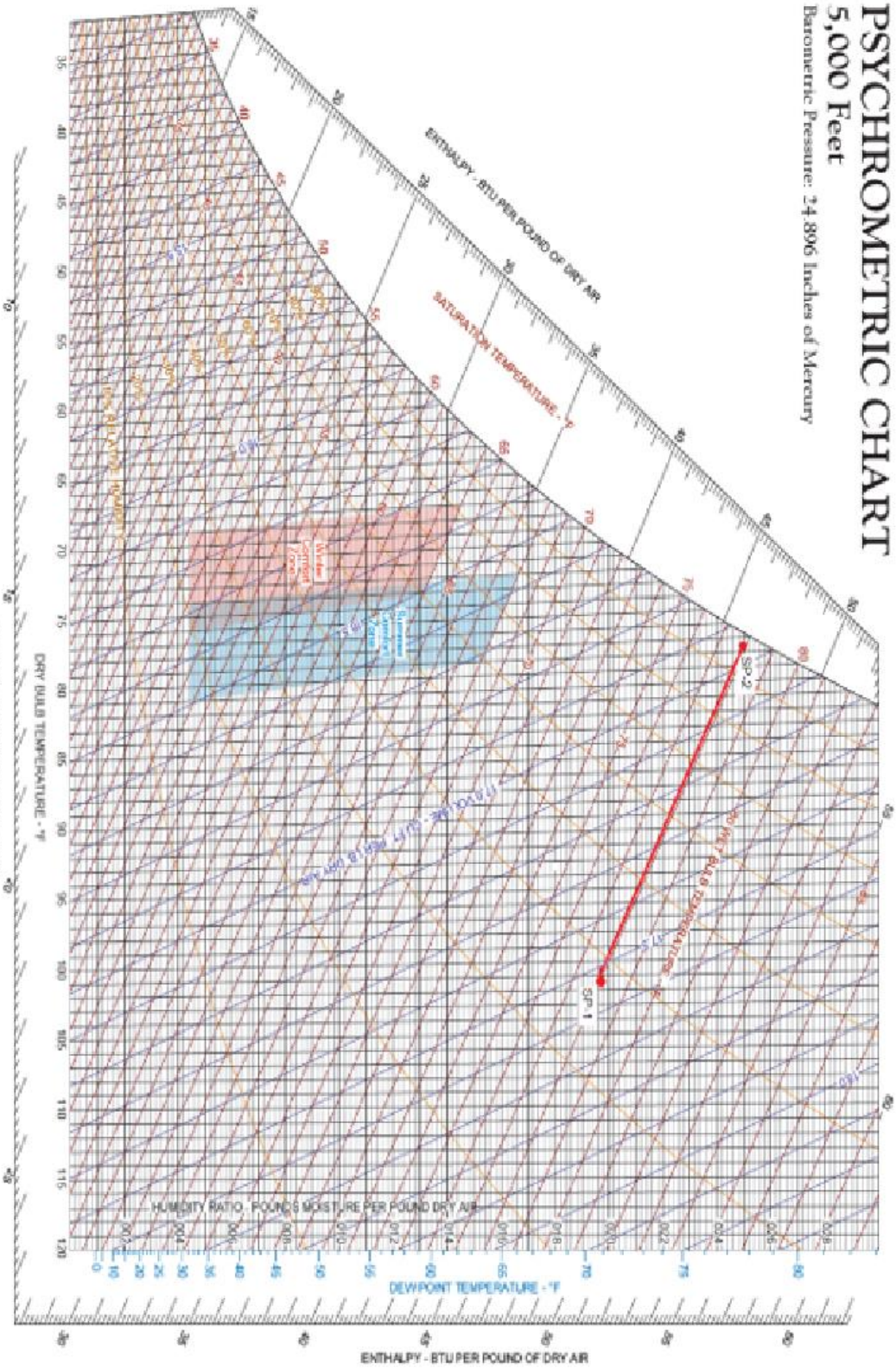

Fig. 4-3: 5000 ft. Elevation Psychrometric chart showing points SP-1 and SP-2 For data collected on September 15, 2023 at 1 pm [31]

is important as it may require a correction factor. For a known quantity of heat, Q, the overall heat transfer coefficient, UA, is:

$$UA = \frac{Q}{LMTD}$$

Where, $LMTD$ is the log mean Temperature difference. And:

$$LMTD = \frac{\Delta T_2 - \Delta T_1}{\ln\left(\frac{\Delta T_2}{\Delta T_1}\right)}$$

Each fluid in the heat exchanger then can be characterized by:

$$Q = \dot{m}_h C_{p,h}(T_{h,i} - T_{h,o})$$

$$Q = \dot{m}_c C_{p,c}(T_{c,i} - T_{c,o})$$

Where the h and c subscripts are hot and cold respectively, and the i and o subscripts are the in and out sides, respectively. So then,

$$Q = \dot{m}_h C_{p,h}\left(T_{h,i} - T_{h,o}\right) = \dot{m}_c C_{p,c}(T_{c,i} - T_{c,o})$$

For our specific purposes, the hot side will be air and the cold side will be water. The mass flow rate of the air will be the density times the velocity times the area.

$$Q = \rho_a V_a A C_{p,a}\left(T_{a,i} - T_{a,o}\right) = \dot{m}_w C_{p,w}(T_{w,i} - T_{w,o})$$

We can then find the UA of the heat exchanger by measuring the in and out Temperatures and flow rates for both the water and air. Using that data, we can find the log mean Temperature difference and then use either the water or air side to replace Q giving either:

$$UA = \frac{\dot{m}_w C_{p,w}(T_{w,i} - T_{w,o})}{LMTD}$$

Or

$$UA = \frac{\rho_a V_a A C_{p,a}\left(T_{a,i} - T_{a,o}\right)}{LMTD}$$

For the physical testing, the heat exchanger was placed in a box such that the air flow across the exchanger could be measured, relatively easily. A blower fan was used to blow air into the box and through the exchanger. The water flow was measured using an inline flow meter in the pump line. The pump was placed in the bottom of a five-gallon bucket and the water was pumped through the exchanger and into a second five-gallon bucket so the Temperature change in the water from the heat exchanger could be measured.

The condenser heat exchanger was tested by itself on July 18, 2023, with heat being supplied by the solar collector. The day was mostly sunny, but there were intermittent clouds. The air pressure remained steady at $P_{amb} = 25.7\ in\ Hg = 653\ mm\ Hg = 12.63\ psi$. The ambient air Temperature was $T_{amb} = 93°F$ to $94°F$ throughout the testing period. The pump delivered a steady $5.0\ gpm = 2500\frac{lb}{hr}$ of water through the heat exchanger. A handheld anemometer at the blower outlet consistently measured $v_a = 1500\frac{ft}{min}$ over a 6" diameter outlet, so:

$$\rho_a = \frac{P}{RT} = \frac{12.63\frac{lb_m}{in^2}}{\left(0.3704\ \frac{psi \cdot ft^3}{lb_m \cdot °R}\right)(460 + 94°R)} = 0.062\frac{lb_m}{ft^3} \qquad Air\ Density$$

$$\dot{V}_a = \left(1500\frac{ft}{min.}\right)\left[\pi\left(\frac{3}{12\ ft}\right)^2\right] = 295\ cfm \qquad Air\ Volumetric\ Flowrate$$

$$\dot{m}_a = \rho_a \dot{V}_a = \left(0.062\frac{lb_m}{ft^3}\right)\left(295\frac{ft^3}{min}\right) = 18.3\frac{lb_m}{min} = 1095\frac{lb_m}{hr} \quad Air\ Mass\ Flowrate$$

Nine measurements were taken over an hour and twenty-minute period, from 12:11 pm to 1:33 pm. The raw data are presented in Appendix B. With occasional cloud passage it was necessary to allow the solar input to reach steady state.

Run 2, taken at 12:20 pm, is typical and bears scrutiny.

$T_{a,i} \quad = 111.3°F$

$T_{a,o} \quad = 74.3°F$

$T_{w,i} \quad = 69.0°F$

$T_{w,o} \quad = 73.1°F$

$$\dot{m}_a C_p = \left(1095 \frac{lb_m}{hr}\right)\left(0.24 \frac{BTU}{lb_m\,°F}\right) = 263 \frac{BTU}{hr\,°F} \qquad Air\ flow\ heat\ capacity$$

$$\dot{m}_w C_p = \left(2500 \frac{lb_m}{hr}\right)\left(1.0 \frac{BTU}{lb_m\,°F}\right) = 2500 \frac{BTU}{hr\,°F} \qquad Water\ flow\ heat\ capacity$$

Clearly the water flow dominates the heat transfer properties in the heat exchanger for this run. In the solar still application this is desirable, as it keeps the Temperatures throughout the system low, increasing heat gained by the solar collector.

The heat lost by the air and delivered to the water is:

$$Q_a = \dot{m}_a C_{pa}\left(T_{a,i} - T_{a,o}\right) = \left(263 \frac{BTU}{hr\,°F}\right)(111.3 - 74.3\,°F) = 9731 \frac{BTU}{hr}$$

The heat gained by the water, Q_w, should equal Q_a:

$$Q_w = \dot{m}_w C_p\left(T_{w,o} - T_{w,i}\right) = \left(2500 \frac{BTU}{hr\,°F}\right)(73.1 - 69\,°F) = 10{,}250 \frac{BTU}{hr}$$

These two values are within $\frac{10{,}250-9731}{10{,}000} = 5.2\%$ of each other and mutually reinforce; the average will be taken as $Q = 10{,}000\,\frac{BTU}{hr}$.

The log mean Temperature difference (LMTD) is defined as [32]:

$$LMTD = F\,\frac{\left[\left(T_{a,i} - T_{w,i}\right) - \left(T_{a,o} - T_{w,o}\right)\right]}{Ln\left[\frac{T_{a,i} - T_{w,i}}{T_{a,o} - T_{w,o}}\right]} \tag{4}$$

where F (<1) is a correction factor to correct for the difference between the actual cross flow geometry and counter flow; Equation 4 sans the F defines counter flow LMTD. F = 0.95, as will be demonstrated below.

$$LMTD = 0.95\,\frac{[(111.3 - 69) - (74.3 - 73.1)]}{Ln\left[\frac{111.3 - 69}{74.3 - 73.1}\right]}\,°F = 10.96°F$$

The heat exchanger overall conductance, UA is a useful parameter.

$$UA = \frac{Q}{LMTD} = \frac{\left(10{,}000\,\frac{BTU}{hr}\right)}{10.96°F} = 937\,\frac{BTU}{hr\,°F}$$

The average of the nine runs was $UA = 762\,\frac{BTU}{hr\,°F}$.

The Number of Transfer Units, NTU is given by:

$$NTU = \frac{UA}{\dot{m}_a\,C_p} = \frac{937}{263}\frac{BTU}{hr\,°F} = 3.6$$

and examination of heat exchanger effectiveness (ε) versus NTU curves [32] shows that an NTU > 3 is generally the point of diminishing returns, so the considered heat exchanger and flowrates are yielding about as much performance as possible. This can also be seen by the heat exchanger effectiveness determined for this run, which is:

$$\varepsilon = \frac{111.3 - 74.3\ °F}{111.3 - 69\ °F} = 0.875 \qquad \text{(for an infinite H. E. } \varepsilon = 1)$$

Consideration of curves of F versus appropriate flow parameters [32] shows in all cases F = 0.95. This heat exchanger test confirms that an appropriate heat exchanger has been selected for the intended application.

In Chapter 5, where data from the final system are reduced, the following UAs for 6 days are calculated and here shown in Table II:

TABLE II

CALCULATED UA FOR THE SIX TESTING DAYS IN SEPTEMBER

Date	UA
September 11	$879\frac{BTU}{hr\ °F}$
September 12	$772\frac{BTU}{hr\ °F}$
September 13	$564\frac{BTU}{hr\ °F}$
September 15	$841\frac{BTU}{hr\ °F}$
September 19	$907\frac{BTU}{hr\ °F}$
September 22	$991\frac{BTU}{hr\ °F}$

The average is $UA = 860\frac{BTU}{hr\ °F}$, which value will be used henceforth.

The average UA from the July 18 testing was $UA = 762\frac{BTU}{hr\ °F}$. Note this value is $\frac{860-762}{860} = 11.3\%$ lower than the still system testing ($860\frac{BTU}{hr\ °F}$). This is not surprising, because the July 18 testing only used dry air from the solar collector. The September testing involved a condensing situation where vapor from the air condensed on the heat exchanger surface, manifesting an appreciably higher heat

transfer than for air only. The distilled water recovery rate $\dot{m}_v$ produced on the condenser surface is:

$$\dot{m}_v = \rho \dot{V}(\omega_2 - \omega_3) \quad (note\ \omega_3 = \omega_1) \tag{5}$$

3. Heat Rejection System

Two types of heat rejection approaches are used in this study: (1) an evaporative cooler, and (2) an air-cooled heat exchanger.

A large conventional house cooling evaporative cooler takes in ambient air, which passes through water cooled filter pads. The warmer air evaporates some of the water, cooling the air. In a traditional evaporative cooler application, the interest is blowing the coolest possible air into the house. But in the considered application, the evaporative cooler is employed as a cooling tower, because the interest is obtaining the coldest possible water to input to the condenser.

The definition of cooling tower efficiency, η_{ct}, is [33]:

$$\eta_{ct} = \frac{(T_{ct2} - T_{ct1})}{(T_{ct2} - T_{wbt})}$$

Where:

T_{ct1} = Water Temperature exit the cooling tower, into the condenser

T_{ct2} = Water Temperature into the cooling tower, exiting the condenser

T_{wbt} = Arbitrary Ambient wet bulb Temperature [33]

For the September 15 run we have:

$$\eta_{ct} = \frac{(T_{ct2} - T_{ct1})}{(T_{ct2} - T_{wbt})} = \frac{(T_{w2} - T_{w1})}{(T_{w2} - T_{wbt})} = \frac{(64.2 - 60.4)}{(64.2 - 54.3)} = 0.38 \tag{6}$$

For the six September runs:

TABLE III

TEMPERATURES AND HUMIDITY FOR EFFCIENCY OF THE COOLING TOWER

date	T_{w1}	T_{w2}	T_{amb}	RH %	T_{wbt}	η_{ct}
11-Sep	67	72.5	83	22	59.5	0.42
12-Sep	63.4	67	82	17	56.5	0.34
13-Sep	63.8	68.6	79	24	57.5	0.43
15-Sep	60.4	64.2	81	14	54.3	0.38
19-Sep	63	66.4	79	25	57.9	0.40
22-Sep	55.6	59	63	34	48.7	0.33

The average of the six values is $\eta_{ct} = 0.39$, which value will be used henceforth. This seemingly low value of η_{ct} is likely due to the age and condition of the evaporative cooler which is an old unit with scale on its filters that had been left in the weather. A newer unit would likely have a higher efficiency and produce cooler water than we observed. Some consideration of the cool air output of the swamp cooler could be made, however, it was beyond the scope of this investigation and would require a different configuration and set up of the system.

The water Temperature differences for the six days ($T_{w2} - T_{w1} = \Delta T_w$) were: $5.5°F,\ 3.6°F,\ 4.8°F,\ 3.8°F, 3.4°F, and\ 3.4°F,$ for an average Temperature difference $\Delta T_w = 4.1°F$. This is the Temperature difference across the condenser, measured when the average insolation incident on the solar air heater was $I =$

$300\frac{BTU}{hr\ ft^2}$. It is reasonable to assume that ΔT_w is proportional to I, or $\Delta T_w = 4.1°F\left(\frac{I}{300}\right)$. Then exercising Equation 5 we get,

$$T_{w2} = T_{wbt} + 4.1\frac{I}{0.39(300)} = T_{wbt} + 0.035I \quad (7a)$$

for different values of I, and

$$T_{w1} = T_{w2} - 0.39(T_{w2} - T_{wbt}) \quad (7b)$$

Thus, both the condenser inlet and outlet water Temperatures are estimated from measured T_{wbt} and I.

The evaporative cooler heat rejection system takes advantage of the ambient T_{wbt} and produces cooling water for the condenser well below the dry bulb Temperature. Such an approach is useful in arid locations featuring low relative humidity because the air egress from the condenser is cooler than the ambient dry bulb Temperature, increasing the solar collector efficiency and therefore heat available to the system. But the evaporative cooler cannot be used when freezing is a risk because the water in the filters and sump will freeze. In such cases, and in locations featuring high relative humidity, an option is to replace the swamp cooler with an air-to-water heat exchanger.

When the heat rejection system consists of an air-cooled heat exchanger, the ambient dry bulb Temperature is the coolest Temperature in the system. Relative to the swamp cooler cooling system, all system Temperatures will necessarily be higher, and the heat gathered, and water production rates will be lower. This was indeed observed, discussed, and quantified in Chapter 5.

4. System Modelling

Now that the component performance parameters have been mathematically described, it is possible to develop a mathematical model predicting instantaneous system performance. This will be done in the form of an algorithm, providing a step-by-step procedure. The values of the various component parameters will be included in the algorithm, such as A_c, UA, et cetera, including a constant air flowrate of 295 cfm. $\dot{m}_a = 1095\frac{lb}{hr}$. The essential inputs include I, T_{amb}, T_{wbt}, and P_{atm}.

It is necessary to start with the cooling system because that provides input to estimate the Temperature into the solar collector, T_{a3}. Using Equation 7a, the heat gained by the water in the condenser is:

$$T_{w2} = T_{wbt} + 4.1\frac{I}{0.39(300)} = T_{wbt} + 0.035I \qquad \text{(A-1)}$$

The intent here is to estimate a reasonable T_{a3} so the performance characteristics of each component can be sequentially estimated, this is an iterative calculation. The system performance data for the September runs manifested the following $\Delta T^* = T_{a3} - T_{w2}$:

TABLE IV

ΔT^* FOR ALL SEPTEMBER RUNS

9/11	9/12	9/13	9/15	9/19	9/22	Average
$\Delta T^* = 3.6°F$	$6.1°F$	$8.6°F$	$6.7°F$	$5.4°F$	$3.0°F$	$5.6°F$

The average was $\Delta T^* = 5.6\,°F$. In each of the September readings the incident collector insolation was close to $I = 300\frac{BTU}{hr\,ft^2}$. We can then estimate as a value to start the calculation:

$$T_{a3} = T_{w2} + 5.6\frac{I}{(300)} = T_{w2} + 0.0187I \qquad \text{(A-2)}$$

After the calculation is completed, the computed T_{a3} will be compared to that calculated from Equation A-2 to determine if another iteration is necessary. Since the air issuing from the condenser is saturated at Temperature T_{a3}, the partial pressure of the vapor can be calculated from a parametric fit of P_v versus T from a table.

$$P_{v3} = 0.2644 - 0.0103T_{a3} + (1.68\text{x}10^{-4})T_{a3}^2 \qquad 40 \le T_{a3} \le 90°F \qquad \text{(A-3)}$$

after which the humidity ratio ω is determined from [34, 35]:

$$\omega_3 = \omega_1 = 0.622\frac{P_{v3}}{P_{atm} - P_{v3}} \qquad \text{(A-4)}$$

ω_3 could also have been found on the saturation line of a 5000-foot psychrometric chart, but the intent here is to establish a mathematical algorithm that incorporates the psychrometric chart, facilitating data reduction in Chapter 5. The humidity ratio ω does not change while the air is being heated in the solar collector, so $\omega_3 = \omega_1$. At the start of the run, it is necessary to determine the atmospheric pressure, P_{atm}. This can either be done via an accurate barometer, or by contacting on-line the local weather service.

Having obtained T_{a3}, one can employ Equations 1 and 3 to estimate the useful heat produced by the solar air heater, Q_u. If heat losses are minimized, this

should be the same heat quantity that passes through the wetting filter, the condenser, and dissipated by the heat rejection system.

$$Q_u = IA_c\eta_c = I(37\ ft^2)\left[0.80 - 1.95\frac{(T_{in} - T_{amb})}{I}\right] \quad \text{(A-5)}$$

The ambient air density is calculated from:

$$\rho_a = \frac{P_{atm}}{\left(0.37\frac{psi\ ft^3}{lb\ °R}\right)(460 + T_{amb})}$$

after which the Temperature exits from the solar collector, T_{a1}, is readily calculated. It is assumed that the blower supplies a steady flowrate of $\dot{V} = 295\ cfm$, which was measured during trials.

$$\dot{m}_a = \rho_{air}\left(295\frac{ft^3}{min}\right)\left(60\frac{min}{hr}\right) = 17{,}700\rho_{air} \quad \text{(A-6)}$$

$$T_{a1} = T_{a3} + \frac{Q_u}{(0.24\frac{BTU}{lb\ °F})(\dot{m}_a)} \quad \text{(A-7)}$$

The intersection of T_{a1} and $\omega_3 = \omega_1$ (from Equation A-4) defines a unique state point (SP-1) where the enthalpy can either be read from a 5000-foot psychrometric chart (Figure 4-4) or calculated from [33]

$$h_1 = h_2 = 0.24T_{a1} + \omega_1(1060.5 + 0.45T_{a1}) \quad \text{(A-8)}$$

which is valid above 70°F. The first term in Equation A-8 accounts for the sensible heat, and the second term for the latent heat required to evaporate liquid water into vapor at T_{a1}. Heated air at SP-1 flows through the Celdek wetting medium, where heat from the air evaporates liquid water flowing through the filter, cooling

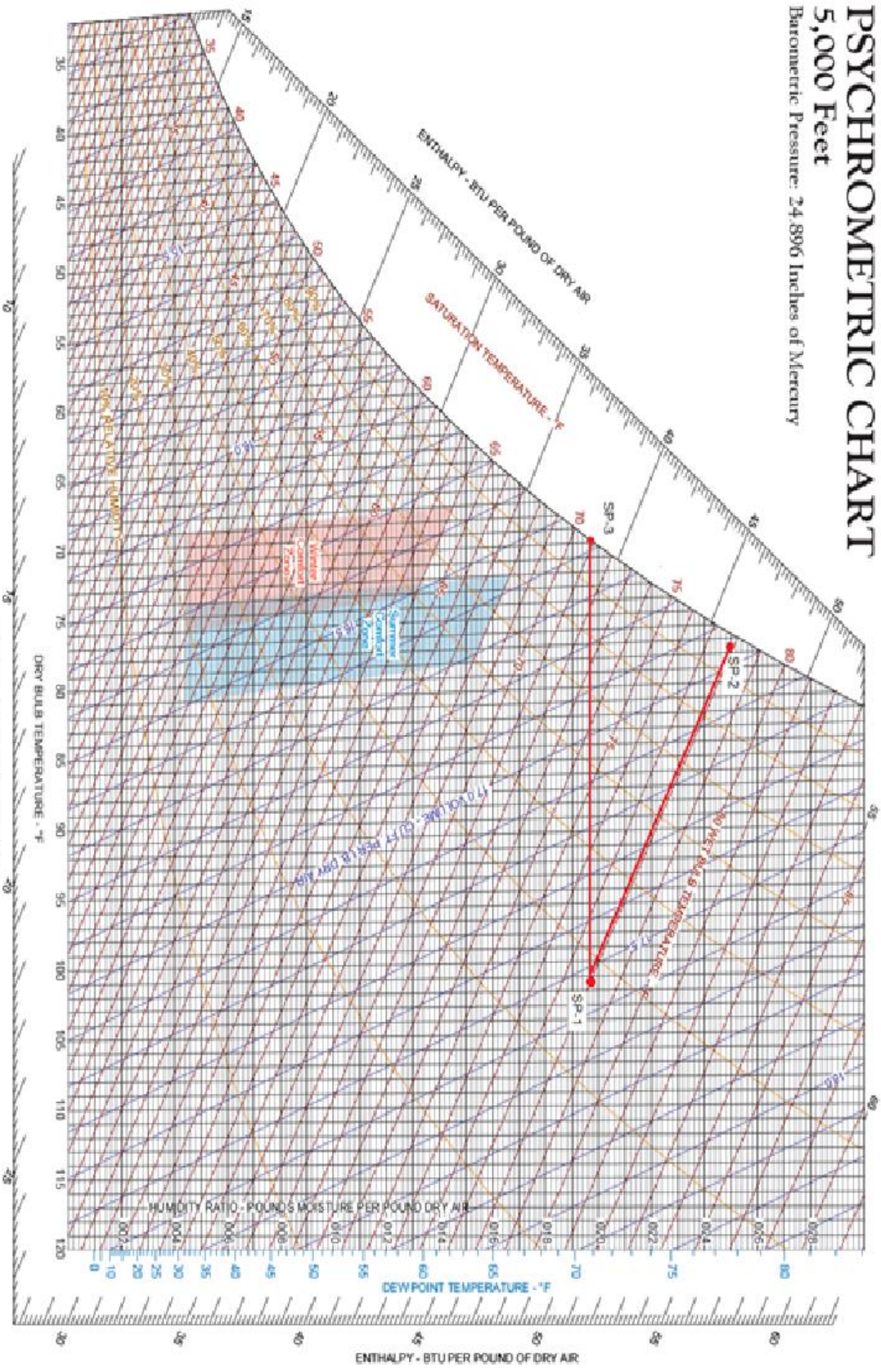

Fig. 4-4: Psychometric chart showing expected SP-1, SP-2, and SP-3 for data from September 15 at 1 pm [31]

the air. Since the process is adiabatic, $h_2 = h_1$. Reference to a 5000-foot psychrometric chart, Fig. 4-4, shows the process from SP-1 to SP-2 moving upward to the left along a line of constant enthalpy. The maximum distance the process could proceed along the enthalpy line is to the saturation curve. Since the wetting pad does not fully saturate the air flowing through it, SP-2 is below the saturation curve. The "Approach" is defined as the actual length of the process line divided by the distance from SP-1 to the saturation curve along the constant enthalpy line, point SP-2s. The September runs indicated that the Approach was generally 95%, which is quite a high wetting efficiency, this is why Celdek is used in newer home evaporative coolers.

In theory equations A-3, A-4 and A-8 could be solved to locate SP-2s, but due to the non-linearity of all three equations, the possibility of a closed-form solution is remote. So, to keep the algorithm mathematical, two parabolas were developed to correlate saturation enthalpy (h_s) to saturation humidity ratio (ω_s), where $h_s = h_{2s} = h_2 = h_1$ is already known. The derived relationship is:

$$\omega_s = -0.0034 + (5.18\text{x}10^{-4})h + (2.07\text{x}10^{-6})h^2 \qquad \text{(A-9)}$$

Examination of the psychrometric chart suggests that $\omega = \omega(T)$ can be represented by a parabola over short distances. The relationship is:

$$\omega_s = 0.0333 - (1.082\text{x}10^{-3})\text{T}_{2s} + (1.255\text{x}10^{-5})T_{2s}^2 \qquad \text{(A-10)}$$

Whereas $\omega(T)$ can be expressed as a parabola, unfortunately T (ω) cannot, so it is necessary to extract T_s from Eq A-10 via the quadratic formula. Therefore, from Equation A-10 (the negative sign in front of the square root is dropped from the quadratic solution as extraneous)

$$T_{2s} = \frac{(1.082\text{x}10^{-3}) + \sqrt{(1.082\text{x}10^{-3})^2 - 4(1.255\text{x}10^{-5})(0.0333 - \omega_s)}}{2(1.255\text{x}10^{-5})} \qquad \text{(A-11)}$$

Since the Approach is $a = 0.95$:

$$T_{a2} = T_{a1} + a(T_{2s} - T_{a1}) \qquad \text{(A-12a)}$$

and

$$\omega_2 = \omega_1 + a(\omega_s - \omega_1) \qquad \text{(A-12b)}$$

The LMTD, defined in Equation (4) is:

$$LMTD = \frac{Q}{UA} = F\,\frac{[(T_{a2} - T_{w1}) - (T_{a3} - T_{w1})]}{Ln[\frac{T_{a2} - T_{w1}}{T_{a3} - T_{w2}}]} \qquad \text{(A-13)}$$

As discussed in Section 2, the $UA = 762\,\frac{BTU}{hr\,^\circ F}$ value was an average of several runs with a wide scatter, so it can only be considered an approximate value. The Q calculated from Equation A-1 also came from a scatter, so the LMTD calculated from them is an approximated value. In Equation A-13 all Temperatures are known from above except T_{a3} (and F = 0.95), but the non-linearity of Equation 13 means solving for T_{a3} would require an iterative technique, using a computer. If we consider the Arithmetic Mean Temperature difference, AMTD, then Equation A-13 becomes:

$$AMTD = \frac{1}{2}F[(T_{a2} + T_{a3}) - (T_{w2} + T_{w1})] = \frac{Q}{UA}$$

and one can quickly solve for T_{a3}:

$$T_{a3} = T_{w2} + T_{w1} - T_{a2} + \frac{2\left(\frac{Q}{UA}\right)}{F} \quad where\ F = 0.95 \qquad \text{(A-14)}$$

The AMTD is always greater than the LMTD, and for the September runs AMTD was approximately 8.3% greater than the LMTD. Considering the scatter from which values of Q and UA were calculated, usage of Equation A-14 is warranted, and obviates the necessity for solving the complicated Equation A-13.

$$\dot{m}_v = \dot{m}_a(\omega_2 - \omega_3) \qquad Note\ \omega_3 = \omega_1 \tag{A-15}$$

Using environmental inputs, I, T_{amb}, T_{wbt}, and P_{atm}, and system inputs specific to the system, which have been measured by field testing, the above algorithm models expected state points and distilled water output. It will be verified or modified according to system test data.

In evaluating solar still performance, a system figure of merit (FoM) will be defined. The FoM will consider the complete system as a black box. In doing so, inputs such as water usage, for cooling, and energy usage, to run the blower and water pumps, are neglected and the focus is placed on the output, ie. the recovered distillate. By neglecting the various inputs into the system, the FoM can be used to compare different configurations of the system as well as potentially compare our system to other distillation methods. The term FoM is preferred to “efficiency,” because in a multi-stage system the merit parameter can exceed 1 (similar to a refrigerator or air conditioner). The potential water evaporation rate of the insolation incident on the solar collector is $\dot{M}_{sc}$:

$$\dot{M}_{sc} = I\frac{A_c}{h_{fg}}$$

The system FoM is defined here as:

$$FoM = \frac{Actual\ Water\ Collection\ Rate}{\text{Potential Water Evaporation Rate of Insolation}}$$

Then:

$$FoM = h_{fg}\frac{\dot{m}_v}{IA_c} \quad (8)$$

This definition incorporates all component and system efficiencies and losses. To estimate a daily performance, several hourly productions need to be calculated.

Sensitivity Analysis

A sensitivity analysis was performed on six relevant variables: T_{w1}, $\dot{V}_a$, UA, the Approach, F_R, and $\dot{m}_w$. These variables were considered as they could potentially be adjusted without a drastic or complete change to the system as a whole. The algorithm presented previously was used to compare the FoM of each variable as it was manipulated. The algorithm was exercised for each variable over an appropriate range.

1. T_{w1}

T_{w1} is the water Temperature entering the condenser from the cold-water reservoir. Using an evaporative cooler the lowest the water Temperature can be is the wet bulb Temperature. While lower Temperatures can be achieved via more active chilling there are energy costs and other considerations that are beyond the scope of this

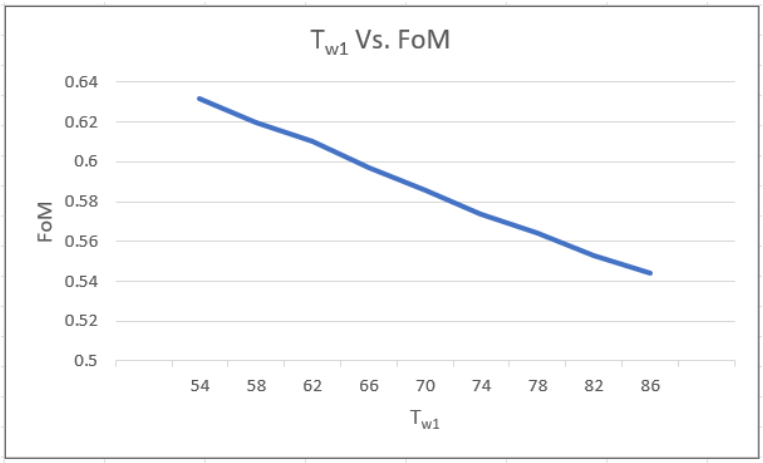

Fig. 4-5: T_{w1} Vs FoM

analysis. To that end, when isolating T_{w1} a range of 54 F to 86 F was chosen. 54 degrees is approximately the average wet bulb Temperature on the testing days, and 86 F is the high end of what is reasonable within the constraints of the algorithm.

2. $\dot{V}_a$ (CFM)

$\dot{V}_a$ is the volumetric flow rate of the air circulating through the system, in this case it is measured as Cubic Feet per Minute or CFM. Initially a blower fan was purchased with an unloaded volumetric flow rate of approximately 500 CFM. Once the system was completed the blower fan was measured to have a flow rate of 295 cfm. Six-inch flexible ducting was used to connect the blower fan to the solar collector and the collector to the distillation unit. A range of 150 to 500 CFM was chosen to exercise the algorithm. 150 CFM is the stall speed of the blower fan, and 500 CFM is the maximum the blower can output. Figure 4-2 shows the data plot.

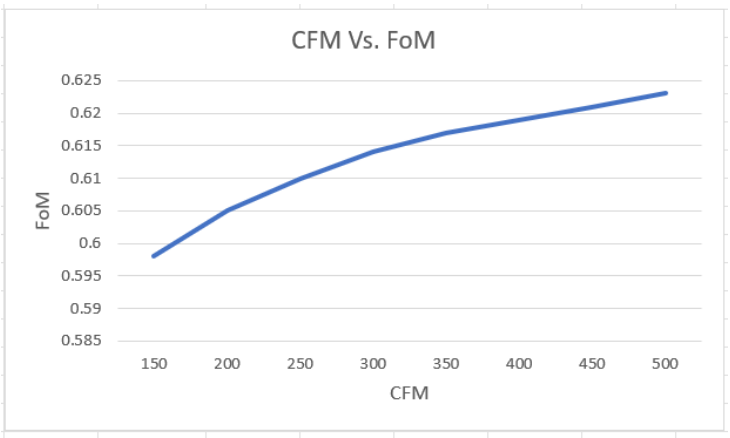

Fig. 4-6: CFM vs FoM

3. UA

UA is the overall heat transfer coefficient of the heat exchanger, specifically the condenser. The UA is affected by the Temperatures of both the air outside the condenser and the water inside as well as both flow rates. Since the UA is a

property of the condenser it is likely that the most effective way to change the UA is to replace the condenser. A range of 500-1000 $\frac{BTU}{hr\,°F}$ was used to exercise the algorithm. This range is approximately 25% above and below the average UA found in testing of 762 $\frac{BTU}{hr\,°F}$.

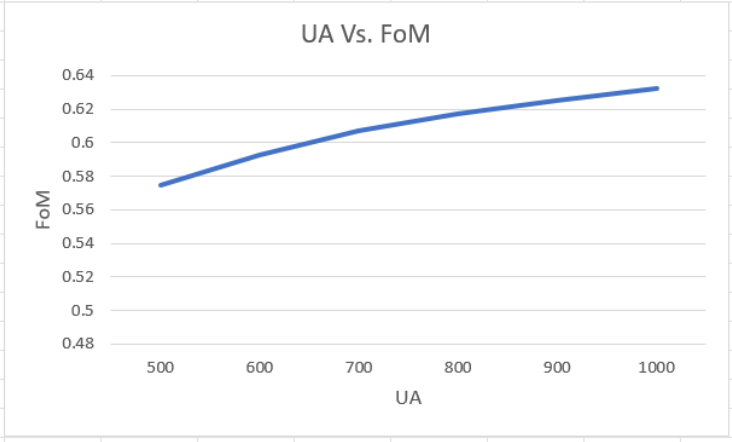

Fig. 4-7: UA vs. FoM

4. Approach

The Approach is the distance between state points 1 and 2 on the psychrometric chart, divided by the distance between state point 1 and the saturation line. In essence the Approach is the percentage of water vapor in the air. A range of 0.75 to 1 was considered. Due to the effectiveness of the Celdek used in the system the Approach was found to range from 87% to 95% in the current system design. While the Approach appeared to have the greatest effect on the FoM,

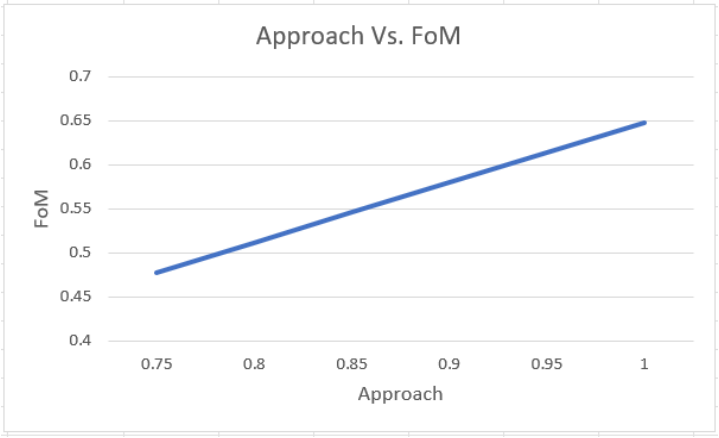

Fig. 4-8: Approach vs. FoM

the current design of the system is nearing the maximum Approach and further exploration may not be especially fruitful.

5. F_R

F_R, the heat removal factor, is the amount of usable heat gained from the solar collector. A high value of the heat removal factor, F_R, is important for efficient solar collector operation, because it indicates most of the insolation captured by the absorber is usefully released heat, Q, to the air working fluid, rather than being radiated or reflected to or through the glazing. F_R is a property of the solar collector design and is indicative of the insolation incident on the collector. F_R is the more useful variable to analyze the effects of a lower insolation incident on the collector. Similar to the Approach, F_R was nearing maximum in the current system design and further exploration may not be useful. However, F_R appears to have a significant effect on the FoM and should be maximized as much as feasibly possible in any future endeavors. The range used was 0.75 to 1, while the actual system showed an F_R of approximately 0.965 or 96.5%.

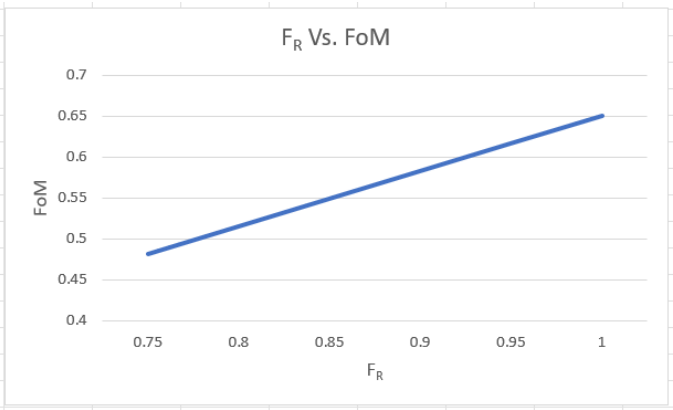

Fig. 4-9: F_R Vs. FoM

Figure 4-9 highlights the necessity of efficient solar collector design. In an effort to maximize F_R, significant effort was invested to install 5 layers of charcoal-colored aluminum bug screen as additional absorbers inside the collector. If the

collector had no additional absorbers and only had the back surface painted black the F_R would be substantially less. Without additional absorbers the F_R would be less than 0.7 or 70%, which would drastically diminish the solar heat gathered and the consequent FoM would have been in the range of [0.44/0.64=] 63% of experienced performance.

6. $\dot{m}_w$

$\dot{m}_w$ is the water flow rate within the condenser. The water flow rate will affect several different aspects of the system. With a higher flow rate, the log mean Temperature difference, LMTD, will go down which will lower the Temperature of T_{a3}. A lower T_{a3} will increase the effectiveness of the heat exchanger, this in turn Raises the UA. The water flow rate is fairly easy to adjust by using a more powerful pump and is likely to show the most drastic improvement. The range of 4 to 7 gpm was used to exercise the algorithm for this variable. During testing the flow rate was static at 5.7 gpm and the range used is approximately 25% above and below.

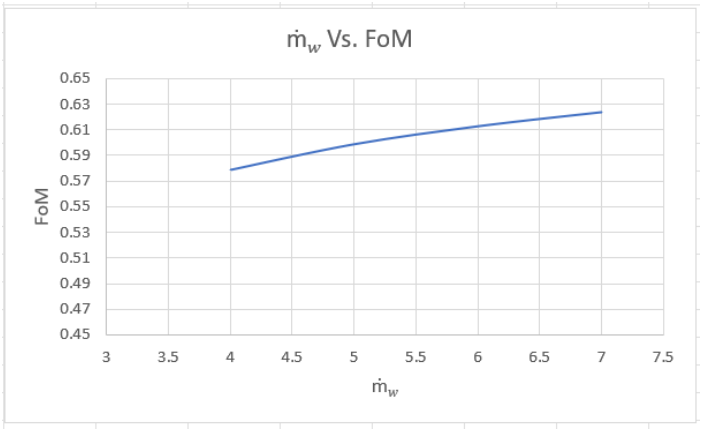

Fig. 4-10: $\dot{m}_w$ Vs. FoM

7. Driving Factors

Figure 4-11 shows the change of the FoM for each variable given a range of 25% above and below the average found in testing. The average of the FoM from the six variables was found to be 0.6. Using that average as the baseline, the

variables were compared and ordered from largest to smallest change of FoM across the range. Of the six variables it was found that the Approach and the F_R have the most drastic effect on the FoM and will need to be reasonably maximized in any future work, however, since the current system maximized both they are less useful to focus on. The third most effective variable was the water

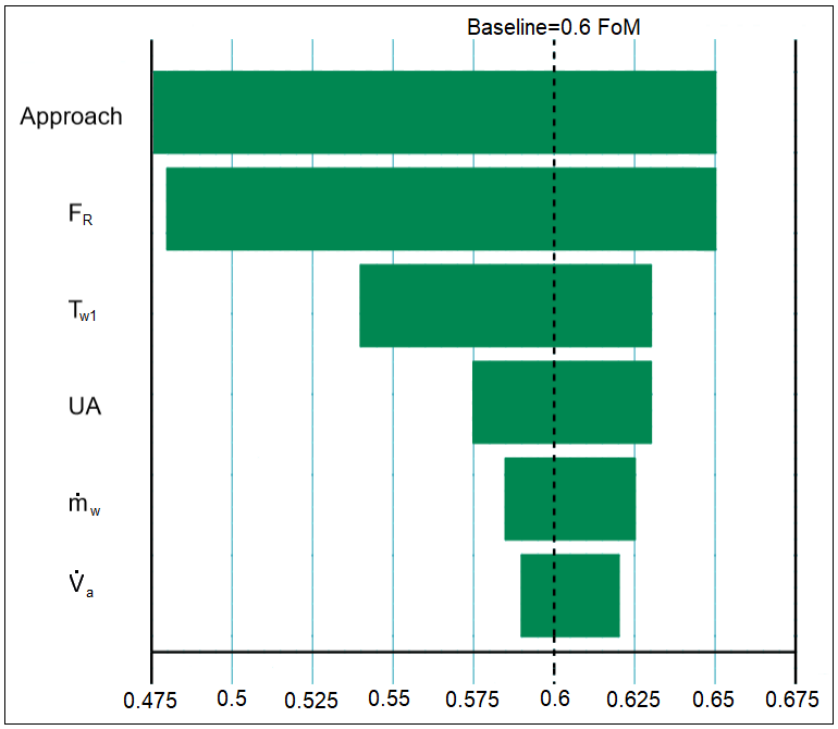

Fig. 4-11: The change in FoM of each variable

Temperature entering the condenser, T_{w1}, and further investigation is warranted. The water Temperature could be lowered by actively cooling the water below the wet bulb Temperature, but this may not be a cost-effective endeavor. The UA and the water flow rate, $\dot{m}_w$, also had reasonable effect on the FoM. To change the UA would most likely require changing to a different condenser, which could alter several aspects of the system design and may not be cost effective. The water flow rate is potentially the easiest variable to adjust as a more powerful pump could

be substituted into the system, and this ease may warrant further investigation even though it will likely have a smaller effect on the system.

Some consideration was given to changing the physical attributes of the system, such as increasing the size of the solar collector or increasing the interior dimensions of the distillation unit. The interconnectedness of those variables with the design of the system would suggest that changing those variables would require a complete redesign of the system. Such redesigns should be considered in future research but go beyond the scope of the current endeavor.

Chapter 5. Data Analysis and Results

In Chapter 4 a mathematical model simulating the solar distillation system was developed. In that model the functioning of various components was estimated, and in some cases (e.g. UA) empirical results from testing were used to assign numerical values. It was found necessary to start with the cooling system to estimate Temperatures so the inlet Temperature to the solar collector could be approximated, as a necessary input to estimate solar heat collected.

Chapter 3 describes construction of the system. Certain parameters were measured and determined to be constant; thus, the system airflow is $\dot{V}_a = 295\ cfm$. A water meter was installed to measure flow from the cooling system and found to remain constant at $\dot{m}_w = 5.7\ gpm$.

The system was tested for two different cooling solutions, and results are described in this chapter. Runs employing an evaporative cooler heat rejection system were run for 6 sunny days from September 12 through September 22. Then the evaporative cooler was replaced by an air-to-water heat exchanger and ambient air was passed through the heat exchanger to achieve system heat rejection; three days of data were collected on October 6, 7 and 8.

September Runs – Evaporative Cooler Heat Rejection

The system tested is depicted in Figure 4-1. The period between September 12 and 22, 2023, were characterized by mostly sunny days with few clouds. The September runs featured the evaporative cooler being used as the heat rejection system.

The data were collected in two modes: (1) automatic computer collection, and (2) visual instrument readings recorded on an excel sheet. The raw data are presented in Appendix A, which shows six days of collection for the considered system. A sample calculation showing the data reduction procedure is presented here for a considered run, on September 15, 2023, at 1 pm PDT (approximately solar noon):

$I = 950 \frac{Watt}{m^2} = 301 \frac{BTU}{hr\ °F}$ Ambient insolation

$T_{amb} = 81\ °F$ Ambient dry bulb Temperature

$RH_{amb} = 14\%$ Ambient relative humidity

$T_{a1} = 101.5°F$ Temperature exiting from solar collector

$T_{a2} = 78.5°F$ Temperature between Celdek and condenser

$T_{a3} = 70.9°F$ Temperature post condenser and entering solar collector

From a 5000 ft psychrometric chart, with $T_{amb} = 81\ °F$ and $RH_{amb} = 14\%$, one immediately reads for other ambient parameters:

$V = 16.5 \frac{ft^3}{lb}$ so $\rho = \frac{1}{V} = 0.061 \frac{lb}{ft^3}$ Ambient air density

$T_{wb} = 52°F$ Ambient wet bulb Temperature

$\omega = 0.0038 \frac{lb_v}{lb_{da}}$ Ambient humidity ratio

1. Solar Heat Collected

It was previously established via testing of the solar hot air heater that the collector efficiency is (refer to Figure 4-2):

$$\eta_c = 0.80 - 1.95\frac{(T_{in} - T_{amb})}{I}$$

So:

$$\eta_c = 0.80 - 1.95\frac{(70.9 - 81)}{301} = 0.865$$ Solar collector efficiency

Then the expected heat collected from the solar collector is:

$$Q_s = IA_C\eta_c = \left(301\frac{BTU}{hr\ ft^2}\right)(37\ ft^2)(0.865) = 9622\frac{BTU}{hr}$$

This value will be accepted as the actual heat generated by the solar collector, for reasons which will become apparent. This value $Q_s = 9622\frac{BTU}{hr}$ is independently validated in Section 4 by the system heat rejected by the evaporative cooler water, $Q = 9500\frac{BTU}{hr}$. This close agreement, within $\frac{9622-9500}{9622} = 1.3\%$, corroborates both results, and $Q_s = 9622\frac{BTU}{hr}$ will be used as the heat input for this run. The solar collector efficiency is:

$$\eta_c = \frac{9622\frac{BTU}{hr}}{\left(301\frac{BTU}{hr\ ft^2}\right)(37.1\ ft^2)} = 0.86$$

From previous testing the airflow through the system was estimated to be $\dot{V} = 295\ cfm$. Then the actual sensible heat collected by the solar collector is:

$$Q_{sen} = \rho\dot{V}C_p(T_1 - T_3)$$

$$= \left(0.061\frac{lb}{ft^3}\right)\left(295\frac{ft^3}{min}\right)\left(60\frac{min}{hr}\right)\left(0.24\frac{BTU}{lb\ °F}\right)(101.5 - 70.9\ °F)$$

$$= 7930\frac{BTU}{hr}$$

This is $\frac{9622-7930}{9622} = 0.176$ or 17.6% below Q_{sen}. However, in Section 2 below we see the evaporated vapor is approximately $5.9\frac{lb}{hr}$, whereas the actual water collected (see Section 3) was estimated at $3.5\frac{lb}{hr}$. This difference is too great to be attributed to experimental error, and unfortunately another phenomenon was operative, which was realized only after field testing was completed and the system was dismantled.

The intake to the blower which circulates air throughout the system is located just a few inches after the condenser. It was anticipated that all of the vapor condensed would occur on the heat exchanger surface, fall off in droplets, and be collected in the basin below the condenser. But reflection shows that did not fully happen, and some of the condensation occurred as atomized droplets in the cooled air, and not on the heat transfer fins. This mist or fog was then entrained by the blower and reentered the solar collector, so rather than being harvested as distilled water product, the mist was lost as useful product. Suppose $\dot{m}_{vc} = 1.6\frac{lb_v}{hr}$ bypassed the collection bucket and reentered the solar collector. Then the latent heat required to evaporate this bypassed fog was:

$$Q_{Lat} = \dot{m}_{vc} h_{fg} = \left(1.6\frac{lb_v}{hr}\right)(1049\ BTU/lb_v) = 1678\frac{BTU}{hr}$$

Then the total heat supplied by the solar collector is:

$$Q_{sl} = Q_{sen} + Q_{Lat} = 7930 + 1678 = 9608\frac{BTU}{hr} \approx Q_s = 9622\frac{BTU}{hr}$$

Therefore, it is concluded that $\dot{m}_{vc} \approx 1.6\frac{lb_v}{hr}$ of distilled liquid water in the form of atomized droplets bypassed harvest and was evaporated in the solar collector in

this particular run. In hindsight this tremendous penalty could have been obviated by employment of a demister.

The elevation of the Desert Research Institute (DRI), where the data were collected, is almost exactly 5000 feet. The data collected for the three state points in the still were:

$T_{a1} = 101.5°F \quad RH_1 = 31\% \quad \text{so} \quad \omega_1 = 0.016 \frac{lb_v}{lb_{da}}$

$T_{a2} = 78.5°F \quad RH_2 = 87\% \quad \text{so} \quad \omega_2 = 0.0215 \frac{lb_v}{lb_{da}}$

$T_{a3} = 70.9°F \quad RH_3 = 69\% \quad \text{so} \quad \omega_3 = 0.0135 \frac{lb_v}{lb_{da}}$ and Dew Point Temp = 60.5ºF

These state points are plotted on the psychrometric chart comprising Figure 5-1. The initial thought was that RH_3 must be 100%, because SP-3 follows a condensing situation, and the two humidity sensors (which confirmed each other within 3%) must be in error. But further investigation revealed that even in a condensing environment the relative humidity can be less than 100%. For example, even during a rain shower the relative humidity may be less than 100% [36]. Rain drops descending from a higher elevation are often colder than ambient air due to the adiabatic thermal lapse rate, so vapor in the air condensing on the cold rain drops leaves a void, manifesting a sub-100% RH. Similarly, vapor condensing on the heat exchanger surface, which is colder than the surrounding air, will form relatively cold drops onto which other vapor can condense. It is no coincidence that the dew point Temperature at SP-3 is 60.5ºF, the same as the cooling water Temperature inlet Temperature (60.4ºF). In Figure 5-1 it is significant to note that the wet bulb Temperature for SP-3, and corresponding humidity ratio,

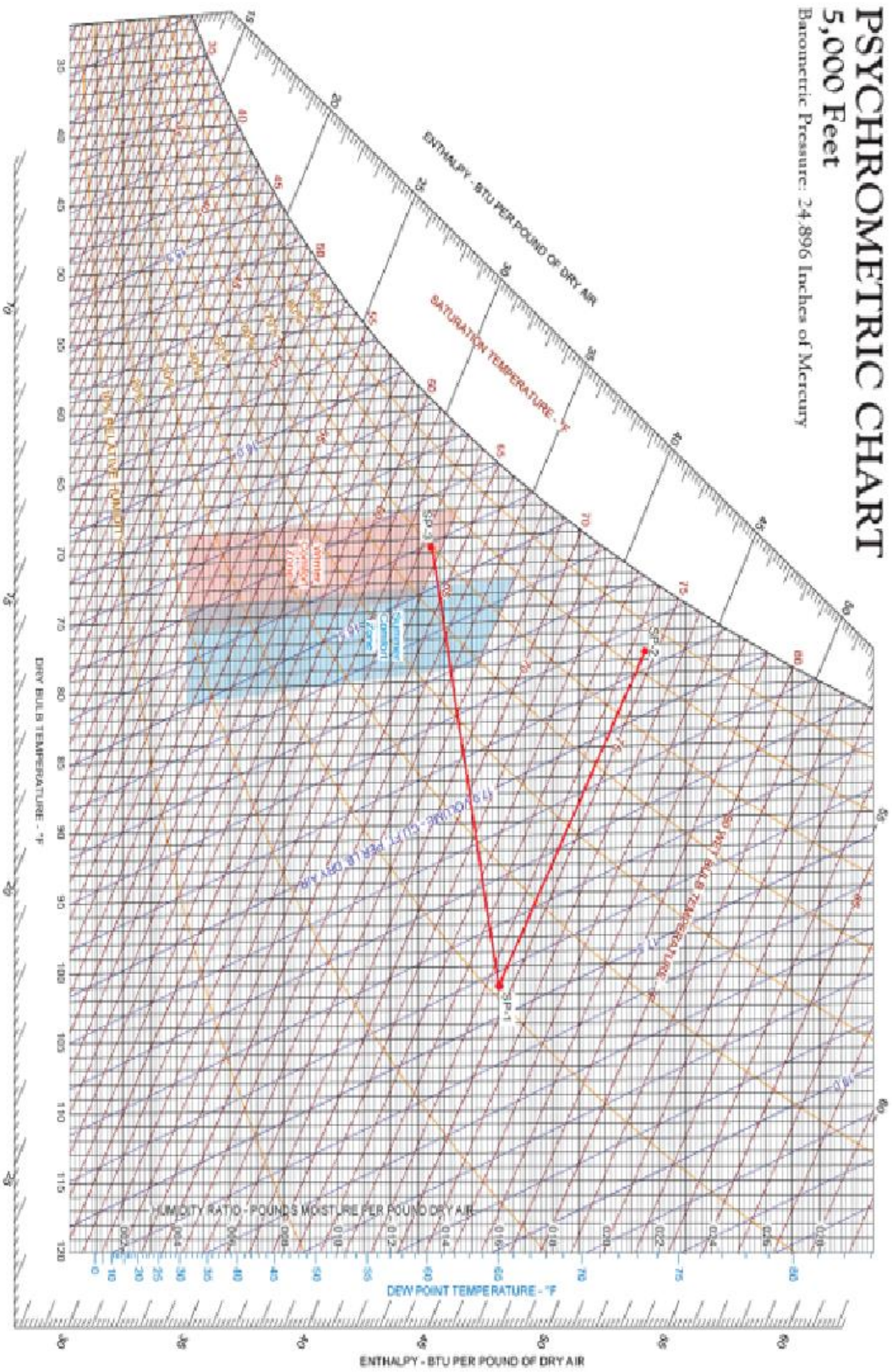

Fig. 5-1: Psychometric chart showing SP-1, SP-2, and SP-3 for data from September 15 at 1 pm

nearly matches the humidity ratio for SP-1, as predicted by theory, so a mass balance on both vapor and liquid droplets matches expectation. Thus, we witness the phenomenon of an unsaturated air mixture at 71ºF, with entrained mist droplets at lower Temperatures, exiting the condenser and entering the solar collector. The air is entering the solar air heater at 70.9ºF but is unsaturated, with entrained water droplets; the three state points for this run are shown on Figure 5-1, where SP-3 is consistent with:

Humidity ratio $\omega_3 = 0.0135\ \frac{lb_v}{lb_{da}}$

Enthalpy $h_3 = 32.0 \frac{BTU}{lb_{da}}$

Density $\rho_3 = \frac{1}{16.4} \approx 0.061 \frac{lb}{ft^3}$

However, the properties above do not account for the presence of liquid water droplets entrained in the air. In the solar heater the air is heated from $T_3 = 70.9°F$ to $T_1 = 101.5°F$, but the humidity ratio increases because the water droplets are evaporated. Therefore, in Figure 5-1 both Temperature and humidity increase going from SP-3 to SP-1.

2. Humidifier Air Moistening

The first component in the still is a 4" thick Celdek evaporative cooling pad. The air exiting the solar collector contains only superheated steam, the liquid mist having been evaporated. Water continually circulated down the pad encounters the warm air from the solar collector and moistens the air. Heat from the air evaporates some of the liquid water, and since the process is adiabatic, $h_2 = h_1$;

in Figure 5-1 the field measurements show this, adding credence in the measurements.

SP-2 is just below the saturation line, where theory predicts SP-2 should be located. The “approach” is defined as the distance between SP-1 and SP-2 divided by the distance along a line of constant enthalpy from SP-1 to the saturation line. Measurement shows the approach is 87%, which indicates efficient wetting of the air. The air humidity ratio rose from $\omega_1 = 0.016 \frac{lb_v}{lb_{da}}$ to $\omega_2 = 0.0215 \frac{lb_v}{lb_{da}}$, so the quantity of water evaporated was:

$$\dot{m}_v = \rho \dot{V}(\omega_2 - \omega_1) = \left(0.061 \frac{lb}{ft^3}\right)\left(295 \frac{ft^3}{min}\right)\left(60 \frac{min}{hr}\right)\left(0.0215 - 0.016 \frac{lb_v}{lb_{da}}\right)$$

$$= \left(1080 \frac{lb_{da}}{hr}\right)\left(0.0051 \frac{lb_v}{lb_{da}}\right)$$

$$= 5.9 \frac{lb}{hr} = 0.71 \frac{gal}{hr}$$

3. Condenser Heat Exchanger

The heat exchanger log mean Temperature difference (LMTD) is of interest, as is the heat exchanger UA conductance. Since there is a condensing situation on the air side, the air specific heat must be modified to account for the condensation. The measured heat exchanger parameter values of interest are, using the 5000 ft psychrometric chart (see Figure 4-3 and Figure 5-1):

$T_2 = 78.5°F$ Air-vapor mix into HE

$T_3 = 71°F$ Air exit from HE including liquid water droplets

$\omega_3 = 0.0135 \frac{lb_v}{lb_{da}}$ as measured

$\dot{V}_a = 295\ cfm \quad \Rightarrow\Rightarrow \quad \dot{m}_{air} = 1080\,\frac{lb_{da}}{hr}$

$T_{w1} = 60.4°F$ Cooling water Temperature from evaporative cooler into heat exchanger

$T_{w2} = 64.2°F$ Return water from heat exchanger

$\dot{m}_a = 5.7\ gpm = 2850\,\frac{lb}{hr}$ Cooling water flowrate

Then:

$$LMTD = F_{cor}\,\frac{\left((T_{a2} - T_{w1}) - (T_{a3} - T_{w2})\right)}{\ln\left(\frac{T_{a2} - T_{w1}}{T_{a3} - T_{w2}}\right)}$$

where F_{cor} is a correction factor to account for the difference between the crossflow heat exchanger employed here and a counter flow heat exchanger. For our purposes we can use $F = 0.95$ [32].

So:

$$LMTD = 0.95\,\frac{\left((78.5 - 60.4) - (71 - 64.2)\right)}{\ln\left(\frac{18.1}{6.8}\right)} = 10.9°F$$

Then the heat exchanger conductance UA is:

$$UA = \frac{Q}{LMTD} = \frac{9622\,\frac{BTU}{hr}}{10.9\,°F} = 883\,\frac{BTU}{hr\,°F}$$

It is reassuring that the calculated value for UA falls within the expected range. However, the realized UA may be higher due to the water droplets in the exit air.

A heat balance on the air through the condenser yields:

$$Q = Vapor\ Heat\ of\ Condensation + Air\ Sensible\ heat$$

$$= \dot{m}_a\left[h_{fg}(\omega_2 - \omega_3) + C_{p-air}(T_{a2} - T_{a3})\right]$$

$$= 1080\frac{lb_{da}}{hr}\left[\left(1049\frac{BTU}{lb_v}\right)\left(0.0215 - 0.0135\frac{lb_v}{lb_{da}}\right) + \left(0.24\frac{BTU}{lb\,°F}\right)(78.5 - 71°F)\right]$$

$$\overset{Latent}{} \quad \overset{Sensible}{}$$

$$= 1080\frac{lb_{da}}{hr}\left[\ 8.4\ +\ 1.8\frac{BTU}{lb_{da}}\right]$$

$$Q = 11{,}000\frac{BTU}{hr}$$

which value is about 14% higher than the estimated solar gain of $Q_s = 9622\frac{BTU}{hr}$. The measured value of $\omega_3 = 0.0135\ \frac{lb_v}{lb_{da}}$ does not include the water droplets which condensed, so is lower than the actual water content in the air. The same quantity of water entering the solar heater at SP-3 must equal the water at SP-1, which consists of unsaturated air sans mist drops. So, at SP-1 the moisture flowrate is:

$$\dot{m}_{v1} = \dot{m}_a\omega_1 = \left(1080\frac{lb_{da}}{hr}\right)\left(\ 0.016\frac{lb_v}{lb_{da}}\right) =\ 17.3\frac{lb_v}{hr} \qquad \text{Water flowrate past SP} - 1.$$

Therefore, the following equality must hold:

$$\dot{m}_{v1} = \dot{m}_{v3} = 17.3\frac{lb_v}{hr} = \dot{m}_a\omega_3 + \dot{m}_{vby} = \left(1080\frac{lb_{da}}{hr}\right)\left(\ 0.0135\frac{lb_v}{lb_{da}}\right) + \dot{m}_{vby}$$

Where $\dot{m}_{vby}$ is the liquid droplet blowby, $\frac{\text{lb}_v}{\text{hr}}$

or

$$\dot{m}_{vby} = 2.7\ \frac{\text{lb}_v}{\text{hr}}$$

The measured distilled water collected during the 5½ hour collection period was 2 gallons = 16.7 lb. In future runs water will be collected and measured every half hour, so the exact quantity will be known for each period. But for now, it is necessary to estimate the water collection rate around 1 pm. It will be assumed

that during the data collection period the water output is proportional to the insolation. From the data sheet, the total insolation recorded over the 12 half-hour periods is approximately:

$$\Sigma I = 0.5\ (\text{first}\ I) + \Sigma\left(2^{\text{nd}}\ to\ 11^{th}\ I\right) + 0.5(12^{th}\ I) = 0.5(930 + 330) + 8388$$

$$= 9018\ Watt - hr$$

Then the water collected over the half-hour period around 1 pm is:

$$\dot{m}_w = \frac{(950\ Watt - hr)(2\ gal)}{9018} = 0.21\frac{gal}{half - hour} = 0.42\frac{gal}{hr} = 3.5\frac{lb}{hr}$$

At the end of Section 2 we estimated from the field testing that the water evaporated between SP-1 and SP-2 was $\dot{m}_v = \rho\dot{V}(\omega_2 - \omega_1) = 5.9\frac{lb_v}{hr}$. Adding the collected water and the bypass water totals $\dot{m}_v = 3.5 + 2.7 = 6.2\frac{lb_v}{hr}$, which values are within $\frac{6.2-5.9}{6.2} = 5\%$ of each other. This is persuasive evidence that an enormous quantity of distilled water which should be collected was instead bypassed from harvest and continually re-evaporated and re-condensed, an egregious penalty. In future studies this bypass must be prevented via use of demisters, baffles, an additional heat exchanger/condenser, or some other device(s).

4. Evaporative Cooler Heat Rejection

A heat balance on the cooling water from the evaporative cooler gives:

$$Q = \dot{m}_w C_{p,w}(T_{w2} - T_{w1}) = \left(2500\ \frac{lb}{hr}\right)\left(1.0\frac{BTU}{lb\ °F}\right)(64.2 - 60.4°F) = \ 9{,}500\frac{BTU}{hr}$$

This value confirms and reinforces the value predicted by the solar collector efficiency equation in Section 1, namely $Q_s = 9622\ \frac{BTU}{hr}$.

Overall, the measurements for this considered run are internally consistent, with no egregious recordings.

Due to the evaporative cooler system, the inlet air Temperature to the solar collector is $T_{a3} = 71°F$, which is cooler than ambient Temperature $T_{amb} = 81°F$. This allows for increased collected solar heat compared to higher inlet Temperatures. The comparison to thermal power plants is complete since both high boiler Temperature and low condenser Temperature impact efficiency.

<u>October Runs – Heat Exchanger Heat Rejection</u>

A limitation of the evaporative cooling approach is it cannot be used when winter ambient Temperatures are too low because ice will form on the filters which will make the swamp cooler useless and may cause damage to the pump and

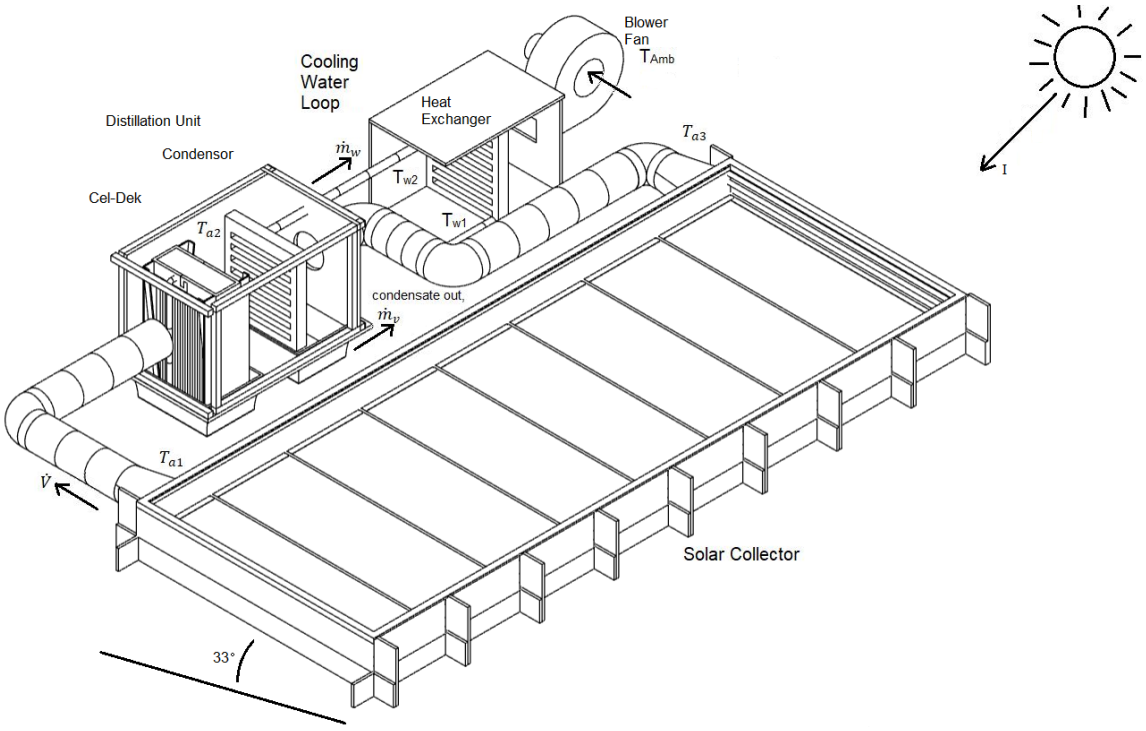

Fig. 5-2: system with a Second heat exchanger and blower fan for cooling

tubing. In some regions blessed with abundant sunshine, this is not a problem, but evaporative cooling cannot be employed in winter in Reno or many other American locations. This may suggest the evaporative cooler heat rejection approach is particularly adapted to locations where ambient freezing is not a consideration, and the swamp cooler can be used year-round.

The evaporative cooler was removed and replaced by an air-to-water heat exchanger, a duplicate of the condenser heat exchanger, and a blower fan. The system is shown in Figure 5-2. System tests were run on three consecutive sunny days, October 6, 7 and 8. System data from October 7 at 1 pm PDT (approximately solar noon) are analyzed in detail. This facilitates system performance differences between the two cooling approaches to be compared and contrasted.

For the considered run, on October 7, 2023, at 1 pm PDT:

$I = 860\frac{Watt}{m^2} = 273\frac{BTU}{hr\ ft^2}$ Ambient insolation incident on collector face

$T_{amb} = 77°F$ Ambient dry bulb Temperature

$RH_{amb} = 30\%$ Ambient relative humidity

$T_{a3} = 84.4°F$ Air Temperature into solar collector

From a 5000 ft psychrometric chart, with $T_{amb} = 77°F$ and $RH_{amb} = 30\%$, one immediately reads for other ambient parameters:

$V = 16.45\frac{ft^3}{lb}$ and $\rho = \frac{1}{V} = 0.061\frac{lb}{ft^3}$ Ambient air density

$T_{wb} = 57°F$ Ambient wet bulb Temperature

$\omega = 0.0070\frac{lb_v}{lb_{da}}$ Ambient humidity ratio

The collector efficiency is (refer to Figure 4-2):

$$\eta_c = 0.80 - 1.95\frac{(T_{in} - T_{amb})}{I}$$

So

$$\eta_c = 0.80 - 1.95\frac{(84.4 - 77)}{273} = 0.747 \text{ Solar collector efficiency}$$

Then the heat collected from the solar collector is

$$Q_{s1} = IA_c\eta_c = \left(273\frac{BTU}{hr} - ft^2\right)(37\ ft^2)(0.747) = \ 7556\frac{BTU}{hr}$$

The measured distilled water collection for this 1-hour period was 29 ounces, or

$$\dot{m}_v = 29\frac{oz}{hr} = 1.81\frac{lb}{hr}$$

It is noted that this water collection does not include atomized water droplets that bypassed collection and were entrained in the air stream return to the solar collector, so neither the September nor October system runs give a true picture of the actual system capability. This $\dot{m}_v$ output will be compared with output from the evaporative cooling heat rejection approach via the Figure of Merit (FoM), described below.

It is of interest to estimate the distilled water collection rate ($\dot{m}_v$) if water bypass had not occurred and compare to the $\dot{m}_v$ of the evaporative cooler cooling system. Since T_3 is close to saturation, we find from Equation A-4 in Chapter 4 (note at $T_3 = 84.4°F$, $P_v = 1.19\ in - Hg$):

$$\omega_3 = \omega_1 = \frac{0.622(1.19)}{24.9 - 1.19} = 0.031\frac{lb_v}{lb_{da}}$$

Then from Equation 4-3

$$\eta_c = 0.80 - 1.95\frac{(84.4-77)}{273} = 0.747 \qquad \text{Solar collector efficiency}$$

and

$$T_{a1} = T_{a3} + \frac{\eta_c I A_c}{(\rho \dot{V}_a C_p)_{air}} = 84.4°F + \frac{(0.747)\left(273\ \frac{BTU}{hr\ ft^2}\right)(37.1\ ft^2)}{\left(1095\frac{lb}{hr}\right)(0.24\frac{BTU}{lb_m\ °F})}$$

$$T_{a1} = 84.4 + 28.8 = 113.2°F$$

Then the enthalpy is (Using Equation A-8 on Chapter 4, page 53)

$$h_1 = h_2 = 0.24(113.2) + (.031)[(1060.5 + 0.45(113.2)] = 27.2 + 34.4 = 61.6\frac{BTU}{lb_{da}}$$

The saturation line on the 5000' psychrometric chart only goes as high as $83°F$, so the chart cannot be directly read, other than via extrapolation. Employing Equation A-9 (Chapter 4 page 55) yields $\omega_{2s} = 0.0362\frac{lb_v}{lb_{da}}$, and with a 95% approach:

$$\omega_2 = \omega_1 + 0.95(\omega_{2s} - \omega_1) = 0.031 + 0.95(0.0362 - 0.031) = 0.0359\frac{lb_v}{lb_{da}}$$

Then the water collection potential from this heat exchanger cooled run is:

$$\dot{m}_v = \dot{m}_a(\omega_{2s} - \omega_1) = \left(1095\frac{lb_{da}}{hr}\right)\left(0.0359 - 0.031\frac{lb_v}{lb_{da}}\right) = 5.36\frac{lb_v}{hr}$$

This value is compared with the evaporative cooler cooled run product collection potential of:

$$\dot{m}_v = \dot{m}_a(\omega_{2s} - \omega_1) = \left(1095\frac{lb_{da}}{hr}\right)\left(0.025 - 0.0196\frac{lb_v}{lb_{da}}\right) = 5.92\frac{lb_v}{hr}$$

This difference is a direct result of cooler air entering the solar collector when the evaporative cooler cooling system is used versus the heat exchanger heat rejection approach.

Comparing the Two Cooling System Methods

As discussed in Chapter 4, the Figure of Merit (FoM) is a consistent parameter to evaluate the solar distillation system performance of disparate runs and considered approaches. The FoM is the actual distilled water collection rate, $\dot{m}_v$, divided by the potential water evaporation rate of the insolation incident on the solar collector, $\dot{m}_{sc}$. This definition allows for all of the system efficiencies and losses to be incorporated into a single metric that can be used to compare different system designs.

$$FoM = \frac{Actual\ Water\ Collection\ Rate}{\text{Potential Water Evaporation Rate of Insolation}} \quad (1)$$

The potential water evaporation rate of the insolation incident on the solar collector is $\dot{M}_{sc}$

$$\dot{M}_{sc} = I\frac{A_c}{h_{fg}} \quad (2)$$

and so

$$FoM = \frac{\dot{m}_v}{\dot{M}_{sc}} = h_{fg}\frac{\dot{m}_v}{IA_c} \quad (3)$$

The two system cooling approaches considered here are:

(1) Evaporative cooling heat removal using sump water to cool the condenser (ECHR), and

(2) Heat exchanger heat removal using ambient air (HEHR).

The two salient performance parameters impacted by each cooling method are:

(1) Solar collector efficiency, η_c

(2) The collected distilled water rate divided by incident insolation evaporation potential on the solar collector, FoM.

The testing results are compared in Table V.

TABLE V

SYSTEM PERFORMANCE COMPARISON

Cooling System Method	ECHR	HEHR	$\frac{\text{ECHR}}{\text{HEHR}}$
Solar Collector Efficiency, η_c	0.864	0.748	1.16
FoM, $\dot{m}\frac{h_{fg}}{IA_c}$	0.33	0.19	1.7

It is expected that ECHR outperformed HEHR, as quantified in Table V. Since the expected overall condensation is less for the HEHR, but due to high air velocity and strong fan induction the same water bypass likely occurs in both systems. Therefore, the apparent FoM would drop drastically due to the same distilled water bypass from a smaller base.

It is of interest to compare the ECHR and HEHR approaches assuming all distilled water is collected. In the present system this would involve a demister of some kind, likely fine screens as discussed below. From the calculations above we see

$$\frac{\dot{m}_{v,ECHR}}{\dot{m}_{v,HEHR}} = \left(\frac{5.92}{5.36}\frac{lb_v}{hr}\right) = 1.1$$

Finally, the FoM for each approach is of interest, assuming no distilled water bypass. For September 15 data:

$$\dot{M}_{sc} = \frac{IA_c}{h_{fg}} = \frac{\left(301\,\frac{BTU}{hr\,ft^2}\right)(37.1\,ft^2)}{1049\,\frac{BTU}{lb_v}} = 10.65\,\frac{lb_v}{hr}$$

$$FoM_{ECHR} = \frac{\dot{m}_v}{\dot{M}_{sc}} = \frac{5.92\,\frac{lb_v}{hr}}{10.65\,\frac{lb_v}{hr}} = 0.56$$

$$FoM_{HEHR} = \frac{5.32}{10.65} = 0.50$$

As a point of interest, data from the Los Salinas sloped glass solar still in the Atacama Desert, at latitude -33.5 South and 4300-foot elevation, averaged FoM = 0.39; this is representative of sloped glass passive stills. From Reference [4] on a good day the system produced $\dot{m}_v = 2.5\,\frac{\text{liter}}{\frac{\text{day}}{\text{m}^2}} = 0.10\,\frac{\text{lb}}{\text{hr ft}^2}$. If $I = 270\,\frac{BTU}{hr\,ft^2}$ then:

$$FoM_{Atacama} = \dot{m}_v\frac{h_{fg}}{IA_c} = \frac{\left(0.1\,\frac{lb}{hr\,ft^2}\right)\left(1050\,\frac{BTU}{lb}\right)}{\left(270\,\frac{BTU}{hr\,ft^2}\right)(1\,ft^2)} = 0.39$$

A secondary consideration is the electrical power requirements for both variations of the system. The only difference electrically between the two is the evaporative cooler and the blower fan on the heat exchanger. Both versions used two water pumps and a blower fan. The water pumps are rated at 60 Watts for each pump and the blower fan is rated at 225 Watts. The evaporative cooler was set on low fan and so is rated at 437 Watts. Power consumption per hour is calculated as:

$$power_{ECHR} = 2(60) + 225 + 437\,Watts = 782\,Watts = 2668\,\frac{BTU}{hr}$$

And:

$$power_{HEHR} = 2(60) + 2(225)\ Watts = 570\ Watts = 1945\frac{BTU}{hr}$$

In comparison to the power of the solar collector the electrical power used in the system is much lower. This gives a ratio of electrical power to thermal power of $\frac{power_{ECHR}}{Q} = \frac{2668}{9622} = 0.277$ and $\frac{power_{HEHR}}{Q} = \frac{1945}{9622} = 0.202$. If a large body of water is available, such as a lake or the ocean, the cooling system could use water directly from that source. This would eliminate the need for the evaporative cooler or the second blower motor and, using the existing pumps and blower, would give a power ratio of $\frac{power_{water}}{Q} = \frac{1177}{9622} = 0.122$. These power ratios are based on the ideal insolation incident on the collector which means these are best case and can only get worse as the insolation drops.

6. Need for a Demister

A demister, when properly employed into the system, would capture a large amount of entrained water vapor. There are several different groups of mist eliminator each with advantages, disadvantages and requirements that require very careful consideration.

	DEMISTER® mist eliminator	FLEXICHEVRON® mist eliminator	DEMISTER-PLUS mist eliminator	FLEXIFIBER® mist eliminator	VORSOMAX® cyclone mist eliminator
100% Efficiency	3-10 µ	10-40 µ	7-10 µ	<0.1 µ	7-20 µ
Pressure Drop wc	<1 in [25 mm]	0.4-3.5 in [10-89 mm]	1-20 in [25-508 mm]	2-20 in [51-508 mm]	8-14 in [200-355 mm]
Gas Capacity	5	6-15	10-20	1	15-20
Liquid Capacity	5	10	5-10	1	10
Solids Handling	3	10	3-10	1	10
Cost	1	2-3	3-6	10	3-5
Cost with Vessel	6	3-4	1-3	10	1
Relative scale based on 1 as the lowest. Others are scaled.					

Fig. 5-3: Comparison table from Koch-Glitsch mist eliminator brochure [38]

> “Mist eliminators belong to one of the following groups: settling tank, fiber filtering candles, electrostatic precipitators, cyclones, impingement van separators and wire mesh. Each of these devices operates under different principles and is applied for the removal of the droplets with a specific size range and effective separation performance. [37]”

Since simplicity and cost are both primary factors in the design considerations the reasonable options are fairly limited. Fiber filters of some sort could be cost effective but would increase the potential need for maintenance as the fibers could degrade or potentially be fouled. A wire mesh demister has the potential to be fabricated by simple means and could be very cost effective. It has gained extensive industrial recognition as low pressure drop, high separation efficiency, reasonable capital cost, minimum tendency for flooding, high capacity, and small size.[37] Wire mesh also has a low pressure drop which is ideal for our system as it employs a blower fan. Al-Dughaither et al. showed the pressure drop across a wire mesh could be as low as 3.8 cm H_2O [37]. The company Koch-Glitsch advertises pressure drops as low as 1 cm H_2O (see figures 5-3 and 5-4) [2]. “When the vessel size is not set by the mist eliminator, such as is normally the case for distillation towers, steam drums, or evaporators, the practical starting point is often the knitted wire mesh pad type. DEMISTER® mist eliminators provide high separation efficiency at the lowest installed cost.[38]”

Fig. 5-4: Several mist eliminators sold by Koch-Glitsch [38]

In Chapter 4 the mathematical model for the expected system performance, without liquid bypass of the distilled water collection just after the condenser, was developed. It was expected that field data would be reduced following that model. When the collected water was found to be appreciably less than predicted, the more complicated model in Chapter 5 had to be developed which fit all the data.

The SP-3 field measurements, which indicated that the relative humidity after the condenser was appreciably less than 100%, were initially considered to be in error, the thinking being that the relative humidity RH_3 must be (close to if not) 100%, despite two separate sensors that indicated the same values within a few percent. Since the mathematical model based on theory corroborates the test data so well, it is expected the Chapter 4 model can provide accurate predictions.

Clearly a demister component is required to make the system work at its full potential. Adding a demister to the system would require a redesign of some of the elements of the distillation unit. For best results, the demister would need to be placed into a duct or chamber with air flow in the vertical direction and there would need to be some separation between the demister and the blower. In such a case

it would be better to have the outlet ducting of the distillation unit come out the top of the box rather than the side. Having the air flow in the vertical direction and the outlet coming out of the top of the box, just above the collection bucket, would allow the condensed vapor to rain down out of the demister into the collection bucket. The demister chamber would then be placed on top of the distillation unit with the wire mesh approximately halfway between the distillation unit outlet and the blower on top of the demister chamber. Having the flow change from the horizontal to the vertical could have some problematic repercussions, such as the flow not being evenly distributed across the entire area of the condenser. Perhaps a duct with a bell mouth could be placed a few inches into the distillation unit to help keep the flow even distributed across the condenser. Another consideration that would need to be made would be the positioning of the condenser in relation to the bell mouth. The length of the distillation unit may need to be increased to facilitate a reasonable space between the condenser and the outlet. A potential design can be seen in figure 5-5.

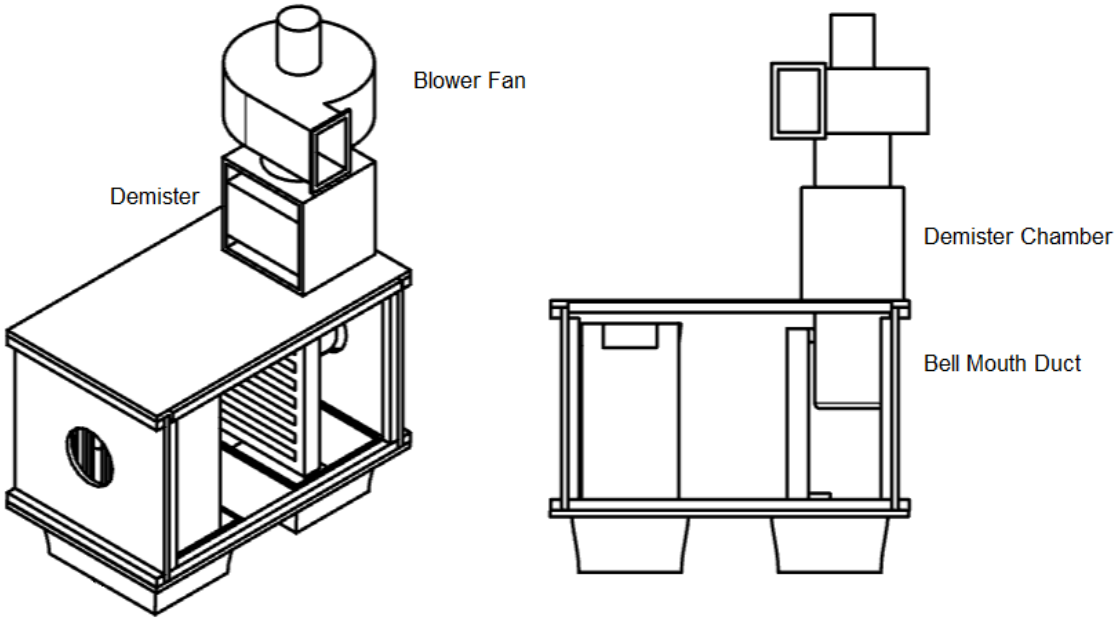

Fig. 5-5: Demister chamber placed on top of the distillation unit.

Chapter 6. Results And Conclusions

Results and Conclusions of this research are discussed, along with recommendations for future efforts.

During the planning, design, system fabrication and initial testing, the idea that small water droplets could and would be blown out of the heat exchanger due to high air velocities and be sucked into the in the air entrained and drawn into the blower, bypassing distilled water collection, was never considered. But during the first round of testing in September, it was noted that the distilled water collection was appreciably less than the mathematical model predicted, well below experimental error tolerance. The system was checked for leaks which would allow for either liquid or vapor escape, but no obvious outflows were found. It was assumed as a necessary phenomenological fact that the output from the condenser must be saturated, and the two humidity sensors that measured substantially less than 100% relative humidity must be in error, despite the fact that both sensors closely corroborated each other.

When the possibility that the post-condenser humidity sensors might really be correct was examined, and the exit air might not actually be saturated, a mass balance comparing water evaporated from the Celdek and exit from the condenser closely accounted for all the water if some of the distilled water was in atomized droplet form and was bypassing collection, being returned to the solar collector in liquid form. A new mathematical model accurately simulated the droplet phenomenon. The missing water was found!

Research comprises an art and science of discovery, and generally raises surprises. Successful end products commonly have non-linear development paths and consume more time than planned due to unexpected developments, and that was certainly the case in this project. So, although the demonstrated solar still did not produce the expected quantity of distilled water, the mathematical models closely predicted the actual result, lending confidence that when the bypass bugs are shaken out the predicted results are attainable.

Conclusions are assembled below.

(1) Two mathematical models were developed. One accurately describes water collection for a flawed system where not all distilled water was able to be collected. The other describes the intended system where all distilled water would be collected.

(2) The system as designed is potentially attractive, especially if combined with a large solar air heater that provides winter space heating but wastes the heat in the summer.

(3) In arid areas an evaporative cooler heat rejection system is more efficient than applying an air-to-water heat exchanger. This suggests such a system would be most applicable in arid regions where winter freezing is not a design concern. This applies to many parts of the world where such a distillation system is most needed. In areas where winter freezing occurs, seasonal switch outs may be necessary.

(4) The electrical power requirements for the system are minimal relative to the thermal power from the solar collector.

(5) If a river, lake, or ocean were available for cooling, the system could work better and be cheaper.

(6) Active energy solar distillation provides more distilled water than the passive sloped-glass approach per unit solar exposed area. Furthermore, the active solar collector can be seasonally adjusted to intercept more insolation, although this may be a minor benefit in equatorial areas.

(7) The air velocity through the condenser heat exchanger must be kept low to avoid small water drops from being blown past the water collection component. In the initial design the heat exchanger was selected with minimal flow area (and maximum thickness) to provide maximum velocity and hence maximum heat transfer coefficient.

(8) Due to subcooling, the air-vapor mixture after the condenser may not be saturated, but instead may contain tiny water droplets, requiring a demister. If testing reveals that water droplets are blown off the condenser, then large area demister screens may be necessary to capture the water droplets.

(9) Two or more stages are possible, with the condenser of the first stage being the heat source for the second stage. An economic analysis would be necessary to assess the viability of multi-stage systems, which would be thermally powered by just one solar air heater.

(10) The water purity of the collected condensate was tested and found to be considerably better than the makeup water. With system cleaning, the water purity would have been higher.

(11) The electrical consumption in the summer mode could be defaulting because of the amount of energy is not minor. The use of an evaporative cooler as the heat rejection component of the system is a less feasible and less desirable solution than initially thought.

(12) The sensitivity analysis suggests the water Temperature, T_{w1}, the overall heat transfer coefficient of the condenser, UA, and the mass flow rate of the water through the condenser, $\dot{m}_w$, warrant further investigation. The heat rejection factor, F_R, and the approach should be maximized in all future endeavors as they could both have a drastic negative effect on the system if not maximized.

Future Effort

Before other similar systems are built, the atomized droplet entrainment versus air velocity through the heat exchanger needs to be addressed. A second condenser heat exchanger in series, at the expense of increased pressure drop and decreased air flow, might capture the water droplets. Or if the second heat exchanger is in parallel, the air velocity might be sufficiently slow to avoid liquid blowby. Or a system of fine screen demisters over a large area (for slow velocity and diminished pressure drop) could be a reasonable solution.

After a 1-stage system has been successfully demonstrated, a two-stage system should be considered.

After the technical performance of a system is characterized, an economic analysis, likely using full year climate bin data, should be performed to determine the economic performance.

Chapter 7. References

[1] UNESCO, Water in a Changing World. 2009.

[2] J. R. Hirschmann, "Solar distillation in Chile," *Desalination,* vol. 17, no. 1, pp. 31-67, 1975/08/01/ 1975, doi: https://doi-org.unr.idm.oclc.org/10.1016/S0011-9164(00)84078-3.

[3] H. S. Aybar, F. Egelioglu, and U. Atikol, "An experimental study on an inclined solar water distillation system," (in English), *Desalination,* Article vol. 180, no. 1-3, pp. 285-289, Aug 2005, doi: 10.1016/j.desal.2005.01.009.

[4] J. HARDING, "APPARATUS FOR SOLAR DISTILLATION," *Minutes of the Proceedings of the Institution of Civil Engineers,* vol. 73, no. 1883, pp. 284-288, 1883, doi: 10.1680/imotp.1883.21702.

[5] A. Al-Garni, "Productivity Enhancement of Solar Still Using Water Heater and Cooling Fan," *Journal of Solar Energy Engineering,* vol. 134, p. 031006, 08/01 2012, doi: 10.1115/1.4005760.

[6] A. H. Abed, H. A. Hoshi, and M. H. Jabal, "Experimental investigation of modified solar still coupled with high-frequency ultrasonic vaporizer and phase change material capsules," *Case Studies in Thermal Engineering,* vol. 28, p. 101531, 2021/12/01/ 2021, doi: https://doi.org/10.1016/j.csite.2021.101531.

[7] Z. M. Omara, A. S. Abdullah, and T. Dakrory, "Improving the productivity of solar still by using water fan and wind turbine," *Solar Energy,* vol. 147, pp. 181-188, 2017/05/01/ 2017, doi: https://doi.org/10.1016/j.solener.2017.03.041.

[8] S. A. Kalogirou, "Chapter 8 - Solar Desalination Systems," in *Solar Energy Engineering (Second Edition)*, S. A. Kalogirou Ed. Boston: Academic Press, 2014, pp. 431-479.

[9] M. C. Garg, "Chapter 4 - Renewable Energy-Powered Membrane Technology: Cost Analysis and Energy Consumption," in *Current Trends and Future Developments on (Bio-) Membranes*, A. Basile, A. Cassano, and A. Figoli Eds.: Elsevier, 2019, pp. 85-110.

[10] M. Rosen and A. Farsi, "CHAPTER TWO - Desalination technologies and their working principles," in *Sustainable Energy Technologies for Seawater Desalination*, M. Rosen and A. Farsi Eds.: Academic Press, 2022, pp. 45-106.

[11] (2023). *STATEMENT OF RATES EFFECTIVE RATES APPLICABLE TO SIERRA PACIFIC POWER COMPANY ELECTRIC SCHEDULES Bundled Rates*. [Online] Available: https://www.nvenergy.com/about-nvenergy/rates-regulatory/electric-schedules-north .

[12] "Buy Distilled water." https://www.medcaresupply.com/Buy-Distilled-Water-s/261.htm (Accessed September 19th, 2023).

[13] R. Singh, "Chapter 3 - Hybrid membrane systems – applications and case studies," in *Hybrid Membrane Systems for Water Purification*, R. Singh Ed. Amsterdam: Elsevier Science, 2005, pp. 131-196.

[14] T. Gullinkala, B. Digman, C. Gorey, R. Hausman, and I. C. Escobar, "Chapter 4 Desalination: Reverse Osmosis and Membrane Distillation," in *Sustainability Science and Engineering*, vol. 2, I. C. Escobar and A. I. Schäfer Eds.: Elsevier, 2010, pp. 65-93.

[15] K. Bourouni, M. T. Chaibi, and L. Tadrist, "Water desalination by humidification and dehumidification of air: State of the art," *Desalination,* vol. 137, no. 1, pp. 167-176, 2001/05/01/ 2001, doi: https://doi.org/10.1016/S0011-9164(01)00215-6.

[16] S. Al-Hallaj, M. M. Farid, and A. Rahman Tamimi, "Solar desalination with a humidification-dehumidification cycle: performance of the unit," *Desalination,* vol. 120, no. 3, pp. 273-280, 1998/12/22/ 1998, doi: https://doi.org/10.1016/S0011-9164(98)00224-0.

[17] K. Bourouni, R. Martin, L. Tadrist, and M. T. Chaibi, "Heat transfer and evaporation in geothermal desalination units," *Applied Energy,* vol. 64, no. 1, pp. 129-147, 1999/09/01/ 1999, doi: https://doi.org/10.1016/S0306-2619(99)00071-9.

[18] M. M. Farid, S. Parekh, J. R. Selman, and S. Al-Hallaj, "Solar desalination with a humidification-dehumidification cycle: mathematical modeling of the unit," *Desalination,* vol. 151, no. 2, pp. 153-164, 2003/01/10/ 2003, doi: https://doi.org/10.1016/S0011-9164(02)00994-3.

[19] M. Farid and A. W. Al-Hajaj, "Solar desalination with a humidification-dehumidification cycle," *Desalination,* vol. 106, no. 1, pp. 427-429, 1996/08/01/ 1996, doi: https://doi.org/10.1016/S0011-9164(96)00141-5.

[20] S. K. Garg, S. D. Gomkale, R. L. Datta, and D. S. Datar, "Development of humidification-dehumidification technique for water desalination in arid zones of India," *Desalination,* vol. 5, no. 1, pp. 55-63, 1968/01/01/ 1968, doi: https://doi.org/10.1016/S0011-9164(00)80192-7.

[21] S. Parekh, M. M. Farid, J. R. Selman, and S. Al-hallaj, "Solar desalination with a humidification-dehumidification technique — a comprehensive technical review," *Desalination,* vol. 160, no. 2, pp. 167-186, 2004/01/15/ 2004, doi: https://doi.org/10.1016/S0011-9164(04)90007-0.

[22] I. Al-Mutaz, "The continued challenge of capacity building in desalination," *Desalination,* vol. 141, pp. 145-156, 12/15 2001, doi: 10.1016/S0011-9164(01)00399-X.

[23] S. Esfandeh, M. Hemmat Esfe, and M. H. Kamyab, "Chapter 11 - Applications of nanofluids in solar energy collectors focusing on solar stills," in *Advances in Nanofluid Heat Transfer*, H. M. Ali Ed.: Elsevier, 2022, pp. 341-373.

[24] S. B. Kedare and N. B. Desai, "Solar Thermal Process Heat," in *Encyclopedia of Sustainable Technologies*, M. A. Abraham Ed. Oxford: Elsevier, 2017, pp. 367-376.

[25] J. W. Saxton, "Solar-vacuum distillation," M.S., University of Nevada, Reno, United States -- Nevada, 1401260, 2000. [Online]. Available: https://unr.idm.oclc.org/login?url=https://www-proquest-com.unr.idm.oclc.org/dissertations-theses/solar-vacuum-distillation/docview/230985086/se-2?accountid=452[Online]. Available: https://unr.primo.exlibrisgroup.com/discovery/openurl?institution=01UNR_INST&vid=01UNR_INST:DEFAULT&genre=dissertations&atitle=&author=Saxton%2C+James+William&volume=&issue=&spage=&date=2000-01-01&rft.btitle=&rft.jtitle=&issn=&isbn=978-0-599-92178-8&sid=ProQuest+Dissertations+%26+Theses+Global_

[26] M. N. Kiley, "Analysis of a site-built active air-solar heater," M.S., University of Nevada, Reno, United States -- Nevada, 1351184, 1992. [Online]. Available: https://unr.idm.oclc.org/login?url=https://www-proquest-com.unr.idm.oclc.org/dissertations-theses/analysis-site-built-active-air-solar-heater/docview/303994456/se-2?accountid=452[Online]. Available: https://unr.primo.exlibrisgroup.com/discovery/openurl?institution=01UNR_INST&vid=01UNR_INST:DEFAULT&genre=dissertations&atitle=&author=Kiley%2C+Matthew+Nichol&volume=&issue=&spage=&date=1992-01-01&rft.btitle=&rft.jtitle=&issn=&isbn=979-8-208-65036-3&sid=ProQuest+Dissertations+%26+Theses+Global_

[27] T. D. Goldade, "Development of Mobile Solar Evaluation Laboratory & Technical and Economic Performance of the Goldade Site-Built Air Collector," M.E., University of Nevada, Reno, United States -- Nevada, 10001601, 2015. [Online]. Available: https://unr.idm.oclc.org/login?url=https://www-proquest-com.unr.idm.oclc.org/dissertations-theses/development-mobile-solar-evaluation-laboratory/docview/1760591338/se-2?accountid=452[Online]. Available: https://unr.primo.exlibrisgroup.com/discovery/openurl?institution=01UNR_INST&vid=01UNR_INST:DEFAULT&genre=dissertations&atitle=&author=Goldade%2C+Travis+D.&volume=&issue=&spage=&date=2015-01-01&rft.btitle=&rft.jtitle=&issn=&isbn=978-1-339-41533-8&sid=ProQuest+Dissertations+%26+Theses+Global_

[28] S. K. Hoekman, B. Broch, C. Robbins, R. Jacobson, and R. Turner, "DRI Renewable Energy Center (REC) (NV)," United States, 2012-12-31 2012. [Online]. Available: https://www.osti.gov/biblio/1061460[Online]. Available: https://www.osti.gov/servlets/purl/1061460

[29] A. Tejero-González and A. Franco-Salas, "Optimal operation of evaporative cooling pads: A review," Renewable and Sustainable Energy Reviews, vol. 151, p. 111632, 2021/11/01/ 2021, doi: https://doi-org.unr.idm.oclc.org/10.1016/j.rser.2021.111632.

[30] Duffie, J.A. and Beckman, W.A., “Solar Engineering of Thermal Processes” Second Edition, Wiley Interscience, 1991.

[31] The Engineering ToolBox (2006). *Moist Air - Psychrometric Chart for Normal Temperatures at 5000 Feet Altitude*. [online] Available at: https://www.engineeringtoolbox.com/psychrometric-chart-d_250.html [Accessed November 16th, 2023].

[32] Cengel, Y.A., “Heat Transfer ~ A Practical Approach”, McGraw-Hill, Boston, MA, 1998.

[33] The Engineering ToolBox (2004). *Cooling Tower Efficiency*. [online] Available at: https://www.engineeringtoolbox.com/cooling-tower-efficiency-d_699.html [Accessed October 28th, 2023].

[34] Jennings, B.H., “Environmental Engineering ~ Analysis and Practice”, Harper and Row, New York, 1970.

[35] Kuehn, T.H. et al., “Thermal Environmental Engineering”, Edition 3, Prentice Hall, 1998.

[36] B. Pontolilo, “What Is the Relative Humidity When It’s Raining?,” *GreenBuildingAdvisor*, Sep. 26, 2018. https://www.greenbuildingadvisor.com/article/relative-humidity-raining (accessed Dec. 08, 2023).

[37] A. A. Al-Dughaither, A. A. Ibrahim, and W. A. Al-Masry, "Investigating pressure drop across wire mesh mist eliminators in bubble column," *Journal of Saudi Chemical Society,* vol. 15, no. 1, pp. 1-9, 2011/01/01/ 2011, doi: https://doi-org.unr.idm.oclc.org/10.1016/j.jscs.2010.09.008.

[38] “Mist Elimination and Phase Separations.” Accessed: Dec. 08, 2023. [Online]. Available: https://koch-glitsch.com/technical-documents/brochures/mist-elimination-liquid-liquid-coalescing-(1) .

Appendix A: Data

This is the raw data collected during testing. Each day of data has two parts. The Tables are the data that were collected manually. The list after each table is the raw consol read out from the Arduino connected to the six humidity sensors for approximately one minute at 1 pm local time. The 1 pm time was selected as being typical of the system performance. Readings were taken every half hour starting at 11 am and ending at 4:30 pm. There are two sets of data, the first set using the evaporative cooler as the heat rejection unit and the second set using the heat exchanger and blower fan as the heat rejection unit.

Evaporative Cooler Runs

	11:00	11:30	12:00	12:30	1:00	1:30	2:00	2:30	3:00	3:30	4:00	4:30
9/11/23	sunny	sunny	sunny	sunny	sunny	cloudy	sunny	sunny	sunny	cloudy/ raining	partially sunny	Partially sunny
Amb Temp (F)	76	79	80	81	83	83	84	84	85	86	86	85
Outside RH (%)	32	28	26	24	22	20	20	21	19	18	18	18
I (w/m^2)	877	920	930	935	947	925	920	856	790	100	710	500
FR (gpm)	5.6	5.2	5.7	5.7	5.8	5.7	5.7	5.7	5.7	5.7	5.7	5.8
sump Temp (F)	61.4	61.7	55.1	67	67	68	69.2	66.2	65.5	60.8	64	61.7
Return Temp (F)	65.4	65.1	66.2	71	72.5	74.5	71.5	69.2	68.2	61.5	66.5	63.2

12:59:58.777 -> Hum1: 35.00 %, Temp: 39.60 C, F = 103.28
13:00:00.747 -> Hum2: 35.00 %, Temp: 39.40 C, F = 102.92
13:00:02.752 -> Hum3: 81.00 %, Temp: 28.90 C, F = 84.02
13:00:04.744 -> Hum4: 86.00 %, Temp: 28.00 C, F = 82.40
13:00:06.750 -> Hum5: 71.00 %, Temp: 24.00 C, F = 75.20
13:00:08.770 -> Hum6: 60.00 %, Temp: 25.00 C, F = 77.00
13:00:10.810 -> Hum1: 35.00 %, Temp: 39.60 C, F = 103.28
13:00:12.808 -> Hum2: 35.00 %, Temp: 39.40 C, F = 102.92
13:00:14.822 -> Hum3: 81.00 %, Temp: 28.90 C, F = 84.02
13:00:16.918 -> Hum4: 86.00 %, Temp: 28.00 C, F = 82.40
13:00:18.834 -> Hum5: 71.00 %, Temp: 24.00 C, F = 75.20
13:00:20.849 -> Hum6: 60.00 %, Temp: 25.00 C, F = 77.00
13:00:22.856 -> Hum1: 35.00 %, Temp: 39.60 C, F = 103.28
13:00:24.866 -> Hum2: 35.00 %, Temp: 39.40 C, F = 102.92
13:00:26.846 -> Hum3: 81.00 %, Temp: 28.80 C, F = 83.84
13:00:28.858 -> Hum4: 86.00 %, Temp: 28.00 C, F = 82.40
13:00:30.892 -> Hum5: 72.00 %, Temp: 24.00 C, F = 75.20
13:00:33.158 -> Hum6: 62.00 %, Temp: 25.10 C, F = 77.18
13:00:34.919 -> Hum1: 35.00 %, Temp: 39.60 C, F = 103.28
13:00:36.909 -> Hum2: 35.00 %, Temp: 39.50 C, F = 103.10
13:00:38.933 -> Hum3: 81.00 %, Temp: 28.90 C, F = 84.02
13:00:40.943 -> Hum4: 86.00 %, Temp: 28.00 C, F = 82.40
13:00:43.197 -> Hum5: 71.00 %, Temp: 24.10 C, F = 75.38
13:00:44.958 -> Hum6: 60.00 %, Temp: 25.20 C, F = 77.36
13:00:46.950 -> Hum1: 35.00 %, Temp: 39.60 C, F = 103.28
13:00:48.980 -> Hum2: 35.00 %, Temp: 39.50 C, F = 103.10
13:00:50.964 -> Hum3: 81.00 %, Temp: 28.90 C, F = 84.02
13:00:52.974 -> Hum4: 86.00 %, Temp: 28.00 C, F = 82.40
13:00:54.986 -> Hum5: 71.00 %, Temp: 24.20 C, F = 75.56
13:00:57.016 -> Hum6: 59.00 %, Temp: 25.20 C, F = 77.36

	11:00	11:30	12:00	12:30	1:00	1:30	2:00	2:30	3:00	3:30	4:00	4:30
9/12/23	sunny	sunny	sunny	sunny	sunny	sunny	sunny	sunny	sunny	sunny	cloudy	cloudy
Amb Temp (F)	74	76	78	80	82	82	83	84	84	86	87	85
Outside RH (%)	26	22	21	19	17	19	19	18	17	16	16	18
I (w/m^2)	960	968	970	970	960	910	904	825	748	675	400	55
FR (gpm)	5.6	5.6	5.7	5.7	5.7	5.7	5.7	5.6	5.7	5.7	5.6	5.7
sump Temp (F)	62.3	61.5	62	63.3	63.4	64.4	64.2	63.6	64.2	64.5	62.2	61.2
Return Temp (F)	66.4	66	66.2	66.7	67	67.5	67.4	66.3	67	67	63.6	62.5

12:59:59.644 -> Hum1: 33.00 %, Temp: 39.10 C, F = 102.38
13:00:01.652 -> Hum2: 31.00 %, Temp: 40.40 C, F = 104.72
13:00:03.639 -> Hum3: 85.00 %, Temp: 27.00 C, F = 80.60
13:00:05.673 -> Hum4: 87.00 %, Temp: 27.10 C, F = 80.78
13:00:07.656 -> Hum5: 71.00 %, Temp: 22.60 C, F = 72.68
13:00:09.691 -> Hum6: 71.00 %, Temp: 23.10 C, F = 73.58
13:00:11.698 -> Hum1: 33.00 %, Temp: 39.20 C, F = 102.56
13:00:13.709 -> Hum2: 31.00 %, Temp: 40.40 C, F = 104.72
13:00:15.708 -> Hum3: 85.00 %, Temp: 27.00 C, F = 80.60
13:00:17.699 -> Hum4: 87.00 %, Temp: 27.10 C, F = 80.78
13:00:19.706 -> Hum5: 71.00 %, Temp: 22.60 C, F = 72.68
13:00:21.745 -> Hum6: 70.00 %, Temp: 23.10 C, F = 73.58
13:00:23.755 -> Hum1: 33.00 %, Temp: 39.30 C, F = 102.74
13:00:25.749 -> Hum2: 31.00 %, Temp: 40.40 C, F = 104.72
13:00:27.770 -> Hum3: 85.00 %, Temp: 27.00 C, F = 80.60
13:00:29.781 -> Hum4: 87.00 %, Temp: 27.10 C, F = 80.78
13:00:31.773 -> Hum5: 71.00 %, Temp: 22.60 C, F = 72.68
13:00:33.787 -> Hum6: 71.00 %, Temp: 23.00 C, F = 73.40
13:00:35.794 -> Hum1: 33.00 %, Temp: 39.40 C, F = 102.92
13:00:37.818 -> Hum2: 31.00 %, Temp: 40.40 C, F = 104.72
13:00:39.816 -> Hum3: 85.00 %, Temp: 27.00 C, F = 80.60
13:00:41.824 -> Hum4: 87.00 %, Temp: 27.10 C, F = 80.78
13:00:43.820 -> Hum5: 71.00 %, Temp: 22.60 C, F = 72.68
13:00:45.834 -> Hum6: 71.00 %, Temp: 23.00 C, F = 73.40
13:00:47.841 -> Hum1: 33.00 %, Temp: 39.40 C, F = 102.92
13:00:49.876 -> Hum2: 31.00 %, Temp: 40.40 C, F = 104.72
13:00:51.879 -> Hum3: 85.00 %, Temp: 27.00 C, F = 80.60
13:00:53.862 -> Hum4: 87.00 %, Temp: 27.10 C, F = 80.78
13:00:55.886 -> Hum5: 71.00 %, Temp: 22.60 C, F = 72.68
13:00:57.919 -> Hum6: 70.00 %, Temp: 23.00 C, F = 73.40

	11:00	11:30	12:00	12:30	1:00	1:30	2:00	2:30	3:00	3:30	4:00	4:30
9/13/23	sunny	sunny	sunny	sunny	sunny	sunny	sunny	sunny	sunny	sunny	sunny	sunny
Amb Temp (F)	74	75	78	Power Outage no data	79	81	81	82	81	83	83	83
Outside RH (%)	31	29	27	no data	24	22	22	20	20	19	19	19
I (w/m^2)	906	917	920	no data	920	900	850	810	700	645	530	300
FR (gpm)	5.6	5.7	5.7	no data	5.8	5.7	5.6	5.7	5.6	5.6	5.7	5.6
sump Temp (F)	61.3	62.5	63	no data	63.8	62.8	62	64	63.4	61.8	61.6	59.2
Return Temp (F)	63.6	65.4	66.5	no data	68.6	66.8	67.7	67.2	66.6	64.3	64	62.1

12:59:57.944 -> Hum1: 57.00 %, Temp: 26.20 C, F = 79.16
12:59:59.934 -> Hum2: 62.00 %, Temp: 26.20 C, F = 79.16
13:00:01.945 -> Hum3: 90.00 %, Temp: 24.20 C, F = 75.56
13:00:03.953 -> Hum4: 87.00 %, Temp: 24.30 C, F = 75.74
13:00:05.980 -> Hum5: 76.00 %, Temp: 25.00 C, F = 77.00
13:00:07.975 -> Hum6: 76.00 %, Temp: 25.20 C, F = 77.36
13:00:12.012 -> Hum1: 63.00 %, Temp: 26.20 C, F = 79.16
13:00:14.034 -> Hum2: 67.00 %, Temp: 26.30 C, F = 79.34
13:00:16.060 -> Hum3: 90.00 %, Temp: 24.20 C, F = 75.56
13:00:18.048 -> Hum4: 89.00 %, Temp: 24.30 C, F = 75.74
13:00:20.078 -> Hum5: 76.00 %, Temp: 25.00 C, F = 77.00
13:00:22.089 -> Hum6: 76.00 %, Temp: 25.20 C, F = 77.36
13:00:26.139 -> Hum1: 65.00 %, Temp: 26.20 C, F = 79.16
13:00:28.129 -> Hum2: 75.00 %, Temp: 26.40 C, F = 79.52
13:00:30.158 -> Hum3: 94.00 %, Temp: 24.20 C, F = 75.56
13:00:32.165 -> Hum4: 98.00 %, Temp: 24.50 C, F = 76.10
13:00:34.160 -> Hum5: 67.00 %, Temp: 24.80 C, F = 76.64
13:00:36.167 -> Hum6: 63.00 %, Temp: 25.00 C, F = 77.00
13:00:40.235 -> Hum1: 67.00 %, Temp: 29.10 C, F = 84.38
13:00:42.245 -> Hum2: 68.00 %, Temp: 28.30 C, F = 82.94
13:00:44.248 -> Hum3: 102.00 %, Temp: 24.50 C, F = 76.10
13:00:46.255 -> Hum4: 102.00 %, Temp: 25.20 C, F = 77.36
13:00:48.270 -> Hum5: 65.00 %, Temp: 24.50 C, F = 76.10
13:00:50.286 -> Hum6: 67.00 %, Temp: 24.60 C, F = 76.28
13:00:54.302 -> Hum1: 51.00 %, Temp: 33.30 C, F = 91.94
13:00:56.323 -> Hum2: 54.00 %, Temp: 32.00 C, F = 89.60
13:00:58.347 -> Hum3: 102.00 %, Temp: 25.00 C, F = 77.00
13:01:00.343 -> Hum4: 100.00 %, Temp: 25.80 C, F = 78.44
13:01:02.362 -> Hum5: 66.00 %, Temp: 24.20 C, F = 75.56
13:01:04.376 -> Hum6: 68.00 %, Temp: 24.40 C, F = 75.92

	11:00	11:30	12:00	12:30	1:00	1:30	2:00	2:30	3:00	3:30	4:00	4:30
9/15/23	sunny	sunny	sunny	sunny	sunny	sunny	sunny	sunny	sunny	sunny	sunny	sunny
Amb Temp (F)	73	76	78	78	81	83	85	84	84	84	85	84
Outside RH (%)	27	20	17	16	14	13	11	12	11	11	11	11
I (w/m^2)	930	970	970	960	950	927	880	800	735	660	536	330
FR (gpm)	5.6	5.6	5.6	5.7	5.7	5.7	5.6	5.6	5.7	5.7	5.7	5.6
sump Temp (F)	56.1	55.7	59.8	60.1	60.4	65.1	61.6	61.2	61.2	59.8	59.1	58.9
Return Temp (F)	58.5	59.5	64.2	63.8	64.2	67.9	64.8	64.3	63.9	62.1	61.4	60.9

12:59:57.378 -> Hum1: 30.00 %, Temp: 38.80 C, F = 101.84
12:59:59.394 -> Hum2: 32.00 %, Temp: 38.50 C, F = 101.30
13:00:01.376 -> Hum3: 85.00 %, Temp: 26.00 C, F = 78.80
13:00:03.412 -> Hum4: 89.00 %, Temp: 25.80 C, F = 78.44
13:00:05.419 -> Hum5: 70.00 %, Temp: 21.50 C, F = 70.70
13:00:07.430 -> Hum6: 70.00 %, Temp: 21.70 C, F = 71.06
13:00:09.433 -> Hum1: 30.00 %, Temp: 38.80 C, F = 101.84
13:00:11.448 -> Hum2: 32.00 %, Temp: 38.50 C, F = 101.30
13:00:13.436 -> Hum3: 85.00 %, Temp: 26.00 C, F = 78.80
13:00:15.465 -> Hum4: 89.00 %, Temp: 25.80 C, F = 78.44
13:00:17.469 -> Hum5: 68.00 %, Temp: 21.50 C, F = 70.70
13:00:19.484 -> Hum6: 68.00 %, Temp: 21.70 C, F = 71.06
13:00:21.463 -> Hum1: 30.00 %, Temp: 38.80 C, F = 101.84
13:00:23.482 -> Hum2: 32.00 %, Temp: 38.50 C, F = 101.30
13:00:25.509 -> Hum3: 87.00 %, Temp: 26.00 C, F = 78.80
13:00:27.521 -> Hum4: 89.00 %, Temp: 25.80 C, F = 78.44
13:00:29.515 -> Hum5: 68.00 %, Temp: 21.50 C, F = 70.70
13:00:31.518 -> Hum6: 67.00 %, Temp: 21.80 C, F = 71.24
13:00:33.538 -> Hum1: 30.00 %, Temp: 38.90 C, F = 102.02
13:00:35.557 -> Hum2: 32.00 %, Temp: 38.50 C, F = 101.30
13:00:37.564 -> Hum3: 87.00 %, Temp: 26.00 C, F = 78.80
13:00:39.538 -> Hum4: 89.00 %, Temp: 25.80 C, F = 78.44
13:00:41.570 -> Hum5: 68.00 %, Temp: 21.50 C, F = 70.70
13:00:43.570 -> Hum6: 67.00 %, Temp: 21.90 C, F = 71.42
13:00:45.597 -> Hum1: 30.00 %, Temp: 38.90 C, F = 102.02
13:00:47.592 -> Hum2: 32.00 %, Temp: 38.50 C, F = 101.30
13:00:49.618 -> Hum3: 85.00 %, Temp: 26.00 C, F = 78.80
13:00:51.602 -> Hum4: 89.00 %, Temp: 25.80 C, F = 78.44
13:00:53.632 -> Hum5: 70.00 %, Temp: 21.50 C, F = 70.70
13:00:55.620 -> Hum6: 67.00 %, Temp: 21.90 C, F = 71.42

	11:00	11:30	12:00	12:30	1:00	1:30	2:00	2:30	3:00	3:30	4:00	4:30
9/19/23	sunny	sunny	sunny	sunny	sunny	sunny	sunny	sunny	sunny	cloudy	sunny	sunny
Amb Temp (F)	71	73	75	77	79	79	80	82	83	81	82	82
Outside RH (%)	35	33	30	28	25	23	23	21	20	20	19	19
I (w/m^2)	890	900	905	915	905	890	853	790	730	275	515	275
FR (gpm)	5.6	5.6	5.7	5.7	5.7	5.8	5.8	5.7	5.7	5.7	5.6	5.7
sump Temp (F)	61.2	62	62.2	62.8	63	64.1	63.7	58	65	61	60.8	61.6
Return Temp (F)	65.8	65.8	65.8	66	66.4	67.3	66.6	63.3	68.5	62.5	62.9	63.8

13:00:00.565 -> Hum1: 36.00 %, Temp: 37.70 C, F = 99.86
13:00:02.572 -> Hum2: 62.00 %, Temp: 35.80 C, F = 96.44
13:00:04.579 -> Hum3: 88.00 %, Temp: 26.20 C, F = 79.16
13:00:06.567 -> Hum4: 92.00 %, Temp: 26.10 C, F = 78.98
13:00:08.585 -> Hum5: 73.00 %, Temp: 21.90 C, F = 71.42
13:00:10.596 -> Hum6: 73.00 %, Temp: 22.30 C, F = 72.14
13:00:12.620 -> Hum1: 36.00 %, Temp: 37.60 C, F = 99.68
13:00:14.607 -> Hum2: 62.00 %, Temp: 35.80 C, F = 96.44
13:00:16.634 -> Hum3: 88.00 %, Temp: 26.20 C, F = 79.16
13:00:18.616 -> Hum4: 92.00 %, Temp: 26.10 C, F = 78.98
13:00:20.623 -> Hum5: 73.00 %, Temp: 21.90 C, F = 71.42
13:00:22.659 -> Hum6: 75.00 %, Temp: 22.20 C, F = 71.96
13:00:24.667 -> Hum1: 36.00 %, Temp: 37.50 C, F = 99.50
13:00:26.674 -> Hum2: 62.00 %, Temp: 35.90 C, F = 96.62
13:00:28.688 -> Hum3: 88.00 %, Temp: 26.20 C, F = 79.16
13:00:30.677 -> Hum4: 92.00 %, Temp: 26.10 C, F = 78.98
13:00:32.706 -> Hum5: 73.00 %, Temp: 21.90 C, F = 71.42
13:00:34.693 -> Hum6: 73.00 %, Temp: 22.20 C, F = 71.96
13:00:36.716 -> Hum1: 36.00 %, Temp: 37.50 C, F = 99.50
13:00:38.735 -> Hum2: 62.00 %, Temp: 35.90 C, F = 96.62
13:00:40.736 -> Hum3: 88.00 %, Temp: 26.20 C, F = 79.16
13:00:42.729 -> Hum4: 92.00 %, Temp: 26.10 C, F = 78.98
13:00:44.737 -> Hum5: 75.00 %, Temp: 21.90 C, F = 71.42
13:00:46.768 -> Hum6: 73.00 %, Temp: 22.20 C, F = 71.96
13:00:48.781 -> Hum1: 36.00 %, Temp: 37.50 C, F = 99.50
13:00:50.784 -> Hum2: 62.00 %, Temp: 36.00 C, F = 96.80
13:00:52.773 -> Hum3: 88.00 %, Temp: 26.20 C, F = 79.16
13:00:54.805 -> Hum4: 92.00 %, Temp: 26.10 C, F = 78.98
13:00:56.803 -> Hum5: 75.00 %, Temp: 21.90 C, F = 71.42
13:00:58.810 -> Hum6: 73.00 %, Temp: 22.20 C, F = 71.96

	11:00	11:30	12:00	12:30	1:00	1:30	2:00	2:30	3:00	3:30	4:00	4:30
9/22/23	sunny	sunny	sunny	sunny	sunny	sunny	sunny	sunny	sunny	sunny	sunny	sunny
Amb Temp (F)	57	58	60	61	63	65	66	67	67	67	68	68
Outside RH (%)	41	40	39	40	34	32	30	30	29	28	27	26
I (w/m^2)	890	920	930	917	894	890	840	784	685	590	470	350
FR (gpm)	5.6	5.6	5.6	5.7	5.4	5.4	5.8	5.7	5.7	5.6	5.8	5.7
sump Temp (F)	56.4	57	57.3	56.8	55.6	56.4	56.7	55.7	55.1	52.6	55.5	53.6
Return Temp (F)	59	61	61	60	59	60.1	60.2	58.8	58.2	55.6	57.8	56.2

12:59:58.208 -> Hum1: 36.00 %, Temp: 32.90 C, F = 91.22
13:00:00.227 -> Hum2: 40.00 %, Temp: 32.20 C, F = 89.96
13:00:02.242 -> Hum3: 91.00 %, Temp: 22.20 C, F = 71.96
13:00:04.233 -> Hum4: 92.00 %, Temp: 22.30 C, F = 72.14
13:00:06.235 -> Hum5: 81.00 %, Temp: 16.40 C, F = 61.52
13:00:08.247 -> Hum6: 76.00 %, Temp: 16.90 C, F = 62.42
13:00:10.270 -> Hum1: 36.00 %, Temp: 32.90 C, F = 91.22
13:00:12.289 -> Hum2: 39.00 %, Temp: 32.30 C, F = 90.14
13:00:14.284 -> Hum3: 90.00 %, Temp: 22.20 C, F = 71.96
13:00:16.299 -> Hum4: 92.00 %, Temp: 22.30 C, F = 72.14
13:00:18.314 -> Hum5: 81.00 %, Temp: 16.40 C, F = 61.52
13:00:20.325 -> Hum6: 76.00 %, Temp: 16.90 C, F = 62.42
13:00:22.309 -> Hum1: 36.00 %, Temp: 32.90 C, F = 91.22
13:00:24.339 -> Hum2: 39.00 %, Temp: 32.40 C, F = 90.32
13:00:26.351 -> Hum3: 91.00 %, Temp: 22.20 C, F = 71.96
13:00:28.358 -> Hum4: 92.00 %, Temp: 22.30 C, F = 72.14
13:00:30.352 -> Hum5: 81.00 %, Temp: 16.40 C, F = 61.52
13:00:32.372 -> Hum6: 76.00 %, Temp: 16.90 C, F = 62.42
13:00:34.375 -> Hum1: 36.00 %, Temp: 32.90 C, F = 91.22
13:00:36.391 -> Hum2: 39.00 %, Temp: 32.50 C, F = 90.50
13:00:38.388 -> Hum3: 91.00 %, Temp: 22.20 C, F = 71.96
13:00:40.411 -> Hum4: 92.00 %, Temp: 22.30 C, F = 72.14
13:00:42.415 -> Hum5: 81.00 %, Temp: 16.40 C, F = 61.52
13:00:44.430 -> Hum6: 76.00 %, Temp: 16.90 C, F = 62.42
13:00:46.437 -> Hum1: 36.00 %, Temp: 32.80 C, F = 91.04
13:00:48.440 -> Hum2: 39.00 %, Temp: 32.50 C, F = 90.50
13:00:50.443 -> Hum3: 91.00 %, Temp: 22.20 C, F = 71.96
13:00:52.466 -> Hum4: 92.00 %, Temp: 22.30 C, F = 72.14
13:00:54.473 -> Hum5: 81.00 %, Temp: 16.40 C, F = 61.52
13:00:56.464 -> Hum6: 76.00 %, Temp: 16.90 C, F = 62.42

Heat exchanger heat rejection runs:

	11:00	11:30	12:00	12:30	1:00	1:30	2:00	2:30	3:00	3:30	4:00	4:30
10/6/23	sunny	sunny	sunny	sunny	sunny	sunny	sunny	sunny	sunny	sunny	sunny	sunny
Amb Temp (F)	66	70	70	72	74	77	78	78	78	78	80	80
Outside RH (%)	41	37	36	34	32	29	28	28	27	25	24	24
I (w/m^2)	865	870	878	904	904	886	856	803	737	652	536	392
FR (gpm)	7.5	7.5	7.6	7.5	7.5	7.6	7.5	7.7	7.7	7.6	7.6	7.7
bucket Temp (F)	73.6	75.3	80.4	82.4	82.8	83.5	83.3	83.8	81.6	81	79.8	78.7
top of exchanger Temp (F)	73.3	74.5	78.8	80.6	81.4	82.5	82.7	82.8	81.4	82	81.1	79.9
clean water output (oz.)			23		32		28		18		16	1

13:00:01.116 -> Hum1: 43.00 %, Temp: 44.30 C, F = 111.74
13:00:03.123 -> Hum2: 42.00 %, Temp: 44.30 C, F = 111.74
13:00:05.130 -> Hum3: 94.00 %, Temp: 32.60 C, F = 90.68
13:00:07.133 -> Hum4: 95.00 %, Temp: 32.80 C, F = 91.04
13:00:09.160 -> Hum5: 84.00 %, Temp: 28.30 C, F = 82.94
13:00:11.168 -> Hum6: 75.00 %, Temp: 28.70 C, F = 83.66
13:00:13.162 -> Hum1: 43.00 %, Temp: 44.30 C, F = 111.74
13:00:15.183 -> Hum2: 40.00 %, Temp: 44.40 C, F = 111.92
13:00:17.172 -> Hum3: 93.00 %, Temp: 32.60 C, F = 90.68
13:00:19.204 -> Hum4: 95.00 %, Temp: 32.80 C, F = 91.04
13:00:21.211 -> Hum5: 84.00 %, Temp: 28.30 C, F = 82.94
13:00:23.203 -> Hum6: 76.00 %, Temp: 28.70 C, F = 83.66
13:00:25.213 -> Hum1: 43.00 %, Temp: 44.40 C, F = 111.92
13:00:27.232 -> Hum2: 40.00 %, Temp: 44.40 C, F = 111.92
13:00:29.239 -> Hum3: 94.00 %, Temp: 32.60 C, F = 90.68
13:00:31.257 -> Hum4: 95.00 %, Temp: 32.80 C, F = 91.04
13:00:33.245 -> Hum5: 84.00 %, Temp: 28.30 C, F = 82.94
13:00:35.277 -> Hum6: 76.00 %, Temp: 28.70 C, F = 83.66
13:00:37.288 -> Hum1: 43.00 %, Temp: 44.40 C, F = 111.92
13:00:39.278 -> Hum2: 40.00 %, Temp: 44.50 C, F = 112.10
13:00:41.285 -> Hum3: 94.00 %, Temp: 32.60 C, F = 90.68
13:00:43.313 -> Hum4: 95.00 %, Temp: 32.80 C, F = 91.04
13:00:45.308 -> Hum5: 84.00 %, Temp: 28.30 C, F = 82.94
13:00:47.315 -> Hum6: 75.00 %, Temp: 28.60 C, F = 83.48
13:00:49.338 -> Hum1: 43.00 %, Temp: 44.40 C, F = 111.92
13:00:51.341 -> Hum2: 40.00 %, Temp: 44.50 C, F = 112.10
13:00:53.360 -> Hum3: 94.00 %, Temp: 32.60 C, F = 90.68
13:00:55.364 -> Hum4: 95.00 %, Temp: 32.80 C, F = 91.04
13:00:57.355 -> Hum5: 84.00 %, Temp: 28.40 C, F = 83.12
13:00:59.389 -> Hum6: 73.00 %, Temp: 28.60 C, F = 83.48

	11:00	11:30	12:00	12:30	1:00	1:30	2:00	2:30	3:00	3:30	4:00	4:30
10/7/23	sunny	sunny	sunny	sunny	sunny	sunny	sunny	sunny	sunny	sunny	sunny	sunny
Amb Temp (F)	66	70	72	76	77	80	80	81	81	84	84	84
Outside RH (%)	41	36	34	31	30	26	24	23	22	19	18	17
I (w/m^2)	797	830	850	858	860	843	803	740	660	563	430	239
FR (gpm)	7.5	7.5	7.5	7.7	7.6	7.7	7.8	7.7	7.7	7.7	7.6	7.6
bucket Temp (F)	79.3	80	81.6	83.5	84.6	86.5	87	87.7	86.4	86.5	84.5	83.7
top of exchanger Temp (F)	77.3	78.4	79.8	82	83	85.3	85.7	86.5	85.8	86.1	84.5	83.7
clean water output (oz.)			28		29		28		8		8	0

13:00:02.090 -> Hum1: 44.00 %, Temp: 44.70 C, F = 112.46
13:00:04.093 -> Hum2: 42.00 %, Temp: 45.00 C, F = 113.00
13:00:06.089 -> Hum3: 91.00 %, Temp: 33.60 C, F = 92.48
13:00:08.109 -> Hum4: 93.00 %, Temp: 33.60 C, F = 92.48
13:00:10.140 -> Hum5: 82.00 %, Temp: 29.00 C, F = 84.20
13:00:12.159 -> Hum6: 73.00 %, Temp: 29.20 C, F = 84.56
13:00:14.162 -> Hum1: 43.00 %, Temp: 44.70 C, F = 112.46
13:00:16.161 -> Hum2: 40.00 %, Temp: 45.00 C, F = 113.00
13:00:18.173 -> Hum3: 91.00 %, Temp: 33.60 C, F = 92.48
13:00:20.171 -> Hum4: 93.00 %, Temp: 33.50 C, F = 92.30
13:00:22.179 -> Hum5: 82.00 %, Temp: 29.00 C, F = 84.20
13:00:24.178 -> Hum6: 71.00 %, Temp: 29.20 C, F = 84.56
13:00:26.211 -> Hum1: 43.00 %, Temp: 44.70 C, F = 112.46
13:00:28.227 -> Hum2: 42.00 %, Temp: 45.00 C, F = 113.00
13:00:30.426 -> Hum3: 91.00 %, Temp: 33.50 C, F = 92.30
13:00:32.242 -> Hum4: 93.00 %, Temp: 33.50 C, F = 92.30
13:00:34.253 -> Hum5: 82.00 %, Temp: 28.90 C, F = 84.02
13:00:36.235 -> Hum6: 75.00 %, Temp: 29.20 C, F = 84.56
13:00:38.259 -> Hum1: 44.00 %, Temp: 44.70 C, F = 112.46
13:00:40.262 -> Hum2: 42.00 %, Temp: 45.00 C, F = 113.00
13:00:42.269 -> Hum3: 91.00 %, Temp: 33.50 C, F = 92.30
13:00:44.300 -> Hum4: 93.00 %, Temp: 33.50 C, F = 92.30
13:00:46.307 -> Hum5: 81.00 %, Temp: 28.90 C, F = 84.02
13:00:48.318 -> Hum6: 73.00 %, Temp: 29.20 C, F = 84.56
13:00:50.329 -> Hum1: 44.00 %, Temp: 44.70 C, F = 112.46
13:00:52.327 -> Hum2: 42.00 %, Temp: 45.00 C, F = 113.00
13:00:54.328 -> Hum3: 91.00 %, Temp: 33.50 C, F = 92.30
13:00:56.329 -> Hum4: 93.00 %, Temp: 33.50 C, F = 92.30
13:00:58.333 -> Hum5: 81.00 %, Temp: 28.90 C, F = 84.02
13:01:00.353 -> Hum6: 76.00 %, Temp: 29.20 C, F = 84.56

	11:00	11:30	12:00	12:30	1:00	1:30	2:00	2:30	3:00	3:30	4:00	4:30
10/8/23	sunny	sunny	sunny	sunny	sunny	sunny	sunny	sunny	sunny	sunny	sunny	sunny
Amb Temp (F)	67	70	74	77	79	81	82	82	85	85	85	84
Outside RH (%)	33	29	25	23	21	17	16	15	14	13	12	12
I (w/m^2)	804	845	860	881	879	862	824	764	698	606	470	256
FR (gpm)	7.5	7.6	7.7	7.7	7.7	7.7	7.8	7.7	7.7	7.7	7.6	7.6
bucket Temp (F)	77.3	79.5	83.5	85.4	87	87.1	88.3	88	87.6	86.5	85.1	84.2
top of exchanger Temp (F)	75.7	78.4	81.7	83.8	85.7	86	87	87	86.6	86.1	85	84.2
clean water output (oz.)			13		21		18		12		6	0

13:00:07.514 -> Hum1: 44.00 %, Temp: 45.70 C, F = 114.26
13:00:09.501 -> Hum2: 43.00 %, Temp: 45.80 C, F = 114.44
13:00:11.539 -> Hum3: 94.00 %, Temp: 34.20 C, F = 93.56
13:00:13.522 -> Hum4: 95.00 %, Temp: 34.40 C, F = 93.92
13:00:15.557 -> Hum5: 79.00 %, Temp: 30.30 C, F = 86.54
13:00:17.569 -> Hum6: 70.00 %, Temp: 30.60 C, F = 87.08
13:00:19.576 -> Hum1: 44.00 %, Temp: 45.60 C, F = 114.08
13:00:21.579 -> Hum2: 43.00 %, Temp: 45.70 C, F = 114.26
13:00:23.583 -> Hum3: 93.00 %, Temp: 34.20 C, F = 93.56
13:00:25.581 -> Hum4: 95.00 %, Temp: 34.40 C, F = 93.92
13:00:27.592 -> Hum5: 79.00 %, Temp: 30.30 C, F = 86.54
13:00:29.595 -> Hum6: 70.00 %, Temp: 30.60 C, F = 87.08
13:00:31.634 -> Hum1: 44.00 %, Temp: 45.60 C, F = 114.08
13:00:33.641 -> Hum2: 43.00 %, Temp: 45.50 C, F = 113.90
13:00:35.649 -> Hum3: 94.00 %, Temp: 34.20 C, F = 93.56
13:00:37.649 -> Hum4: 95.00 %, Temp: 34.40 C, F = 93.92
13:00:39.676 -> Hum5: 78.00 %, Temp: 30.30 C, F = 86.54
13:00:41.682 -> Hum6: 68.00 %, Temp: 30.60 C, F = 87.08
13:00:43.656 -> Hum1: 44.00 %, Temp: 45.70 C, F = 114.26
13:00:45.693 -> Hum2: 43.00 %, Temp: 45.50 C, F = 113.90
13:00:47.700 -> Hum3: 93.00 %, Temp: 34.20 C, F = 93.56
13:00:49.703 -> Hum4: 95.00 %, Temp: 34.40 C, F = 93.92
13:00:51.710 -> Hum5: 78.00 %, Temp: 30.30 C, F = 86.54
13:00:53.732 -> Hum6: 68.00 %, Temp: 30.60 C, F = 87.08
13:00:55.719 -> Hum1: 44.00 %, Temp: 45.70 C, F = 114.26
13:00:57.726 -> Hum2: 43.00 %, Temp: 45.40 C, F = 113.72
13:00:59.766 -> Hum3: 93.00 %, Temp: 34.20 C, F = 93.56
13:01:01.752 -> Hum4: 95.00 %, Temp: 34.40 C, F = 93.92
13:01:03.780 -> Hum5: 79.00 %, Temp: 30.30 C, F = 86.54
13:01:05.791 -> Hum6: 68.00 %, Temp: 30.60 C, F = 87.08

Appendix B: solar collector and UA testing data

The UA testing data has been split into three tables here.

Run	Time	Ta-in (F)	Ta-out (F)	Tw-in (F)	Tw-out (F)	LMTD (F)
7/18/23						
1	12:11	113.8	75.6	69.4	74.3	11.596
2	12:20	111.3	74.3	69	73.1	10.960
3	12:27	104.3	73.5	68.7	72	10.229
4	12:37	89	71.3	67.4	69.3	7.825
5	12:41	88	70.8	67.6	69.9	5.935
6	12:56	105.2	73.8	67.1	70.8	13.119
7	1:15	120	73.8	67.2	71.5	15.309
8	1:24	119.8	77	66.9	71.4	20.010
9	1:33	117.7	76	67	72.5	16.774

Run	Time	Flow water (gal/min)	flow water (lb/min)	flow water (lb/hr)
7/18/23				
1	12:11	5	41.75	2505
2	12:20	5	41.75	2505
3	12:27	5	41.75	2505
4	12:37	5	41.75	2505
5	12:41	5	41.75	2505
6	12:56	5	41.75	2505
7	1:15	5	41.75	2505
8	1:24	5	41.75	2505
9	1:33	5	41.75	2505

Run	Time	Qw (BTU/H)	Qa (BTU/H)	Qave (BTU/H)	UA
7/18/23					
1	12:11	12274.5	10038.96	11156.73	962.096
2	12:20	10270.5	9723.6	9997.05	912.130
3	12:27	8266.5	8094.24	8180.37	799.699
4	12:37	4759.5	4651.56	4705.53	601.344
5	12:41	5761.5	4520.16	5140.83	866.073
6	12:56	9268.5	8251.92	8760.21	667.715
7	1:15	10771.5	12141.36	11456.43	748.304
8	1:24	11272.5	11247.84	11260.17	562.730
9	1:33	13777.5	10958.76	12368.13	737.333